





Chair:  
**Prof. Marco Finazzi**

# DOCTORAL PROGRAM IN PHYSICS

The Doctoral Program in Physics at Politecnico di Milano aims at attracting bright students with good scientific background and clear interest towards development and applications of new ideas and technologies. It offers a wide range of opportunities in the fields of advanced applied physics, such as photonics and optoelectronics (lasers, ultrafast optics), biomedical optics (optical tomography), vacuum technologies (thin film depositions), material technologies (microelectronics and nanotechnologies, micromechanical processing), and advanced instrumentation (electronic and atomic microscopy, nuclear magnetic resonance).

Scientific education and training to develop general research abilities in all areas of applied physics is increasingly needed by advanced technological companies. Through a general education in the basic areas of applied physics and a specific knowledge in condensed matter physics, as well as optics and lasers, the PhD Program aims at the development of an experimental approach to problem solving techniques and at the attainment of a high level of professional qualification.

The Doctoral Program has strongly experimental character. The contents are strictly related to the research activities carried out in the laboratories at the Department of Physics. They can be divided into two main areas:

- a) Condensed Matter Physics, including photoemission; spin-resolved electronic spectroscopy; magneto-optics; X ray diffraction; magnetic nanostructures for spintronics; synchrotron radiation spectroscopy, positron spectroscopy, semiconductor nanostructures.
- b) Photonics and Quantum Electronics, including ultrashort light pulse generation and applications; UV and X optical harmonics generation; biomedical applications of lasers; diagnostics for works of art; laser applications in optical communications; time domain optical spectroscopy and diagnostic techniques.

All research activities rely on advanced experimental laboratories located at Politecnico di Milano (Milano-Leonardo Campus and Como Campus) and are performed in collaboration with several international Institutions. Consistent effort is devoted to experimental research, development of

innovative approaches and techniques, and design of novel instrumentation.

The educational program can be divided into three parts: 1) Courses specifically designed for the PhD program as well transdisciplinary courses; 2) Activities pertaining to more specific disciplines which will lay the foundation for the research work to be carried out during the Doctoral Thesis; 3) Doctoral Thesis. The thesis work is the major activity of the Program. It has a marked experimental character and will be carried out in one or more laboratories at the Department of Physics.

The students are also encouraged to perform part of their thesis work in laboratories of other national or foreign Institutions. Collaborations that may involve the PhD students are presently active with several national and international research and academic Institutions, such as: ETH-Zürich, EPL-Lausanne, Lund Institute of Technology, University of Paris-Sud, Ecole Polytechnique-Paris, University of Berkeley, University of Cambridge, University College London, Massachusetts Institute of Technology, Harvard University, European Space Agency, ENEA, Elettra-Ts, PSI-Villigen, Agenzia Spaziale Italiana, European Synchrotron Radiation Facility (ESRF-Grenoble), IFN-CNR, IIT-Istituto Italiano di Tecnologia.

At present, the number of students in the three-year course is 122, and 119 of them have a fellowship.

The PhD Program Faculty, who takes care of organizing and supervising teaching and research activities, consists of members (listed here below), who are all highly qualified and active researchers covering a wide spectrum of research fields. This ensures a continuous updating of the PhD Program and guarantees that the students are involved in innovative research work.

FAMILY NAME	FIRST NAME	POSITION*
BERTACCO	RICCARDO	FP
BRAMBILLA	ALBERTO	AP
CAIRONI	MARIO	ST
CERULLO	GIULIO	FP
CICCACCI	FRANCO	FP
COMELLI	DANIELA	AP
CUBEDDU	RINALDO	FP
DALLERA	CLAUDIA	FP
D'ANDREA	COSIMO	FP
DELLA VALLE	GIUSEPPE	AP
DUÒ	LAMBERTO	FP
FARINA	ANDREA	ST
FINAZZI	MARCO	FP
GAMBETTA	ALESSIO	AP
GHIRINGHELLI	GIACOMO	FP
ISELLA	GIOVANNI	FP
LANZANI	GUGLIELMO	FP
LAPORTA	PAOLO	FP
MARANGONI	MARCO	FP
MORETTI	MARCO	AP
NISOLI	MAURO	FP
PETTI	DANIELA	AP
PICONE	ANDREA	AP
POLLI	DARIO	AP
RAMPONI	ROBERTA	FP
STAGIRA	SALVATORE	FP
TARONI	PAOLA	FP
TORRICELLI	ALESSANDRO	FP
VIRGILI	TERSILLA	ST
ZANI	MAURIZIO	AP

\*Position: FP = Full Professor; AP = Associate Professor; ST = Scientist.

# PROGRAMMABLE INTEGRATED PHOTONIC DEVICES PRODUCED WITH FEMTOSECOND LASER MICROMACHINING FOR QUANTUM APPLICATIONS

Riccardo Albiero – Supervisor: Roberto Osellame

Profound technological advances are anticipated from the exploration of the complex and counter-interactive phenomena in quantum mechanics. Specifically, harnessing purely quantum phenomena, including quantum superposition, entanglement, and teleportation, holds the potential to enhance secure communications, amplify measurement sensitivity, and achieve substantial speed-ups in various computational tasks. Quantum states, however, exhibit a fragile nature, susceptible to the slightest environmental interactions. In this sense, photonics stands out as a promising choice among the proposed platforms for quantum technology advancement. Indeed, photonic-based quantum states exhibit resilience to noise and unwanted interactions, possessing weak coupling with the surrounding environment and thereby requiring less stringent error protection measures. Additionally, they do not suffer from the decoherence problems that matter-based systems do and can operate without the need for extremely low temperatures or high vacuum conditions. On the other hand, implementing large instances of quantum algorithms or establishing a global quantum communication

network will necessitate new levels of sophistication in the manufacturing of quantum technologies with numerous components. In this framework, integrated optics offers significant advantages over bulk optic quantum setups in terms of compactness, scalability, control, and phase stability. Furthermore, integrated quantum photonics can leverage the recent technological advancement of classical integrated photonics and enable a seamless connection with standard optical components, resulting in robust and reliable devices. Different technologies have been proposed as integrated photonics fabrication platforms, and femtosecond laser micromachining (FLM) in transparent media stands out as an exceptionally versatile one.

This technique leverages the nonlinear interaction between a focused femtosecond laser beam and a transparent substrate, inducing a localized increase in the refractive index of the bulk material. This allows the direct inscription of integrated optical waveguides by translating the sample into three dimensions. Notably, the confined material modification to the focal spot and its immediate surroundings facilitates the inscription of circuits with distinctive 3D geometries. Moreover, FLM can process various materials and does not require clean room facilities, enabling fast prototyping of optical circuits. The cost-effectiveness and rapid fabrication times of FLM often permit the design of devices through an iterative fabrication

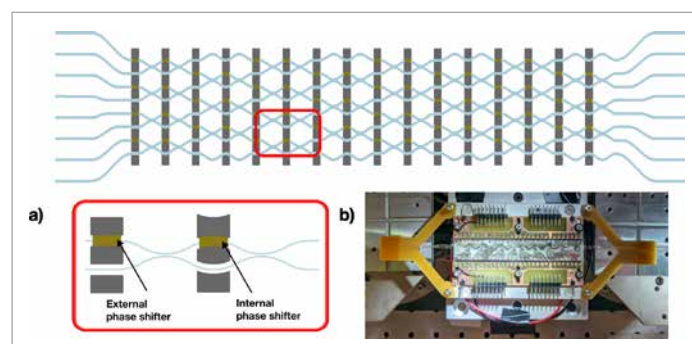


Fig.1 - a) Scheme of the eight-mode universal photonic processor. A rectangular mesh of fully reconfigurable MZI-base unit cells, depicted in the inset. b) A photo of the completed and packaged device.

and characterization processes, bypassing the need for complex numerical simulations. Finally, the low induced refractive index contrast, approximately  $10^{-3}$ , optimally interfaces with optical off-the-shelf optical fibers, eliminating the necessity for lossy grating couplers. Despite inherent limitations, such as modest miniaturization capability and a sequential fabrication process, FLM proves to be a crucial asset in ongoing quantum photonics research. In this thesis work, we present the implementation of several integrated circuits by FLM for the manipulation of quantum states of light in the context of a quantum photonic system. In our first experiment, we employed FLM to create a portable, monolithically integrated chip proficient in efficiently generating and characterizing Greenberger-Horne-Zeilinger (GHZ) states. This chip is tailored to be interfaced with quantum dot single-photon sources, the optical layout features 3D waveguide swaps leveraging the unique capabilities of FLM, and it incorporates low-power thermo-optic phase shifters for the precise characterization of GHZ states using quantum state tomography. The applications of this technology extend beyond quantum computing, encompassing entanglement swapping, quantum repeaters, implementation of secret sharing algorithms, entanglement measurements, and non-locality tests. The second theme of this thesis centers on the implementation of photonic circuits designed for scalable

quantum information processing. Our focus is centered on the optimization of femtosecond laser-written waveguides to obtain reconfigurable photonic circuits with high layout complexity. Particular attention was devoted to universal photonic processors, i.e. fully reconfigurable integrated circuits that can implement any  $N \times N$  unitary transformation of an  $N$ -mode input state. The layout of these circuits consists of a rectangular mesh of programmable Mach-Zehnder Interferometers (MZIs) unit cells featuring an external and internal phase shifter. Our optimization strategies were twofold: first, we worked on the geometrical paths and the optimization of the inscription parameters of the FLM waveguides. Secondly, we developed a novel approach for the isolation structures. In particular, the curve profiles are smoothened, and the waveguide parameters are tailored to minimize the radius of curvatures of the guiding structures without the introduction of additional bending losses. This optimization led to the halving of the curvature radius achievable with FLM waveguides. Secondly, we introduced a novel deep isolation structure design to thermally isolate waveguides. Compared to the previous state-of-the-art, this new isolation structure enables the implementation of compact circuit layouts while maintaining the same fabrication time. Together with a smaller curvature radius, this approach allowed us to demonstrate MZI-based unit cells with a total length

reduced approximately by 20%, representing the new state-of-the-art for programmable photonic integrated circuits fabricated through FLM. This work paved the way for the realization of a low-loss and low-power eight-mode universal photonic processor. The reconfigurability required for its universality is achieved through a mesh of 28 MZIs, whose internal and external phases can be controlled by 56 thermal phase shifters fabricated between isolation structures to reduce both their thermal crosstalk and their power consumption. The device is the most complex circuit fabricated by FLM to date. After a characterization with classical light, we show that the inscribed circuit can implement any arbitrary unitary transformation with the highest fidelity present in literature.

# HARNESSING ORBITAL ANGULAR MOMENTUM AS A MULTIFACETED TOOL FOR STRUCTURED LIGHT

Michael Almeida de Oliveira – Supervisor: Antonio Ambrosio

The quest to harness the full spectrum of light's properties has led to remarkable advances in the generation of new light distributions. At the core of these developments is the ingenious combination of different electromagnetic modes – the building blocks of light's spatial, temporal, frequency, and polarization structures – representing its multifaceted degrees of freedom. The rapidly evolving field of multimode photonics is at the forefront of these innovations, where the coherent manipulation of light's many degrees of freedom offers sophisticated electromagnetic solutions that redefine what is possible with light. Supported by an ever-evolving toolkit, this field is driving a wave of innovation across diverse applications from enhanced imaging techniques, microscopy, metrology, high-capacity optical communication, quantum information processing, and light-matter interactions. This thesis captures this journey, pushing the boundaries of what is possible in familiar 2D transverse patterns towards the realm of 4D spatiotemporal structured light. Here, we explore the

challenge of unraveling the intricate interplay between the topological properties of light, mediated by the orbital angular momentum (OAM) it carries, and its spatial and temporal dimensions, to realize sophisticated light sources exhibiting unprecedented phenomena. Overcoming the constraints of traditional approaches, the study showcases nanostructured metasurface devices and spatial light modulators employed in innovative configurations to effectively couple light's OAM with its other degrees of freedom, including polarization, space, frequency, and time (Fig. 1). The thesis ventures into the realm of structuring light directly at the source, demonstrating a laser cavity emitting coupled

vortex laser arrays (Fig. 2). Here, an active feedback mechanism orchestrates the interplay and evolution of the beams, enabling the engineering of vortex arrays with customizable topologies and tunable collective dynamics. On the other hand, by synthesizing a non-separable correlation between OAM and frequency via a novel space-time pulse shaper, we generate wave packets that follow helical trajectories through space-time (Fig. 3). Further, by employing pioneering multiplexing strategies in space and time, we present novel methods to manipulate their spatiotemporal properties, including time-varying OAM and angular acceleration of helical wave packets, thereby enabling control of novel light properties such as self-torque.

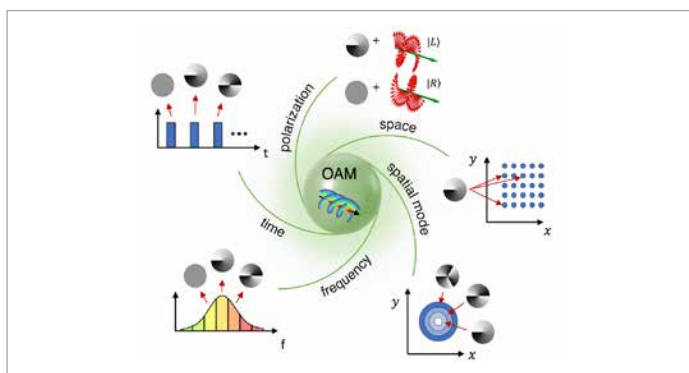


Fig.1 - This schematic captures our objective of integrating orbital angular momentum (OAM) of light with lights various degrees of freedom.

Ultimately, by extending our control and understanding of light's fundamental properties, we present a suite of new tools and methodologies that could transform how we probe, transmit, process, and visualize information.

*The research presented in this dissertation was conducted at the Center for Nano Science and Technology, part of the Italian Institute of Technology in Milan. Funding for the work was provided by the ERC Consolidator Grant "METAmorphoses" (Grant Agreement No. 817794). This work constitutes part of the research activities within the "Vectorial Nano-imaging" research line, led by Dr. Antonio Ambrosio.*

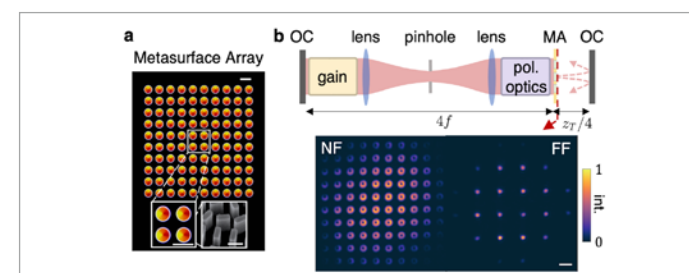


Fig.2 - (a) Optical image of the fabricated metasurface array (MA) with OAM  $\ell=1$ . Scale bars are 300  $\mu\text{m}$ . (b) Our laser cavity comprising of a  $4f$  telescope that images the MA onto the left output coupler (OC). The vortex array is coupled by diffraction via the Talbot effect. Experimental near-field (NF) and far-field (FF) intensity distributions of the arrays emitted from the cavity.

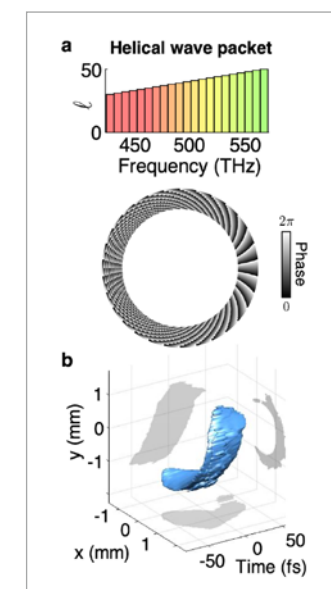


Fig.3 - (a) Hologram used to synthesize a helical wave packet with a broadband linear topological-spectral correlation between  $\ell = 30$  and 50. (b) Iso-intensity surfaces at 10% of the intensity peak for the generated helical wave packet.

# TOWARDS NEXT GENERATION OF TIME RESOLVED DEVICES FOR BIOPHOTONICS APPLICATIONS

**Elisabetta Avanzi** – Supervisor: Alberto Dalla Mora

Co-Supervisor: Laura Di Sieno

Time-domain diffuse optics (TD-DO) is a technique for non-invasive analysis of diffuse samples such as biological tissue. It involves injecting picosecond laser pulses (~10–100 ps) into the sample and collecting the temporal distribution of the re-emitted photons (distribution of time of flight, DTOF). Compared to its counterparts (e.g., continuous wave technique), it has a highly informative content since it can encode the mean depth reached by the photon in the arrival time and distinguish the absorption and scattering coefficients with a single measurement. Moreover, the ability to theoretically probe diffusive media accurately and deeply (up to 6 cm in depth) is another significant benefit. This suggests that the technique may be used to sample organs deep within the body—like the heart or lungs—that have never been investigated through optical methods.

These advantages have been inaccessible for a long time due to two main limitations: a limited light-harvesting capability of the detectors used, and a too slow timing electronics that cannot properly process high incoming signals. Modern research laboratories technologies allow to have high useful signal to the

detector, overcoming all these obstacles. The temporal signal is reconstructed using the time correlated single photon counting technique (TCSPC). Each time that a single photon is detected within an excitation cycle, its arrival time is recorded into a histogram. After many of these events the whole DTOF is reconstructed. The hardware of traditional TCSPC systems is unable to record a second photon in a single signal period since they can only timestamp one photon per cycle. This leads to the loss of the second photon. The recorded temporal signal is distorted since this phenomenon is more likely to occur in the later part of the waveform. This is the so-called pile-up distortion. Reliable reconstructed DTOFs are ensured when the ratio between the photon counting rate and the laser rate is kept < 1–5% (i.e., single photon statistics). The issue of pile-up distortion becomes increasingly important as the intensity of the detected signal rises, due to the advancements in laser technology, detector sensitivity and high-throughput TCSPC chains. This challenge has necessitated the development of innovative solutions to preserve the correctness of the DTOF data.

One such solution is the increase of the distance between the source and the detector. This approach reduces the intensity of the incoming signal without changing the depth selectivity. In doing so, it facilitates a transition from reflectance to transmittance measurement geometries, enabling the exploration of new measurement approaches. In particular, in collaboration with Fondazione Bruno Kessler, with my research activity a detector featuring a significantly large active area (100 mm<sup>2</sup>) has been developed and validated in DO thanks to the use of standardized protocols. It shows an enhanced light collection efficiency, making transmittance measurements feasible for the very first time on several fruits. Indeed, it has been possible to reach a maximum thickness of 9.6 cm. This could open the way to a new way of assessing fruit ripeness and quality, addressing challenges associated with reflectance measurements by potentially simplifying non-contact detection schemes and reducing sensitivity to artifacts. On the other hand, post-processing techniques have been proposed as a reliable solution for pile-up distortion. An algorithm has been proposed to

correct DTOFs shape, enabling accurate analysis of optical properties even under conditions of extreme signal intensity. It does not require any a priori assumptions about the photon distribution or the uniformity of time bins, being a powerful tool for TD-DO data analysis. It has been possible to show through a systematic in-silico study that the optimal counting rate of about 83% is suitable for detecting localized perturbation, and that homogeneous optical properties can be retrieved with an average error of less than 1% up to a photon collection rate greater than 99% of the laser repetition rate. Experiments validate these findings too. After correction, the results obtained under extreme pile-up conditions are better than (or at least comparable with) those of state-of-the-art systems. Because of its ability to acquire data quickly and with a good signal-to-noise ratio, this high-throughput regime may find use in several in vivo biological studies, enabling, so, the tracking of dynamic phenomena and real-time measurements. In particular, a pseudo-wearable high-throughput TD-DO system based on a 256-channel single photon avalanche diode line sensor and a CMOS driver with a laser diode emitting at around 800 nm has been chosen to be tested in high-throughput regime. After a collaboration with the University of Oulu (Finland), to adapt the device to TO-DO, we validated it. Therefore, a photon count rate equal to 83% of the laser rate has been reached at a SDD of 2 cm, allowing fast

acquisitions with increased SNR. The system has been tested under internationally agreed protocols, depicting a higher precision in detecting perturbation and optical properties reconstruction, when an alignment method based on cross-correlation maximization is applied. Measurements on two body locations in a resting-state enable the detection of heartbeat-induced absorption and scattering changes. To the best of our knowledge, this is the first compact pseudo-wearable instruments able to detect this pattern. Additionally, the extreme pile-up condition has been extended also to a high-throughput TCSPC fluorescence lifetime imaging microscopy (FLIM) system based on a compressive single-pixel camera scheme with a SiPM detector. This system offers great detection efficiency and throughput, with a considerable reduction in acquisition time thanks to compressive sensing optimization. It can perform wide-field FLIM at video rates of 20 frames per second, thus it has been used to monitor moving samples and get real-time fluorescence lifetime estimates. The ability to scale SiPMs into arrays may enable multidimensional acquisition by including spectral information to lifetime data for enhanced application specificity. Therefore, a small and cheap multifunctional time-resolved single-photon detection chain with 16 channels has been realized by taking advantage of the recent trend in component miniaturization. These channels

can be set up as a linear array for multispectral fluorescence lifetime imaging or as 16 independently located channels for TD-DO applications, such as tomographic measurements. With its 16 detection channels based on 1.3 x 1.3 mm<sup>2</sup> active area SiPM and its custom-made electronics specifically designed for avalanche sensing and amplification, capable of optimizing the single photon timing resolution, the multifunctional instrument takes advantage of the high time resolution and high light harvesting capability of SiPM. In fact, thanks to the combination of the linear array together with a 16-channel TDC and computational techniques, as pile-up correction, it has been possible to record fluorescence emission spectrum together with the calculation of the fluorescence lifetime of dynamical fluorescent biological samples. Furthermore, by evaluating the 16-channel detection chain with standard DO protocol, it has been possible to demonstrate that, because of its in-line performance with cutting-edge technologies, it may be used for TD-DO applications as well. In conclusion, this thesis work has exploited the latest developments in technology and computational techniques to provide previously unseen results for non-invasive time-resolved biophotonic applications. It opens the way to new working scenarios, like potentially simplifying non-contact detection on fruits, or real-time measurements with wearable instruments for physiological monitoring or multispectral fluorescence lifetime imaging.



# INTEGRATED GLASS DEVICES FOR THE GENERATION AND MANIPULATION OF EXTREME ULTRAVIOLET RADIATION

**Pasquale Barbato** – Supervisor: Rebeca Martinez Vázquez

Extreme Ultraviolet (EUV) radiation, the range of the electromagnetic spectrum spanning from 10 to 121 nm, is of great significance both in academic and industrial settings. From a scientific perspective, it allows to investigate the structure of matter down to dimensions of few nanometers or explore the water window in spectroscopic studies. From an industrial point of view, advanced lithography using EUV at 13.5 eV and beyond is the state-of-the-art in the semiconductor industry for silicon integrated circuits manufacturing. The availability of bright EUV sources and adequate optical components working at these wavelengths is therefore extremely important and, today, satisfied mostly by huge facilities like synchrotrons and free-electron laser, or by commercial laser-induced plasma sources. In both cases, the high footprint and the substantial costs strongly limit their adoption to a restricted number of laboratories. An interesting source of EUV radiation lies in the physical phenomenon known as High-order Harmonic generation (HHG). HHG is a highly non-linear effect arising from the interaction of an intense focused ultrafast laser beam (1013 – 1015 W/cm<sup>2</sup>) with an adequate non-linear

medium, usually a noble gas jet, leading to the emission of coherent radiation in the form of high-order odd harmonics of the driving laser frequency with a duration of attosecond timescale. HHG sources are typically compact and relatively easily accessible, but their practical use is strongly limited by the very low conversion efficiency, intrinsic of the phenomenon, and by the non-trivial manipulation of the emitted light. Such high-energy photons are in fact prone to be absorbed by both the harmonic-generating medium, resulting in a depletion of the source, and by the subsequent optics, which are thus limited to cumbersome grazing configurations. The main goal of my PhD is the development of integrated EUV and ultrashort UV laser sources, consisting of networks of empty structures in bulk fused silica.

These structures, realized with a technique known as Femtosecond Laser Irradiation followed by Chemical Etching (FLICE), allow the confinement of the gas target and the manipulation of the driving field to trigger the nonlinear interaction (Fig.1 and Fig. 2). What makes this approach unique is that with a careful design of the glass chip one can precisely control both strong laser fields and gas density spatial distributions, optimizing at unprecedented levels the generation efficiency. Exploiting the 3D capabilities of FLICE, different functionalities can be added to the integrated devices. As an example, Fig. 2 shows a device integrating differential pumping stages to remove the gas after the generation and decrease the probability of reabsorption of

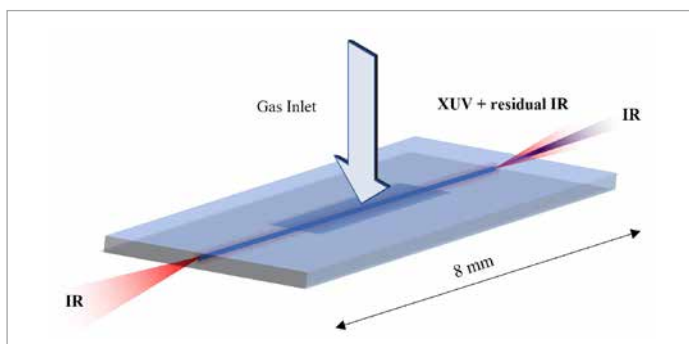


Fig.1 - Scheme of an integrated glass device for HHG. A femtosecond IR beam is focused into a hollow waveguide filled with gas to trigger EUV emission.

the emitted radiation. Other schemes include filtering stages for the removal of the driving field and beam splitters for EUV interferometry. A key aspect of my work was the demonstration that, by replacing the bulk by empty, it is possible to manipulate the propagation of EUV radiation in nanometer profile optical waveguides. To do so I had to perform a development of the fabrication technique itself. FLICE is a well-established micromachining technology which has been extensively used in the last two decades to realize optofluidic device in transparent materials for a variety of applications. It consists in the non-linear absorption of a focused femtosecond laser beam by a proper substrate, followed by the chemical etching of the resulting permanent

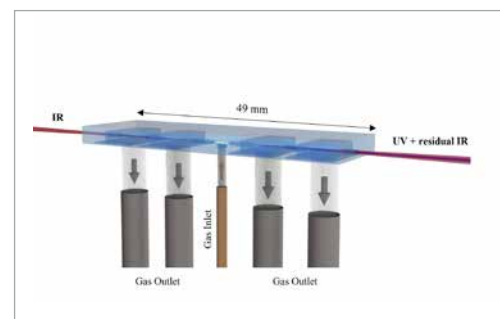


Fig. 2- Optofluidic device for UV generation integrating a gas-ejection differential pumping scheme.

modification. It is possible to realize hollow structures in bulky materials with dimensions ranging from some centimeters to few micrometers. To realize EUV waveguides, it is necessary to approach dimensions comparable to EUV wavelengths, i.e., tens of nanometers. To do so, I pushed FLICE to unprecedented level of minuteness. Working at extreme focusing conditions, low repetition rates and near-threshold energies, I was able to explore a new modification regime that confines the modification to a sub-micrometer region. Under these conditions it was possible to unveil the existence of two fabrication conditions, associated to a different number of pulses per unit length delivered to the material, that leads to very different cross-sectional profiles of the channel

(Fig.3). Studying the etching properties of a highly selective etchant, NaOH, rarely adopted with FLICE, I managed to create high-aspect ratio nanochannels, with diameter of ~300 nm and exceeding 1 mm in length.

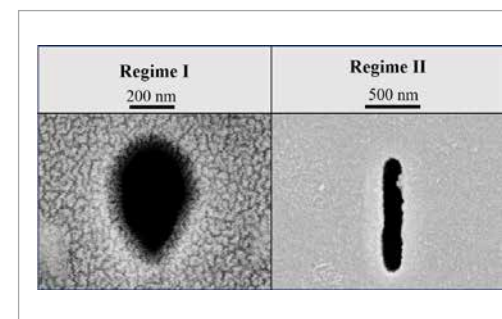


Fig. 3 - Scanning Electron Microscope images of the cross section of hollow channels in bulk fused silica with submicrometric profiles.

# APPLICATION OF ELECTRON SPECTROSCOPY TO THE STUDY OF PHOTOPHYSICS IN BIOMOLECULES

**Matteo Bonanomi** – Supervisor: Caterina Vozzi

My research activity mainly focuses on studying the ultrafast dynamics in biomolecules by photoelectron spectroscopy techniques. I spent most of my PhD at FERMI Free Electron Laser (FEL) in Trieste, Italy, at the Low-Density Matter beamline (LDM). In the last decades, fundamental processes of biological systems have been extensively studied on an ultrafast time scale. Particularly, the ability to track in time the energy transfer in molecules has provided new insights in the knowledge of reaction mechanisms. The dynamics of biomolecules almost invariably involve the non-adiabatic coupling of vibrational with electronic degrees of freedom, leading to the redistribution of charge and energy within the molecule. A well-established method to observe the first stages of a photochemical process is to prepare a photoexcited state with an optical laser, the so-called pump. Then a delayed probe pulse acts as the shutter of an ultrafast camera. Time-resolved photoelectron spectroscopy (TRPES) is the first-choice technique to follow the electronic relaxation processes in molecules as it is sensitive to molecular orbital configurations and vibrational dynamics.

Furthermore, it provides information on states which are not reachable by absorption methods. TRPES is an important technique for the study of non-adiabatic dynamics in polyatomic molecules and has been applied to a range of problems including internal conversion, photoisomerization, excited state proton and electron transfer, and photodissociation. Although TRPES is a commonly used technique for femtochemistry studies with table-top laser sources, applying TRPES to Free Electron Lasers (FEL) has several advantages. The use of XUV or X-ray FEL pulse for the probe step allows for site- and chemical-specific probing via inner-shell ionization. Also probing via valence ionization makes it possible to follow the molecular dynamics not just in the electronically excited state but also subsequent dynamics on the electronic ground state. In principle, both advantages are also applied to TRPES with HHG sources, but the lower photon flux of most HHG sources often poses a practical challenge for gas phase TRPES studies, both for valence photoelectron spectroscopy but especially for inner-shell photoelectron spectroscopy. I will present two topics addressed in my PhD

project: first, our results on the UV induced photodynamic in norbornadiene, a promising candidate for future application in energy storage. Then, our study on the photodynamics of the Uracil nucleobase. We studied the electronic relaxation dynamic of UV-excited norbornadiene using time-resolved gas-phase valence photoelectron spectroscopy, at LDM beamline. Norbornadiene (NBD) is a highly strained multicyclic hydrocarbon that isomerizes into Quadricyclane (QC) upon absorption in the ultraviolet (UV). QC undergoes the reverse reaction at similar wavelengths, resulting in a reversible molecular photoswitch that attracts a great deal of interest. Furthermore,

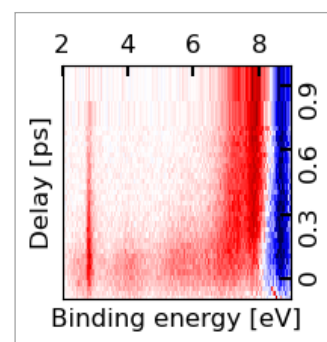


**Fig.1** – Experimentally measured photoelectron binding energy spectra of UV-excited NBD as a function of the pump-probe time delay between UV (6.2 eV) and XUV (18.9 eV) pulses, plotted as the electron yield difference between spectra taken with and without the UV-excitation pulse.

the QC-NBD system, and its derivatives, constitute promising candidates for high density molecular solar thermal (MOST) energy storage, that can absorb, store, and later release solar energy as heat. The study of QC-NBD conversion mechanism has both a photochemical interest and an application perspective. The time-resolved photoelectron spectra are shown as a two-dimensional false-color map in Figure 1.

Several prominent features are apparent. A relatively narrow and long-lived feature centered at 2.8 eV is assigned as the 3s Rydberg states of NBD. A spectrally broad but short-lived structure extending from the Rydberg states to approximately 7 eV merges into two long-lived bands approximately centered respectively at 7.3 and 7.8 eV. We assigned the feature at 7.3 to QC isomerization products and the band at 7.8 to NBD photoproducts. The pronounced negative signal in the difference spectrum at

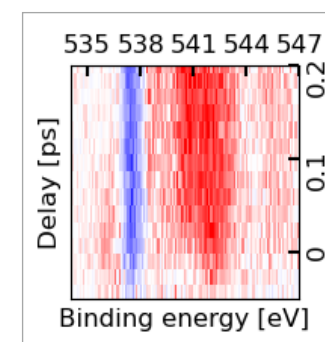


**Fig.2** – Experimentally measured photoelectron binding energy spectra of UV-excited Uracil as a function of the pump-probe time delay between UV (4.7 eV) and X-ray (600 eV) pulses, plotted as the electron yield difference between spectra taken with and without the UV-excitation pulse.

8.5 to 9 eV corresponds to the depletion of the NBD ground state. Pump-probe photoelectron spectroscopy using XUV photons from an FEL reveal rich chemical dynamics, detailing the relaxation pathways of excited state NBD from highly excited Rydberg states all the way to vibrationally hot ground state products. We have identified a new fast relaxation pathway (<100 fs) that competes with the slower decay via the Rydberg states already discussed in the literature, leading to the formation of vibrationally excited photoproducts. Nucleobases are a fundamental basic building block of nucleic acids. The photoreaction mechanisms have been extensively studied over many decades by various spectroscopic techniques; however, the dynamic of these molecules remains unclear. To shed light on those mechanisms, we investigate the photodynamics of Uracil with Time-Resolved X-ray photoelectron spectroscopy (TR-XPS) at the Oxygen K-edge. We did our experiment at the SQS beamline, European XFEL in Hamburg. Like all other nucleobases, Uracil absorbs photons strongly at a wavelength of 267 nm and exhibits an ultrafast relaxation process with experimentally observed relaxation times between 50 fs and 2.4 ps. In this way, excess energy dissipates as heat, rather than bond cleavage. It is thought to be why nucleobases evolved as the “alphabet of life” in a period when the Earth was strongly

irradiated by UV radiation. The two lowest valence excited states are involved in the photoinduced dynamics of Uracil: the first  $\pi\pi^*$  dark state (labeled  $S_1$ ) and the first  $\pi\pi^*$  bright state (labeled  $S_2$ ). Since core-level spectroscopy is site- and chemical-sensitive, TR-XPS can detect an ultrafast change in the electronic distribution around a specific atom.  $S_1$  and  $S_2$  orbitals differ significantly around one of the oxygen atoms. Thus, we expect our probe to capture the relaxation dynamic and particularly the transition from  $S_2$  to  $S_1$ . This is what we observed clearly in our experiment (Figure 2).  $S_2$  is the short-lived feature at 536 eV that decay in  $S_1$  in a timescale of 60 fs. The signature of  $S_1$  appears at higher binding energy as two delayed broad bands centered respectively around 541 eV and 546 eV. Calculations supporting our data demonstrate that the broad bands observed originate from different geometries of the molecules in the  $S_1$  state. TR-XPS has enabled us to identify the different electronic states involved in the relaxation pathway with molecular structure sensitivity.

# NONINVASIVE MORPHO-MOLECULAR IMAGING FOR CANCER AND DEVELOPMENTAL BIOLOGY

Arianna Bresci – Supervisor: Dario Polli

My doctoral research leverages biophotonics to propel biomedical discovery. Valuable information to trace the history and fate of cell states is encoded in their pristine morpho-chemistry under living physiological conditions. Conventional cell characterization tools, such as label-based microscopy, proteomics, metabolomics, and genomics, require extensive sample manipulation, thus failing to unlock original information and introducing artifacts and biases into the results, which limits our biological and biomedical understanding. Also, the complex sample preparation and labelling protocols used in standard methods are not time- and cost-effective, calling for user-friendly methods with comparable or superior rigor in cell phenotyping tasks. In my research, I exploited the noninvasive nature of different all-optical light-matter interactions, in the linear and nonlinear regime, to monitor unexplored biological dynamics occurring in non-perturbed systems. I merged advanced tools for quantitative label-free chemical imaging, including spontaneous and Coherent Raman Scattering (CRS) microspectroscopy and multi-photon microscopy, with cutting-edge morphological

imaging, based on holography and Tomographic Phase Microscopy (TPM). I combined these different optical microscopy techniques with systematic experimental workflows that involve large sample populations, designed to overcome the intrinsically high variability of biological phenomena. I achieved a comprehensive and quantitative description of evolving morpho-molecular traits of cell states, uncovering statistically significant patterns that define the chronological evolution of biological processes of major interest for current cancer and developmental biology. In cancer research, therapy-induced senescence (TIS) is considered an enigmatic cell state fuelling cancer dormancy, resistance

to treatments, and relapse: its prompt identification in cancer cells that underwent therapy is critical. Leveraging CRS (in both its versions: coherent anti-Stokes Raman scattering and stimulated Raman scattering), two-photon excitation fluorescence, and TPM, I revealed and characterized the early onset and progression of TIS in human hepatic cancer cells. My work identifies unprecedentedly early TIS features, including mitochondrial rearrangement, morphological enlargement and flattening, and alterations in the lipid profile. I corroborated these findings, achieved on an *in-vitro* model of TIS, by assessing their reproducibility on human cancer cells that received the standard radiotherapy protocol currently used in clinics. I proved that

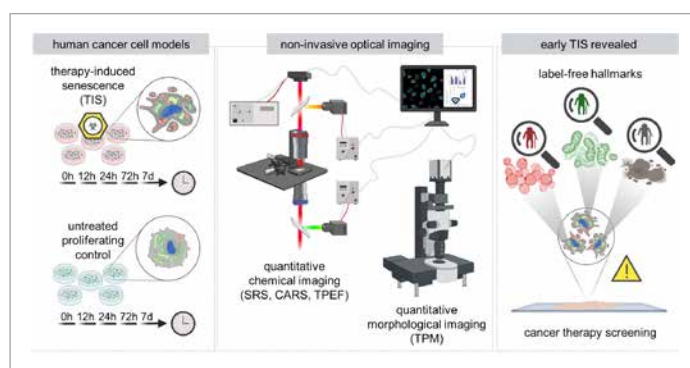


Fig.1 - Schematic workflow to reveal early onset of TIS in human cancer cells that underwent anticancer therapy. SRS: stimulated Raman Scattering. CARS: Coherent Anti-Stokes Raman Scattering. TPEF: Two-Photon Excitation Fluorescence

advanced all-optical microscopy is a quick and effective tool to screen anticancer treatment options and spot first evidence of TIS (Fig. 1). In regenerative medicine and developmental research, Embryonic Stem Cells (ESCs) play a central role, and their characterization under biocompatible conditions is a strict requirement for their actual usage in therapeutic procedures. Merging spontaneous Raman scattering microspectroscopy (RS) and TPM, I profiled the early morpho-molecular events occurring through the first four days of embryonic development (Fig. 2). I uncovered the initial morpho-molecular dynamics of pluripotency-to-multipotency transition in living three-dimensional embryonic colonies, including the generation

of the first ectodermal and endodermal germ layers. To corroborate my findings and highlight their generalizability, I trained a machine-learning model for the prediction of the differentiation state of unseen label-free embryonic colonies. I propose the use of all-optical RS and TPM technology to achieve non-perturbative analysis and quality control of ESCs products to advance current protocols in developmental research and stem cellbased biomedicine. In conclusion, my doctoral work proves the potential of leveraging multimodal light-matter interactions to uncover the hidden dynamics of living cells and cell colonies, escaping the limitations of traditional methods and opening new frontiers in biomedical

understanding. The diverse biological investigations I tackled in my research contribute to the validation and generalization of advanced label-free and quantitative imaging technology for understanding critical cell states and cell dynamics with statistical rigor. Laser-based microscopy and spectroscopy hold a huge potential in providing noninvasively new insights into cellular processes of living and pristine systems, with direct implications for diagnostics and therapeutics.

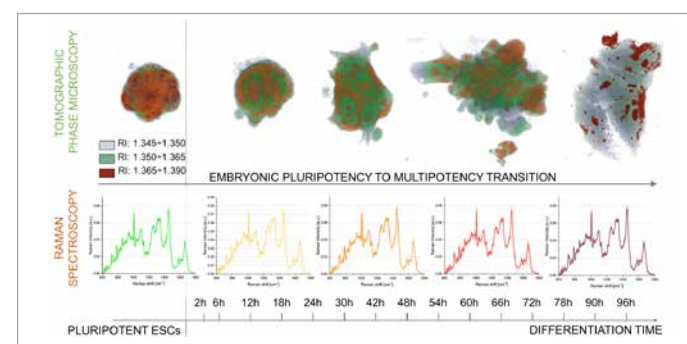


Fig.2 - TPM refractive-index (RI) tomograms (on top) and RS spectra (below) of living label-free embryonic colonies through the first four days of embryonic development (96 hours of differentiation), encoding quantitative morphological and molecular information, respectively.



# WIDE-FIELD VIDEO-RATE BROADBAND CARS MICROSCOPY

Chiara Ceconello – Supervisor: Dario Polli

Spontaneous Raman (SR) microscopy is a powerful tool in the life sciences, enabling label-free, chemically-specific and non-destructive mapping of cells and tissues. SR offers excellent chemical specificity and sensitivity, but its low cross-section prevents high-speed imaging. Coherent Raman scattering (CRS) methods, like coherent anti-Stokes Raman scattering (CARS), significantly increase acquisition speeds by several orders of magnitude, employing ultrashort pulses to trigger third-order nonlinear optical processes. Single-wavelength CARS (SW-CARS) delivers to the sample two spatially and temporally overlapped picosecond pulses, namely pump and Stokes, at frequencies  $\omega_p$  and  $\omega_s$ , respectively. The frequency difference  $\Omega_R = \omega_p - \omega_s$  resonates with the sample's vibrational mode  $\Omega_R$ , creating a signal in the anti-Stokes frequencies area. This signal is blue-shifted compared to the pump and Stokes beams, allowing for investigation of a single vibrational mode. Broadband CARS (B-CARS) combines rapid image acquisition from SW-CARS with SR's chemical specificity to access the entire vibrational spectrum via a broadband Stokes pulse.

B-CARS microscopy employs raster scanning where signals are generated pixel by pixel using tightly focused laser beams and high NA objectives. Despite advancements in reaching  $\approx 1$  ms pixel dwell time, capturing a single image can still take minutes limiting real-time analysis of rapid biological dynamics. Wide-Field (WF) illumination offers a potential solution to this challenge by enabling parallel signal creation over a large field of view, by loosely focusing the beams onto the sample. Signal collection is achieved by using a two-dimensional camera, like a sCMOS, placed in the optical plane conjugated with the sample and appropriately magnified. In particular, non-phaseshifting WF illumination, where the two driving beams are collinear, is a simple arrangement for generating WF-CARS. In this work, I demonstrated a novel

and high-speed approach to WF-CARS with video-rate and broadband imaging capabilities. The laser source (Fig. 1) is an amplified ytterbium laser with 1035 nm central wavelength and 2 MHz repetition rate, allowing to generate broadband Stokes pulses (1050–1500 nm) via white-light continuum (WLC) in bulk media. This is a compact, robust, simple and alignment-insensitive approach with great long-term stability and minimal pulse-to-pulse fluctuations. The red-shifted pump and Stokes wavelengths, as opposed to traditional CARS microscopy set-ups (with sources in the 800–1000 nm region), decrease multiphoton sample photo-damage, allowing the use of higher laser intensities. Furthermore, due to its non-linear optical nature, the increased pulse energies from the lower repetition rate of 2 MHz rather than traditional systems

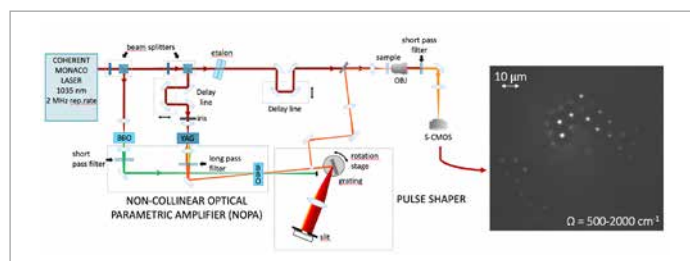


Fig.1 - Schematic of the WF-CARS experimental setup. BBO:  $\beta$ -barium borate, OBJ: objective. Right: WF CARS image of 10- $\mu$ m PS (Polystyrene) and 8- $\mu$ m PMMA (Polymethyl methacrylate) beads in a solution of DMSO (Dimethylsulfoxide). 100 $\mu$ m  $\times$  100 $\mu$ m, 10 ms integration time.

running at 40–80 MHz, contribute to a stronger CARS signal. To further reduce acquisition times, I included in the system design a non-collinear optical parametric amplifier (NOPA) to increase the white-light broadband Stokes power. In this way, it is possible to generate WF-CARS images at a single vibrational frequency with low acquisition times for even quicker and state-of-the-art comparable multiplex CARS imaging. From the common driving source, the laser beam is divided into three branches, with two generating pump and seed for the NOPA and the third serving as the pump of the CARS process. The latter passes through an etalon to generate  $\approx 1$  W narrowband pulses with  $\approx 1$  nm bandwidth, determining spectral resolution of the system. The driving pump beam for the

NOPA is obtained by focusing a 16 W fraction of the laser into a  $\beta$ -barium borate (BBO) crystal (cut at  $\theta = 23.4^\circ$ ) generating 4 W of second harmonic (SH) at 515 nm. The seed is produced through white-light supercontinuum in a 10-mm-thick YAG crystal, and parametric amplification occurs in a 2-mm thick BBO crystal cut for type-I phase matching ( $\theta = 23.4^\circ$ ) with a non-collinear interaction angle of  $5^\circ$ , resulting in 400 mW of amplified broadband Stokes beam covering the entire vibrational fingerprint region (400–1800  $\text{cm}^{-1}$ ). After amplification, the Stokes beam enters a 4-f pulse shaper system with a slit mounted in the Fourier plane, allowing for single wavelength selection from the broadband beam. To select a specific output wavelength, the grating angle is properly tuned by

acting on a motorized rotational stage. The generated WF-CARS signal is collected using a NA=0.3, 20x objective and recorded with a 4.2 MP sCMOS camera after excitation beams filtration. I tested the setup by acquiring a hypercube of pure toluene (Fig. 2, left). Each frame, measuring 100 $\mu$ m  $\times$  100 $\mu$ m, is obtained with an integration time of 5 milliseconds, resulting in a total of 350 frames. The exposure time for a single pixel for the entire CARS spectrum is 45  $\mu$ s/pixel, comparable to the best result in literature of 42  $\mu$ s/pixel. The phase-retrieved spectrum closely matches a related spontaneous spectrum from the literature (Fig. 2, right), with an estimated spectral resolution of 20  $\text{cm}^{-1}$ . This novel WF-CARS configuration represents a significant advancement in CARS microscopy, enabling real-time investigation of dynamic biological processes. The improved video-rate imaging speed and chemical specificity offered by WF-CARS hold great promise for deeper insights into live cellular behavior and tissue dynamics, paving the way for exciting future research and applications in the life sciences.

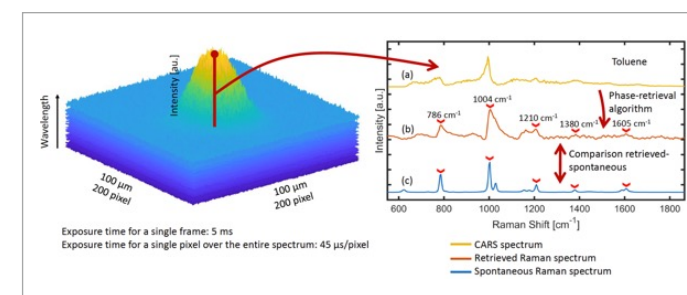


Fig.2 - Left, Wide-field CARS hypercube of toluene acquired as sequential frames at different Raman shifts from 500 to 1900  $\text{cm}^{-1}$ . Right, (a) broadband CARS spectrum of toluene, the peaks are embedded in non-resonant background (NRB). (b) Phase-retrieved Raman spectrum (c) Spontaneous Raman spectrum of toluene.

# STUDYING SUB-STOICHIOMETRIC TUNGSTEN OXIDE THIN FILMS TOWARDS INFRARED TRANSPARENT-CONDUCTIVE OXIDE AND PLASMONICS

Hao Chen – Supervisor: Silvia Maria Pietralunga

Tungsten oxide is a versatile semiconducting material. Its structure exhibits remarkable flexibility due to its ability to crystallize into different crystalline phases and to accommodate oxygen vacancy defects at varying concentrations, thus changing its stoichiometry without compromising overall stability of the lattice. The complex structural polymorphism and poly-stoichiometry trigger various intriguing properties that can be in principle controllably mastered through structural manipulation. For example, the free electron density can be widely tuned from  $10^{18}$  to  $10^{22}$   $\text{cm}^{-3}$  through stoichiometry adjustment, making tungsten oxide switchable from dielectric to metal-like. Such versatility, stability and adjustability of the structures and properties has attracted great research interests in scientific community in recent decades and has promoted a wide span of possible applications such as smart windows, sensors, photo-electro-catalysts, etc. This work aims at studying optic-quality films of tungsten oxide, from amorphous to crystalline phases and from stoichiometric ( $\text{WO}_3$ ) to sub-stoichiometric ( $\text{WO}_{3-x}$ ) states, and aims at characterizing them as tailorable dielectric materials for possible

applications in transparent-conductive oxide (TCO) and plasmonic fields. A set of tungsten oxide films with thickness varying from 30 nm to 200 nm have been deposited by non-reactive RF-sputtering, followed by different thermal annealing treatments to tailor their properties. Annealing processes lasted for 8 hours and were performed in dry air,  $\text{N}_2$  and vacuum at temperatures varying from 300°C to 650°C. Eventually 25 samples were fabricated, each of them was deposited onto two different substrates, i.e., p-doped silicon wafer and fused silica slide. The films were firstly characterized generally for surface morphology, structure at both at long- and short-range, and relative stoichiometry. Then, functional TCO performance was evaluated through quantitative measurements of optical transparency and electrical conduction. The complex dielectric function was also extracted in a wide spectroscopic range from ultraviolet (UV) to mid-infrared (MIR), in view of designing plasmonic structures. Scanning Electron Microscopy (SEM) and Atomic Force Microscopy (AFM) measurements verified the compactness and surface smoothness for

the as-deposited and the 300°C-annealed films. Annealing at higher temperatures modified the surface morphologies differently: flat grains were observed in films annealed at 400°C in air, still of good optic quality in spite of a slightly increased surface roughness; rock-like grains were observed in films annealed in  $\text{N}_2$  at 650°C, and nanorods were observed in films annealed in vacuum at 650°C. The latter two annealing conditions largely increased the surface roughness. Long-range crystallographic structure was examined by X-Ray Diffraction (XRD) and Raman spectroscopy, both confirming the amorphous nature of as-deposited and 300°C-annealed films, and the crystalline nature of films annealed at higher temperatures. In particular, they verified the formation of  $\text{WO}_2$  structure in the film annealed in vacuum at 650°C. Local electronic and atomic structures were probed by X-ray Absorption Spectroscopy (XAS), which provides information about splitting of W 5d orbitals into 2 sub-bands, and upshift of electronic states from low-energy sub-band by annealing in air and in  $\text{N}_2$ , and downshift of electronic states from high-energy sub-band by annealing

in vacuum. Low-valence W ions ( $\text{W}^{5+}$  and/or  $\text{W}^{4+}$ ) are suggested in vacuum-annealed film, which is in good agreement with long-range structural characterizations. Moreover,  $\text{WO}_6$  octahedron units are shown to undergo distortions of a different degree, in the meantime to undergo shrinkages during atomic re-ordering by annealing in various conditions. Relative compositional ratio between O and W was checked by Energy-Dispersive X-ray Spectroscopy (EDXS), which shows a qualitative trend of increasing O/W ratio by annealing in air and in  $\text{N}_2$ , and of decreasing O/W ratio by annealing in vacuum. Optical transmittance was measured by CW spectrophotometry, and the amplitude of optical bandgaps was retrieved by using Tauc plot method. Lower bandgap values are found in  $\text{N}_2$ - and vacuum-annealed films, likely due to the presence of defect levels below the conduction band so that the bandgap is narrowed. A strong increase in optical transmission is reached by annealing in air at 300°C, which on the other hand does not significantly hinder the electrical conduction according to 4-probe measurements. Evaluation on transparent-conductive functionality is performed by adopting Haacke's

figure of merit, which shows good performance of film annealed in air at 300°C as TCO in near-infrared (NIR). Complex dielectric function over UV-NIR range was extracted by Variable Angle Spectroscopic Ellipsometry (VASE). Custom models have been developed to fit experimental data, by including a Tauc-Lorentz oscillator for inter-band transitions and a Lorentz oscillator for NIR absorption (in case if needed). Functionally graded models have also been developed as they are proved to be significantly essential for the fitting of films that show non-homogeneity of indexes along film depth as a result of differential oxidation dynamics during annealing process. Complex dielectric function at extended optical range from NIR to MIR was extracted by Fourier-transform infrared spectroscopy (FTIR). Negative real part of complex dielectric function was detected for post-treated films, in particular, the vacuum-annealed film was found to present a negative real part over a large optical range from 1.7  $\mu\text{m}$  to 20  $\mu\text{m}$ . The collection of reliable complex dielectric functions for differently-treated tungsten oxide films over the large spectroscopic range provides basic and

essential information for the design of plasmonic structures, which is quite interesting and promising thanks to the wide tunability of free electron density and thus of plasma frequency in tungsten oxide. Alternative to traditional lithography and lift-off techniques, electron beam irradiation has been experimentally proved in current work to be effective in controllably tailoring the stoichiometry of tungsten oxide, which is advantageous for its convenience in direct writing of plasmonic patterns without the need for resist material, and flexibility for the shaping of plasmonic patterns at high space resolution. Hence, in perspectives, the achieved results in this study can be a solid milestone for the next-step design and development of e-beam tailored sub-stoichiometric  $\text{WO}_{3-x}$  nanopatterns embedded in dielectric  $\text{WO}_3$  matrix, towards plasmonic applications.

# DEVELOPMENT OF QUANTUM TECHNOLOGICAL DEVICES THROUGH FEMTOSECOND LASER MICROMACHINING OF EMERGING QUANTUM MATERIALS

Giulio Coccia – Supervisor: Shane M. Eaton

In the framework of the European ITN LaslonDef project, the focus of the work has been the development of quantum devices through the laser microfabrication of promising quantum materials. In particular, the focus has been on the development of quantum sensors in diamond and the production of colour centres in other materials, i.e. impurities in the crystal structure with convenient properties for applications in the fields of quantum information, quantum communication and quantum simulation. In the field of diamond quantum sensing, the goal of the experiments was the production of devices with unprecedented sensitivities. A simple device has been demonstrated through the laser microfabrication of an innovative diamond sample from Element6, characterized by an intrinsic high concentration of Nitrogen-Vacancy (NV) centres, the typical diamond colour centre with excellent properties for quantum sensing. In detail, optical waveguides were fabricated through the laser in the bulk of the crystal enabling the interaction with the colour centres themselves and hence the possibility to exploit the crystal as a sensor, as shown in Figure 1. A laser can be coupled

to the waveguide, exciting the colour centres which provides a response to external electric or magnetic fields measurable through the emitted red light coupled to the waveguide and measured through conventional techniques, such as the Optically Detected Magnetic Resonance (ODMR) measurement. For such a sensor a sensitivity of 200 pT Hz<sup>-1/2</sup> has been estimated, one order of magnitude better than a similar device fabricated in a different diamond sample. The characterization of the colour centres' properties and the measurement of the sensitivity has been performed in Cardiff University's laboratories. Alternatively, a sensor has been developed through a combined approach of ion implantation and laser fabrication in collaboration with Ulm University (Figure 2). In such case, an ultrapure diamond has been ion implanted with NV centres from our collaborators in Ulm and waveguides have been fabricated in our lab in an array-like fashion. In this case, it is possible to exploit the shallow-implanted colour centres in high density ensembles to measure electric and magnetic fields, while avoiding that the excitation light would compromise the measurement itself. Moreover, in such device one gains some

locality in the measurement, due to the fact that only the colour centres in the core of the waveguide contribute to the measurement. The fabrication of waveguides' arrays paves the way to the independent excitation of each single waveguide, behaving as a single pixel for the measurement of magnetic fields with spatial resolution. In such case, the characterization of the device has been conducted from our collaborators in Ulm University. Finally, in the framework of the fabrication of photonic components in diamond, the possibility to develop balanced Y-splitters has been demonstrated, structures capable of dividing a single mode in a waveguide into two



Fig.1 - Optical microscope image of the waveguide integrated quantum sensor in the DNV-diamond sample from overhead (top) and cross-section (bottom) point of view.

identical modes in the two planes perpendicular to the light propagation direction (Figure 3). Eventually, also the control of the NV centres concentration in Optical Grade diamond through laser fabrication has been studied and the relative sample has been characterized by the collaborators in Calgary University. The second part of the project was focused on the ondemand formation of colour centres through the laser microfabrication technique. In particular, samples of hexagonal-Boron Nitride (hBN), Silicon Carbide (SiC), Gallium Nitride (GaN) and Aluminium Nitride (AlN) have been furnished from the respective collaborators of Ulm University, RMIT in Australia and Cardiff University. Different samples with diverse properties for each of the materials have

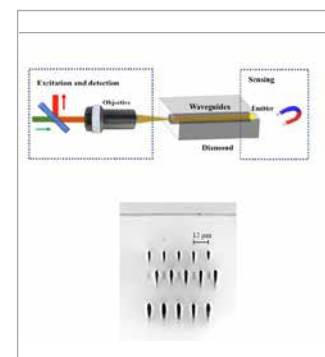


Fig.2 - Schematics of the hybrid quantum sensor mechanism (top). Example of a waveguide array (bottom).

been directly fabricated and characterized in the laboratories of Politecnico di Milano and relative collaborators. In such a context, the characterization and validation of the results requires an extended time and effort and several measurements are still ongoing from the collaborators themselves. The deterministic production of colour centres in such materials will enable the use of these quantum components for the aforementioned quantum applications and integration in more complex devices. This thesis provides an extensive analysis on the exploitation of femtosecond laser writing and crystal defects for the development of quantum devices. The versatility of the femtosecond laser microfabrication technique emerges as one of the main

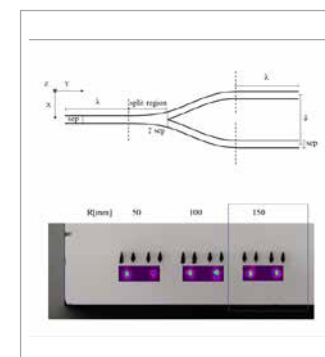


Fig.3 - Layout of a Y-splitter (top). Example of the output modes from Y-splitters with different properties (bottom).

strengths of our platform, which enables the fabrication of fully functional quantum devices through a simple approach, which can be easily scaled for mass production. Advancements in the usable laser systems for the fabrications and progress in the synthesis methods of the considered quantum materials will play a pivotal role for the establishment of these protocols for the production and diffusion of colour centres based quantum devices.

# MODELLING AND DESIGN OF NONLINEAR METASURFACES FOR THE ALL-OPTICAL CONTROL OF LIGHT

**Giulia Crotti** – Supervisors: Giuseppe Della Valle, Remo Proietti Zaccaria

In the last two decades, the outstanding progresses in nanofabrication techniques have granted the capability to miniaturize optical components. These advancements have opened the possibility of transposing well-established technologies for controlling radio- and microwave frequency radiation to the optical and near-infrared range of the electromagnetic spectrum, allowing manipulation of visible light at sub-wavelength scale, thus revolutionizing the field of optics. Nanophotonics exploits nanostructured materials to implement functionalities which traditionally demanded bulky components, such as lenses, mirrors and diffractive elements, with key technological advances, e.g., from the point of view of integration within electronic circuits. Beam steering, polarization control and wavefront manipulation have become achievable within lengths of few hundreds of nanometers. Most importantly, the investigation of light-matter interaction down to the nanoscale has disclosed new phenomena impossible to attain otherwise; this has paved the way to the development of exotic applications such as negative refraction, invisibility cloaking and

focusing beyond the diffraction limit. In general, the goal of tailoring the electromagnetic fields on the nanometer scale is now within reach, especially considering the change of paradigm brought forward by metamaterials and, more specifically, by metasurfaces. These are quasi-2D arrangements of nano-objects, packed in sub-wavelength configurations. As their electromagnetic behaviour is governed by the resonances of the constituent “meta-atoms”, metasurfaces provide unparalleled flexibility: the notable number of degrees of freedom, to be leveraged at the design stage, offers the possibility of complete control over their response. The advantageous characteristics of metasurfaces, stemming from their exceptional optical properties and ultra-compact nature, led to the development of flat optics. In parallel with the aforementioned linear applications, nanophotonic structures represent the ideal platform for exploiting nonlinear phenomena, thanks to their capability of concentrating and enhancing fields with localized resonances. Among these effects, the ones triggered by intense, femtosecond-laser pulses are of particular interest, especially

in relation to the light-induced modulation of matter properties on an ultrafast timescale. Nanomaterials constitute suitable architectures for the application of the all-optical paradigm. This approach is based on the idea of manipulating light by using light: by causing third order nonlinearities in matter, i.e., transient, intensity-dependent variations of the refractive index by a control laser pulse, a second beam, coming at a later time, experiences a modified interaction with the material. Engineering the platform properties can thus allow to tailor light manipulation beyond the fundamental speed limits of electronics. Thus, nano-objects become the building blocks of reconfigurable components, which can be envisioned for integration in active devices. In this context, the importance of understanding the mechanisms regulating the photo-induced modification of matter and their impact on the optical response of nanostructured systems is crucial. Experimental investigations via ultrafast pump-probe spectroscopy have to be complemented by accurate predictive modelling, an indispensable tool also for the design process. This task is far from immediate, given that

physical phenomena taking place upon photoexcitation belong to different temporal, spatial and energetic scales. Moreover, a multi-physics approach is required, to combine analysis of solid state, electromagnetic and thermal problems. Finally, numerical simulations have to be optimized so to keep the design of real-world devices agile. The work presented in this thesis can be inscribed within the efforts of achieving a comprehensive picture of ultrafast effects in nanostructured optical materials. The introduced description of light-matter interaction is employed to rationally design such architectures for selected applications, with a special focus on platforms for the all-optical modulation of light. In particular, the thesis presents the theoretical framework in which nanophotonic systems have been described, including both the numerical and analytical tools constituting the computational laboratory for the engineering of light-matter interaction. The relevant methods for electromagnetic modelling are summarized, the reviewed techniques for the solution of Maxwell equations being the basic toolbox for describing the optical response of nanostructures in both steady-state and out-of-equilibrium conditions. Subsequently, attention is dedicated to the processes taking place inside the active medium upon photo-excitation with the intense pump pulse: namely, the generation and internal relaxation of a population of electron-hole pairs (“hot” carriers), followed by

the energy transfer to the lattice. Thermodynamic rate equation systems, detailing the evolution of such energy exchanges, are the starting point for an account of the photo-induced variation of the medium permittivity. The proposed models of third-order optical nonlinearities in metals and semiconductors are ascribed to a semi-classical, semi-analytic description of matter, and correspond to the sum of various contributions coming from diverse photo-physical effects. The interplay of phenomena and their impact on the system optical response are also discussed, thus linking the dynamics of out-of-equilibrium, internal degrees of freedom to the electromagnetic problem. With the described tools, rational design and modelling of nanostructured systems for all-optical control becomes attainable. First, this expertise is applied to the engineering of dielectric metasurfaces for the modulation of light polarization both in terms of high-contrast polarization-selective switching and transient modification of the dichroic and birefringent properties. In this respect, our results show that the exploitation of hot carrier-mediated effects can yield considerable efficiency improvements. Moreover, metasurface configurations for more advanced, novel photonic functionalities are explored: in particular, we present the design of i) an all-optically reconfigurable metalens and ii) a device for switching a quasi-bound state in the continuum resonance, via ultrafast symmetry

breaking photo-induced at the nanoscale. The working principle shared between the reported works is based on the intriguing concept of photo-induced spatial inhomogeneities, based either on non-uniform delivery of energy, reflecting the anisotropic shape of the pump pulse, or on spatio-temporal transients in the hot carrier distribution, at the nanometric scale of the single meta-atom. This aspect, which until recently had been almost overlooked, is revealed to be another relevant degree of freedom to be leveraged in the design process of both plasmonic and semiconductor-based optical systems. Taken together, the work reported in this manuscript demonstrates that the synergy between this modelling approach and the available experimental techniques can unravel new routes for the understanding and efficient control of light-matter interaction, both by pushing existing technologies to their full potential and by unveiling new, interesting regimes to be exploited.



# EXPANDING TIME-DOMAIN DIFFUSE OPTICS TOWARDS NON-CONVENTIONAL SENSING SCHEMES FOR BIOMEDICAL APPLICATIONS

Sai Vamshi Krishna Damagatla – Supervisor: Antonio Pifferi

Time-domain diffuse optical spectroscopy (TD-DOS) is the field of study that aims to retrieve information from photons that have diffusely propagated through multiple scattering and absorption interactions in a medium. It is based on the detection of the Time-of-flight (TOF) of the photons to obtain their temporal distribution, which encodes the spatial paths travelled. Over the past years, it has progressed in leaps and bounds and found applications in various areas. Nowadays, most TD-DOS measurements are performed in standard configurations with source-detector separations ( $\rho$ ) in the order of a few cm. Most commonly, the measurements are performed placing the probes on the surface of the subject/sample and the models used are those of a semi-infinite or a slab geometry, either as a homogenous case, or a bi/tri-layer. Currently, these techniques have been gone through ethically approved in-vivo trials on volunteers and many of them are undergoing clinical trials in various areas such as breast cancer imaging and monitoring, functional brain monitoring, broadband spectroscopy, functional oximetry, etc to name a few. As part of this PhD, we attempted to expand

these boundaries of TD-DOS by pushing the limits of the measurement scenarios to non-conventional and comparatively extreme cases. These included different aspects – interstitial spectroscopy for single needle as well as high-throughput tomographic measurements, non-standard bioresorbable fibers for spectroscopy up to 1600 nm, spectroscopy in non-contact geometries, measurement of solid powder samples, etc. Here, we will discuss few of these important measurement campaigns. Our first experimental adventure was to test the suitability of TD-DOS for interstitial fiber spectroscopy (IFS). In recent times, IFS has gained importance for its use as a guidance tool in minimally invasive procedures. The problem with using TD-DOS for IFS is

the necessity for the injection and the detection of photons to occur through a single probe/fiber to reduce the invasiveness. This is known as the Null-source detector separation (NSDS) configuration and is generally unusual for standard TD-DOS measurements which are usually performed at  $\rho = 2-3$  cm. In this case, we need to collect and analyse the photons that have diffused deeper and have longer TOF, and are hence known as the 'late photons', all the while avoiding saturating the detector. We attempted to work around this through two different paths:

i) 'Software' gating – Using a high dynamic range detector with extremely low background counts and almost ideal Instrument response function (IRF) to acquire the low intensity, late photon

ii) 'Hardware' gating – Using an ultrafast gated detector with an ability to be turned off and on extremely quickly, hence being able to reject the early photons.

As a first case, we employed the first approach and used a superconducting nanowire single photon detector (SNSPD) with an almost gaussian response function and a dark count rate of <10Hz, which helped us acquire a dynamic range of >55dB with almost negligible dark counts. By working at  $\rho = 0$  in an interstitial setting, we were able to use the greens function solution for the infinite homogenous medium and showed that at  $\rho = 0$ , the effect of scattering theoretically vanishes. Conversely, it could be possible to retrieve the absorption independently of the scattering by fitting only the late photons. Having tested this theory by comparing it to the gold standard of Monte Carlo simulations, we then verified it experimentally on Intralipid based liquid phantoms and demonstrated the scattering independent absorption retrieval by obtaining the water spectrum in the range of 600-1100 nm within a good error margin. Then, we went one step further to perform interstitial measurements with a non-standard specialized bioresorbable fiber made from Calcium phosphate glass. Bioresorbable fibers have an exciting scope as they can be left inside the body for long term therapy, drug diffusion monitoring, thermal treatment, etc. For this second campaign, we decided to use the second

method of utilizing a hardware gate. We used an ultrafast gated single photon avalanche diode (TG-SPAD) built, developed, and tested previously at Politecnico di Milano. By being able to turn on and off the detector very quickly (few tens of ps), we had a very sharp gate, and with a variable delay line, were able to shift this gate, thus acquiring the later photons without saturating the detector. After testing the absorption linearity, we reverified the scattering independent absorption retrieval hypothesis and then tried to spectrally detect the presence of an inclusion placed in a background. Having prepared biological phantoms of speck (porcine processed meat) inclusions in two spectrally different backgrounds – Intralipid based water phantoms and solidified strutto (porcine fat); we acquired spectra while moving closer to the surface of the inclusion. We could successfully detect the expected changes in the spectrum – in particular the presence of blood components at 600-700nm – from a distance of 1 cm from the inclusion surface. The next campaign too utilized the common concept of the NSDS configuration, yet, in terms of measurement configuration was opposite of the interstitial story. Rather than going inside the medium, we decided to go away from it in an endeavour to perform TD-DOS in a non-contact configuration. Non-contact spectroscopy (NCS) has a huge potential for use in various applications such as remote monitoring, burn victims, household medical devices, etc.

The principal problem in this case too was the direct reflections from the surface and from the initial surface scattering events and so we reused the same detection techniques as before. However, in this case we also played about with the optics to inject the photons through a focused or a collimated beam rather than a power losing, diverging one. We also integrated some polarization optics to firstly polarize the light and consequently reject the direct reflections with an analyser. Consequently, with the TG-SPAD and the SNSPD we were able to get high dynamic range DTOFs and observe the diffusion tails due to late photons. We then went on to attempt the absorption retrieval from these data to obtain the absorption and scattering spectra as a proof-of-concept. All these campaigns were spread in different directions, but at their heart had the goal of pushing the limits of TD-DOS to research the next breakthrough though innovation. In conclusion, with a growing research and availability of new, exciting detectors, laser sources and computational methods, TDDOS could be a promising prospect for interstitial and non-contact spectroscopy, with a goal to help in the shift to minimally invasive procedures and personalized remote monitoring and thus better support the field of medical diagnostics, treatment and monitoring.

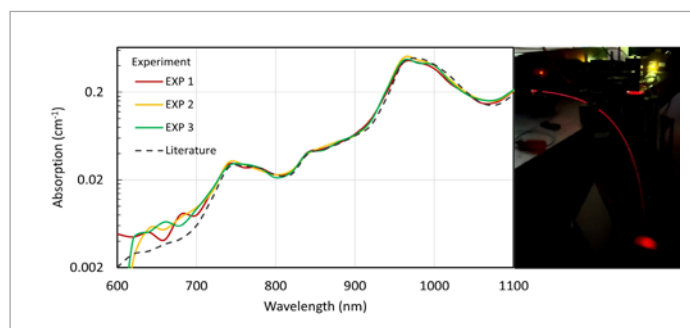


Fig.1 - (left) Absorption spectrum of water retrieved from an interstitial measurement as compared to that of literature (right) A bioresorbable fiber in use for a measurement, with the visible diffusion of the light in the liquid phantom it is immersed in

# PHOTOINDUCED PHASE TRANSITIONS AND ULTRAFAST DYNAMICS IN STRONGLY CORRELATED AND TWO-DIMENSIONAL MATERIALS

Oleg Dogadov – Supervisor: Stefano Dal Conte

Implementation of modern optoelectronic technologies, based on novel materials, requires a profound knowledge of non-equilibrium dynamics of generated photocarriers, which play a major role in the performance of the devices. Understanding the mechanisms of interaction between photoexcited carriers is therefore of primary importance for advanced technological applications. The progress in non-equilibrium spectroscopic methods allows to investigate microscopic processes in condensed matter on their inherent timescales. In my Thesis, broadband optical pump-probe spectroscopy was applied to study dynamics of complex effects in photoexcited materials. In the first part of my Thesis, ultrafast transient reflectivity spectroscopy was used to study the photoinduced insulator-to-metal transition in rare-earth perovskite neodymium nickelate. The high temporal resolution of the applied technique allowed to detect coherent phonons, which had not been observed before in this material with optical techniques. It was found that upon crossing the threshold fluence, both incoherent and coherent parts of the signal experience drastic changes.

When the sample was excited well above the insulator-to-metal transition threshold, the changes of the coherent phonon spectrum were found to appear within ca. 100 fs, similarly to the timescale of electronic modifications. The understanding of these dynamical effects allowed to make an additional step forward towards comprehension of the phase transition origin in this compounds. In the following, I investigated the transient optical response of a monolayer tungsten diselenide upon photoinjection of high carrier densities. In monolayer transition metal dichalcogenides, in which the optical properties are dominated by excitonic species, a transition to the metallic state (the so-called excitonic Mott transition) appears as a result of significant modification of

carrier-carrier interactions, which can be obtained, for instance, by a strong optical perturbation. In this regard, the temporal evolution of excitonic species in the presence of high excitonic or free electron-hole pair densities was studied with the broadband transient reflectivity spectroscopy. Additional information about the temporal evolution of the excitonic state was obtained by a quantitative line shape analysis. The photoinduced insulator-to-metal transition was manifested by a complete suppression of the excitonic transition. The performed work allowed to quantify the role of elevated carrier densities on excitonic effects in two-dimensional materials and in direct-gap semiconductors in general. The work presented in my Thesis was further extended beyond

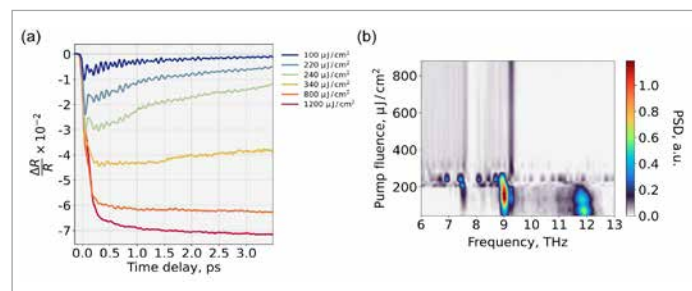


Fig.1 - Insulator-to-metal transition in neodymium nickelate. (a) Drastic changes in the transient signal indicate a strong modification of the electronic system with increasing pump fluence. (b) The Fourier transform of transient traces demonstrates significant changes of the lattice coherences, and hence, the structural phase transition.

photoinduced phase transitions and addressed a complex exciton relaxation dynamics in a heterostructure of two-dimensional semiconductors. In particular, the dynamics of the bright interlayer exciton formation was found to be around 800 fs, being almost an order of magnitude longer than the interlayer charge transfer timescale. A combined experimental-theoretical

approach, introduced in my Thesis, allowed to attribute such delay in the formation of the excitonic signal to the interplay between intervalley scattering and cooling of hot exciton population. The advanced experimental methods utilised in my work provided an opportunity to disentangle competing relaxation processes contributing to the observed dynamics in the photoexcited material. Besides

the fundamental interest of my work, the delayed formation of interlayer exciton signal could explain a long-standing puzzle in optoelectronic devices based on transition metal dichalcogenide heterostructures, namely the observation of efficient generation of photocurrent despite the large binding energy of the interlayer exciton. To summarise, the studies presented in my Thesis made an additional step towards understanding of complex out-of-equilibrium phenomena in strongly correlated and two-dimensional compounds and provided material for further research.

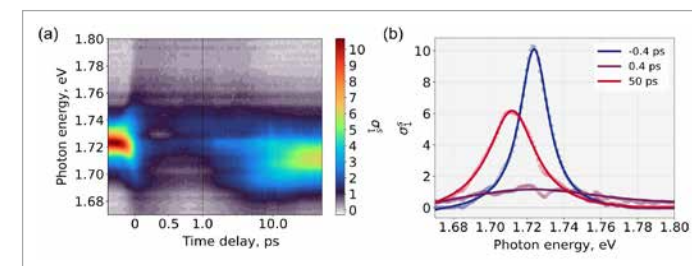


Fig.2 - Excitonic Mott transition in monolayer tungsten diselenide. (a) Pump-probe map, showing a complete quench of the excitonic resonance upon strong photoexcitation. (b) Select transient spectra from the map (a). Real part of optical conductivity is reported in atomic units.

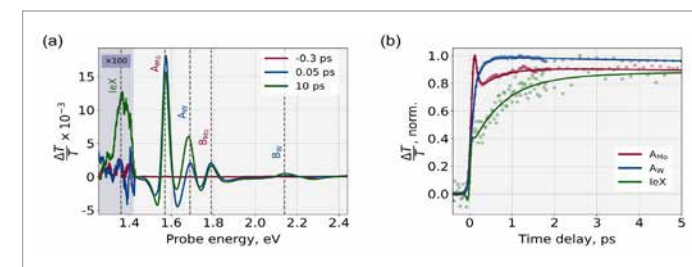


Fig.3 - Interlayer exciton dynamics in a transition metal dichalcogenide heterostructure. (a) Transient spectra at select time delays, showing the presence of the interlayer exciton signal along with the excitons of constituent monolayers. (b) Delayed formation of interlayer exciton signal on a picosecond scale.

# ATTOSECOND ELECTRON DYNAMICS IN MONOCRYSTALLINE DIAMOND

Gian Luca Dolso – Supervisor: Matteo Lucchini

The advent of attosecond science has revolutionized our ability to probe the motion and dynamics of electrons in matter, offering profound insights into the physical processes governing atomic, molecular, and solid-state systems. Recognized by the Nobel Prize in Physics in 2023, the experimental innovations driving attoscience have ushered in a new era of exploration, enabling the generation and utilization of isolated attosecond pulses and pulse trains for the study of electron dynamics. Our focus here lies in the investigation of solid-state systems and the phenomena unfolding during their interaction with intense fields. Within this framework, attoscience aims to achieve unprecedented control over charge carriers, holding the promise of transformative technological advancements. By harnessing light fields to manipulate charge carriers, future electronic applications could operate at frequencies extending into the petahertz domain, heralding a paradigm shift in high-speed electronics. In this context, wide-gap dielectrics emerge as highly promising materials due to their inherently fast response times, dictated by their large band gaps. Moreover, these materials mitigate photodoping, a phenomenon where injected

carriers exhibit prolonged decay times, thus impeding femtosecond-scale conductivity modulation.

For an accurate assessment of the femto- and attosecond dynamics unfolding when a strong light field interacts with light, a precise temporal characterization of the employed ultrashort pulses is mandatory, guaranteeing a correct interpretation of time-resolved investigations. Experimentally, the pulse characterization can be achieved with a two-color photoemission experiment: both the infrared (IR) pump and the attosecond extreme ultraviolet (XUV) probe pulses are directed onto a gas jet, where XUV pulses induce ionization and the IR field dresses the process. By collecting IR-dressed photoelectron

spectra generated by the XUV pulses, we construct a streaking trace, comprising multiple photoelectron spectra obtained at different XUV-IR time delays. The electron wavepacket closely resembles the impinging XUV pulse, while the IR accelerates the electron in the continuum, imprinting its vector potential on the photoelectron spectra. This data, therefore, encodes both the temporal profile of the XUV intensity and the IR vector potential.

Extracting the relevant temporal and spectral information from the photoemission experiment, however, remains a non-trivial task, typically requiring different methodologies depending on the specific temporal profiles of the pulses under scrutiny. Here, we introduce and validate a pioneering approach for

reconstructing ultrashort XUV pulses generated through high-order harmonic generation in gases, catering to three distinct conditions: isolated attosecond pulses, attosecond pulse trains, and few-femtosecond pulses obtained via spectral selection of individual harmonics. Central to this method, called Simplified Trace Reconstruction in the Perturbative Regime (STRIPE), is a novel mathematical model that offers a simplified description of the two-color photoionization process. Notably, this approach allows unveiling the temporal characteristics of XUV pulses while significantly reducing computational overhead compared to existing reconstruction techniques. Through direct comparison with conventional approaches, STRIPE showcases superior flexibility, reliability, and robustness against noise and artifacts, thus positioning itself as a promising tool for pulse characterization.

In our experiments on solids, we employ intense few-cycle IR pulses to trigger electron

dynamics in solid-state systems, while the isolated attosecond pulses are used to follow the system's evolution in time. Experimentally, the two-color photoemission measurements that enable the pulse characterization are recorded simultaneously with the experiment on the solid, thanks to the two-foci geometry of the attosecond beamline. With this technique, we investigate the time-resolved response of a diamond monocrystal, when subjected to an intense near-infrared field, using attosecond all-optical spectroscopy in reflection geometry. Specifically, we measure the IR-induced modifications in the material reflectivity, in the spectral region of the attosecond probe pulse, as a function of XUV photon energy and the pump-probe delay. By accessing a wide range of photon energies, from 20 to 45 eV, coupled with comprehensive theoretical calculations based on time-dependent density functional theory, we effectively discern the various electron states and concurrent physical processes at play. The pump-induced variations of the material reflectivity consist of signals present only in the temporal region of pump-probe overlap, oscillating at twice the frequency of the IR pump.

These dynamics are governed by multiple transitions within the material's band structure, probed by the attosecond pulse. Employing an orbital decomposition approach facilitates the disentanglement

of contributions from different transitions. The time evolution of the dielectric function is accurately reproduced through the coherent superposition of individual transition contributions. The material excitation is initiated by the intense pump pulse. At the investigated photon energies, we reveal the dynamics to be virtual, associated with transient, field-induced changes in band structure, rather than photoionization across the band gap. Contrary to prior studies performed in similar light-matter interaction regimes, attributing observations to intraband motion alone, our comprehensive analysis underscores the non-negligible contribution of vertical coupling between different subbands. This refined understanding sheds light onto the intricate interplay between intra- and inter-band phenomena, highlighting the significant role of interband effects on virtual electron dynamics—an important revelation in the pursuit of attosecond science.

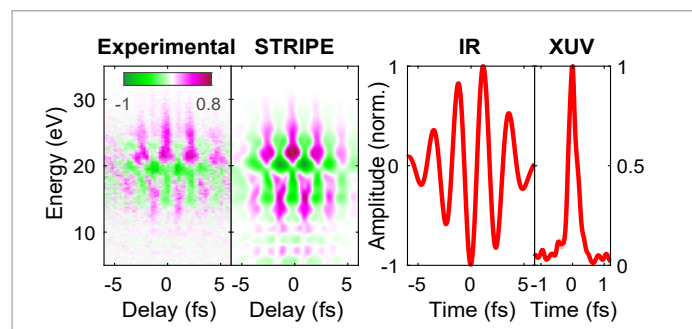


Fig.1 - Left: experimental and reconstructed differential streaking trace. Right: IR and XUV fields retrieved by STRIPE, defined in time.

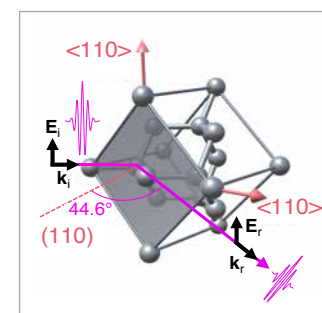


Fig.2 - Representation of the pump-probe experiment, with an illustration of the crystallographic directions and the experimental geometry.

# HARNESSING FERROELECTRICITY AND SPIN-ORBIT COUPLING TOWARDS ULTRALOW POWER SPINTRONICS

Federico Fagiani – Supervisors: Christian Rinaldi

Information and communication technologies' power usage is growing unsustainably, underpinned by the von Neumann architecture in data processing. However, its reliance on separate memory and computing units introduces a bottleneck, partly addressed by transistor scaling up to 10 nm or less. Yet, this approach is nearing economic and physical constraints, prompting exploration of alternatives. One potential avenue is logic-in-memory architectures, which integrate storage and computational functions within a single unit.

In 2019, Intel introduced the MESO (magneto-electric spin-orbit) device, aiming for a new logic-in-memory unit with ultra-low energy consumption. The MESO combines a magneto-electric (ME) module that takes advantage of collective phenomena like ferroelectricity and ferromagnetism to enable information writing and storage, and a spin-orbit (SO) module for processing and readout, leveraging phenomena that conveniently scale with the size of the device (Fig. 1a). Examples of such physical processes are spin-to-charge current conversion (S2CC) phenomena, like spin Hall (SHE) and Rashba-Edelstein

(REE) effects, which translate a spin current into a transverse charge current and vice versa. However, achieving operation in the desired aJ range demands efficient materials and interface optimization, posing challenges for full realization. In search of an efficient and low-energy consumption readout module, part of this thesis thoroughly investigates the MESO spin-orbit readout unit using NiFe/Pt heterostructures. NiFe, a soft ferromagnet, facilitates magnetization reversal, reducing energy dissipation; Pt, through inverse SHE, enables S2CC for memory retrieval. Here, we demonstrate the capability to perform field and angular dependent experiments to access the spin, anomalous and planar Hall effects. Experimental results show a significant spin Hall signal (Fig. 1b); by fitting our results with

micromagnetic and analytical models, we infer a spin Hall angle  $\theta_{\text{SHE}}$  for Pt of 3.5% comparable with literature. Moreover, we provide a detailed analysis of both the energy aspects and the single contributions to the output signal (i.e. spin, anomalous and planar Hall effects).

In the realm of energy-efficient materials for ultralow power devices, ferroelectric Rashba semiconductors (FERSC) emerge as promising candidates. Thanks to their inherent multifunctionality, this family of materials is predicted to be suitable for in-memory computing, combining ferroelectricity (memory) and the Rashba effect (computing) in a single semiconducting material. Recently, we demonstrated that in FERSC's father compound GeTe the ferroelectric (FE) polarization can be reversed by electric pulses

and used to change the sign of S2CC, offering the non-volatile FE control of information processing within the same physical area. However, the efficiency of S2CC mechanism in GeTe remains insufficient (i.e. low S2CC efficiency  $\theta_{\text{SHE}} = 1\%$  and coercive voltage  $VC = 5$  V). Therefore, it is necessary to provide methods to tailor material properties for lower switching voltages and larger S2CC. In this thesis we show how combining GeTe and SnTe FERSCs tunes ferroelectric and Rashba properties in  $\text{Ge}_x\text{Sn}_{1-x}\text{Te}$ . Supported by ab-initio calculations, spin- and angular-resolved photoemission spectroscopy (SARPES) and FE characterizations, we demonstrate engineering of the giant Rashba effect and associated ferroelectricity, which remain stable up to  $T_{\text{room}}$  in GeSnTe. (Fig. 2a,b). We prove the increase of Curie temperature

in  $\text{Ge}_{0.3}\text{Sn}_{0.7}\text{Te}$  up to 500 K (for pure SnTe  $T_C$  is 100 K) and the significant reduction of the coercive voltage  $VC$  with respect to pure GeTe (Fig. 2c shows  $V_{C,\text{GeSnTe}} < 2$  V).

The two aforementioned studies were conveyed to develop an innovative device surpassing MESO by integrating its spin-orbit module with FERSCs. This cutting-edge technology is the *ferroelectric spin-orbit logic (FESO)* and is shown in Fig 3. FESO stores information in FE polarization, enabling processing and readout through polarization-dependent spin-to-charge current conversion. This new paradigm offers a logic-in-memory unit within a single material, facilitating non-volatile voltage-controlled switching without external magnetic fields; moreover, it presents new opportunities in electronics,

potentially exceeding CMOS transistors and von Neumann architecture. Thanks to the knowledge acquired both with S2CC experiments in MESO-like structures and the FERSC's materials investigation, the manuscript concludes with the fabrication of the FESO device and its seminal magneto-transport measurements.

This work highlights the potential for a scalable and energy efficient MESO readout module operating in aJ regime, alongside insights into FERSC alloy's energy bands and the exploration of FESO devices. FERSC materials and the innovative FESO paradigm present a promising path towards logic-in-memory spintronics devices with minimal power consumption.

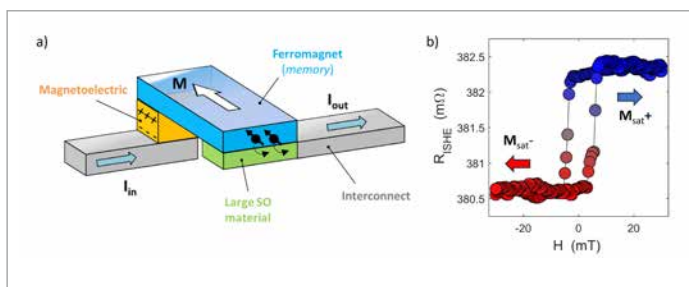


Fig.1 - a) A sketch of the magneto-electric spin-orbit (MESO) device. b) The spin Hall signal measured in NiFe/Pt heterostructures

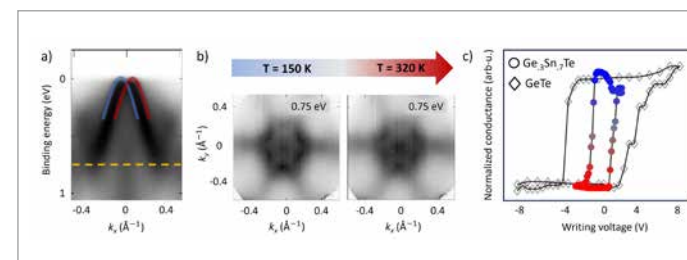


Fig.2 - a) Band dispersion and Rashba splitting detected in GeSnTe. b) Persistency of the Rashba features up to room temperature. c) Ferroelectric hysteresis loops of GeTe and GeSnTe acquired by electro-resistive measurements.

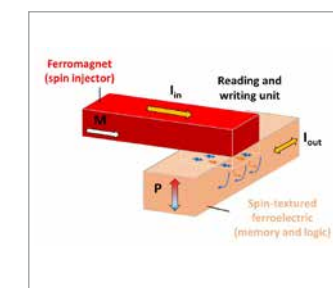


Fig.3 - A sketch of the full FESO device, only comprising a passive ferromagnetic spin injector and a specific spin-textured ferroelectric capable both of storing and processing information.



# ENGINEERING FOOD-GRADE MATERIALS FOR EDIBLE ELECTRONICS

**Fabrizio Mario Ferrarese** – Supervisor: Mario Caironi

One of the great problems of the 21<sup>st</sup> century is the disposal of electronic waste (e-waste) and plastics. For this reason, in recent decades a new ideal has been born in the research of organic electronics which aims at the manufacture of “green” electronic devices which can represent an alternative for the technological industry aimed at respecting the environment and human health. . In this context, edible electronics is a further, much more ambitious approach, which aims not only at reducing costs and preserving the environment, but also at the possibility of being able to ingest future devices safely, allowing the human body to digest and break down them once their function has been completed. The impact of this revolutionary idea goes far beyond the possibility of integrating wearable electronic devices into the human body and allows us to extend the possibilities of diagnostic medicine and the food industry. In order to carry out this ambitious project, it is necessary to exploit edible materials to be used as electronic constituents such as insulators, semiconductors and conductors. In fact, for example, albumin has been shown to be a good dielectric, some food dyes behave like semiconductors and metals such as gold are already

widely used in cooking. To create real functional electronics with these materials it is necessary to demonstrate the fabrication and functionality of basic building blocks such as circuits and power supplies. Furthermore, an important constrain for edible electronics is the operation at low voltages so that they can be ingested by the user in a totally safe manner. The selection of manufacturing materials is therefore fundamental because it dictates the operating characteristics and performance of the devices. This thesis work therefore focused on the investigation of different materials for the manufacturing of transistors, which represent the fundamental building block of any circuit, which can work at low voltages using edible materials and addressing all typical manufacturing and characterization phases. of common FETs (field effect transistors). In first place, the work explores the process of manufacturing an EGOFET, predominantly using edible materials with the semiconductor being the only component recognized as biocompatible in literature. Demonstrating field effect using chitosan as an electrolyte at low voltages (<1 V), along with operational

stability in air and the feasibility of fabrication through liquid phase deposition techniques like ink-jet printing. Optimizing the design to enhance performance with the coplanar gate over the top-gate structure was a significant aspect of this endeavour. The fundamental aspect of the work is the prospect of integrating transients into complex circuits. The design in this sense is fundamental, a coplanar structure greatly facilitates integration into a complex circuit compared to the top gate structure. Electrochemical analysis techniques were employed to investigate the interfaces between the electrolyte and semiconductor/metal under external potentials. The work also highlights the potential of using chitosan, an economical and edible substance, as a viscous dielectric with an electrolytic gate in organic field-effect transistors. Subsequently, the thesis work focuses on the investigation of electrolyte/ semiconductor interfaces using electrochemical techniques, in particular electrochemical impedance spectroscopy (EIS). This technique is critical for evaluating the capacitance of the double layer of a semiconductor that drives electrolytic devices. Copper phthalocyanine, an

edible dye commonly found in toothpaste, served as the standard semiconductor for these investigations. The chapter discusses the different structures and behaviours of the material based on the deposition techniques, which influence the characteristics of the devices. The EIS proves crucial in examining these differences. In fact, during the work, the structure of the semiconductor deposited by evaporation and acid solution deposition was investigated and the impedance measurements offer an extremely precise insight into the interface mechanics between semiconductor and electrolyte. Finally it is proposed a study where bacterial cellulose was obtained through a simple and cost-effective bio fabrication process, commonly used in producing the commercial

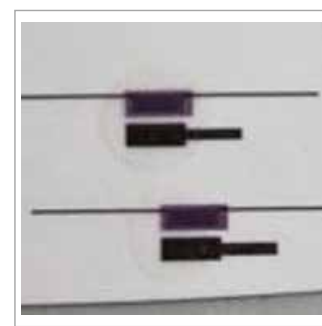


**Fig.1 -An example of the fully solution processed coplanar EGOFET**

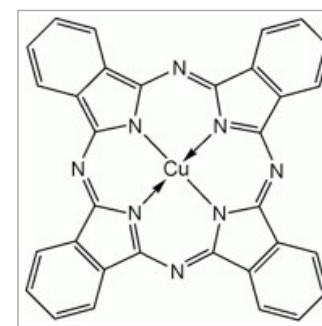


**Fig.2 -Copper-Phthalocyanine molecule. An edible semiconductor investigated in this thesis**



**Fig.3 -Pristine Bacterial Cellulose from Kombucha beverage fermentation**

beverage Kombucha, indicating its potential application in edible electronics. The chapter explores using this material as a scaffold for producing solid electrolytes, leveraging its absorbent properties to trap edible materials like glycerol and sodium sulphate within its fibrous matrix for EGOFET fabrication. Additionally, bacterial cellulose is examined as a substrate for inkjet-printed high-resolution Au patterns, facilitated by a planarization layer of ethyl cellulose. The fabrication of fully printed BC gated EGOFETs on the same BC substrate is achieved, characterized by stability in air and a one-month shelf life. During this work, the possibility of recycling and reusing Kombucha substrates for multiple productions was also explored. In fact, by using ethanol, a solvent orthogonal to bacterial cellulose, it is possible

to wash away the planar layer of ethyl cellulose by removing the devices manufactured on it without damaging the surface of the bacterial cellulose, thus being able to reuse it for further manufacturing. Finally, considering the many layers of materials involved in the manufacturing, bending tests were carried out to validate the actual structural stability of the transistors in each of its components.

# FROM SULFATE ADSORPTION TO THE COPPER DISSOLUTION REGIME BY COMBINING EC-STM AND EC-AFM

**Claudia Filoni** – Supervisor: Gianlorenzo Bussetti

The combination of Scanning Probe Microscopy (SPM) and Electrochemistry (EC) techniques allows to successfully explore the morphological changes of electrodes' surface during oxidation and reduction processes. This experimental approach is very fruitful to correlate morphological/ structural changes to specific EC potentials and *vice-versa*. In principle, corrosion and dissolution regimes (i.e., where the electrode's surface is significantly affected) can also be explored properly choosing the microscopic technique. When the experimental system offers the opportunity of changing the acquisition mode (e.g., from Scanning Tunneling (STM) to Atomic Force Microscopy (AFM)), then a wide interval of the EC potential can be explored. In this context, a Cu(111) single crystal electrode, immersed inside a diluted sulfuric acid solution, is revealed as model system. It is characterized by the adsorption of sulfate ions, for certain potential values, and the dissolution for other ones, as pointed out from the cyclic-voltammetry reported in Figure 1. At +0.2 V (vs. SHE), the anodic current extension (A) indicates the copper dissolution. In the reverse potential scan at +0.15 V,

the peak (B) corresponds to the copper re-deposition part; the peak C at -0.36 V indicates the sulfate desorption process. The hydrogen evolution (D-H) starts at about -0.3 V. The positive peak E corresponds to the sulfate adsorption regime.

Figure 2a shows the EC-STM image of the clean Cu(111) surface, as acquired at about -0.3 V. The height of the steps dividing two contiguous Cu(111) terraces is a multiple of 0.2 nm [i.e., the Cu(111) monoatomic step height]. Panel b indicates respectively the Moiré superstructure (larger unit cell) and the adsorbed sulfate pattern (smaller unit cell), as prescribed and reported in the literature, when the EC potential reaches +0.1 V. The Moiré pattern has cell parameters of  $(2.4 \pm 0.3)$  nm,  $(2.6 \pm 0.3)$  nm, whereas the corresponding parameters for the adsorbed sulfates are  $(0.44 \pm 0.03)$  nm,  $(0.52 \pm 0.03)$  nm. Conversely to the STM, the EC-AFM allows to study the entire dissolution process of the sample, up to the surface dissolution phase. As it can be seen in Figure 3, the flat Cu(111) terraces lose their clear contours as soon as the anodic dissolution potential is reached (white line in panel a). If the applied potential is reversed (white line in panel b),

in correspondence of point B of Fig. 1, the Cu(111) terraces come into sight again and the copper morphology is recovered, even if with a much greater roughness. In conclusion, generally EC-STM and EC-AFM require a different instrumentation layout and do not run on the same system. Despite that, it is possible to successfully couple the two scanning probe microscopies together with traditional electrochemical methods. When the faradaic currents are almost negligible, STM offers the possibility to reach the atomic resolution while, when a significant increase in the faradaic current (e.g., sample

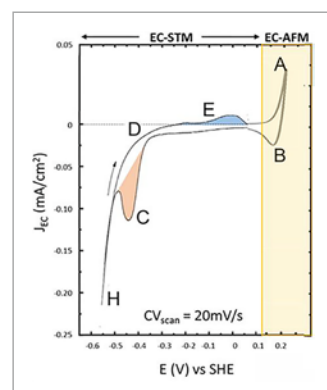


**Fig.1 - cyclic-voltammetry (CV) of Cu(111) immersed in diluted  $H_2SO_4$  electrolyte (pH = 2). In the graph, letters indicate respectively: A: anodic dissolution; B: copper re-deposition; C: sulfate desorption; D-H: hydrogen evolution; E: sulfate adsorption regime. The regions where EC-STM and EC-AFM are appropriately employed are also reported.**

dissolution) is measured and the STM acquisition becomes instable, AFM can overcome these difficulties allowing a correct analysis of the electrode surface. Consequently, the combination of STM and AFM provides a complete picture of the overall process, occurring at different EC potentials.

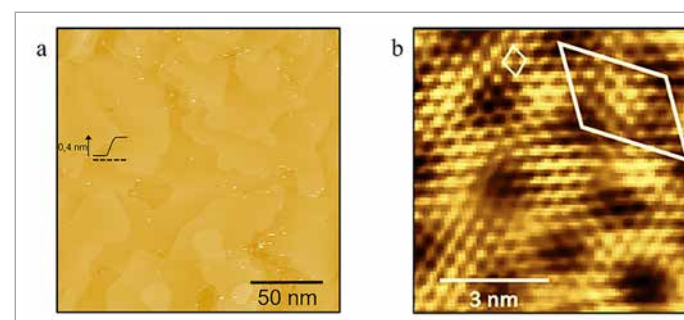


**Fig.2 - (a) EC-STM image of the clean Cu(111) surface ( $I_t = 1.53$  nA;  $V_{bias} = +1.1$  V); a biatomic step is pointed out in the picture. (b) Blow-up image of the Moiré superstructure (larger unit cell) and of the adsorbed sulfate ( $SO_4^{2-}$  anions) structure ( $(\sqrt{3} \times \sqrt{7})R30^\circ$ , smaller unit cell).**

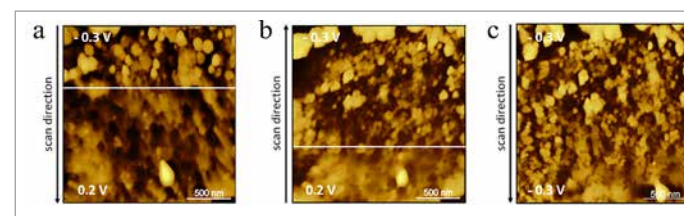


**Fig.3 -  $(2 \times 2)$   $\mu m^2$  EC-AFM images synchronized with the CV cycle in the anodic dissolution potential regime. (a) Dissolution process: the white solid line highlights when the EC potential reaches 0.2 V. After that, the scanning acquisition continues at +0.2 V. (b) Copper re-deposition process: the potential comes from +0.2 V to -0.3 V (see the reported scan directions). The white line highlights the re-deposition phase, corresponding to peak B of the graph in Fig. 1. (c) Potential is then kept fix at -0.3 V whereas flat lamellar copper terraces start to form again.**

# INVESTIGATION OF LIGHT MANAGEMENT MECHANISMS IN PHOTOSYNTHETIC ORGANISMS USING TIME-RESOLVED FLUORESCENCE

Ariel García Fleitas – Supervisor: Guglielmo Lanzani

Photosynthetic organisms exhibit remarkable adaptability to diverse light conditions, a key factor contributing to their survival and success. Their ability to finely adjust their photosynthetic machinery in response to varying light conditions not only enhances energy conversion but also serves as a protective measure against potential light-induced damage. The development of photoprotection mechanisms is a story of nature's ingenuity in coping with the challenges posed by dynamic light environments. Over centuries, these organisms have evolved a range of sophisticated strategies to shield themselves from the potential harm of excessive light. From the early adaptation of light-dependent reactions, such as energy spill-over between photosystems and dynamic phycobilisome mobility in red algae, to the utilization of non-photochemical quenching (NPQ) mechanisms that dissipate excess energy as heat, photoprotection has been a driving force behind the evolution of efficient and resilient photosynthesis. This thesis investigates how photosynthetic organisms can modulate the energy arriving at the reaction center using unconventional

strategies. We exploited time-resolved photoluminescence techniques for following energy transfer processes involved in light regulation inside the photosystems of a variety of photosynthetic organisms: red and green algae, diatoms, leaves and corals. In Chapter 1, we explore the main characteristics of the light matter interaction in photosynthetic organism, the main wavelengths absorbed, scrutinize the energy transfer processes directing light energy to the reaction center, and discuss the management of light through photoprotection mechanisms. Finally, the main techniques for measuring energy transfer and the data analysis are included. The methodology followed in this study is described in Chapter 2. It includes the description of the time-resolved photoluminescence and reflectivity setups. Furthermore, collection and handling of photosynthetic organisms are included in this chapter. How red algae can couple a photonic structure with the external photosynthetic antenna to regulate the amount of light that directly excites chlorophylls is aborded in Chapter 3. A mechanism is proposed for light management through the external antenna involving the decoupling

of the structure and the reduction of energy transfer. Chapter 4 talks about how proteins synthesized by an animal can influence the photosystem of the symbionts living inside. This is the case of corals in which we are going through the fluorescence proteins energy transfer and scattering. Methodology and instrumentation of using fluorescence lifetime as parameter for following non-photochemical processes in leaf are included in Chapter 5. Furthermore, measuring the fluorescence lifetime of photosynthetic organism through their movement is aborded. This last technique could be used in future for following non-photochemical processes of the organism during its displacement. Based on the comprehensive findings obtained from our study, we have gained invaluable insights into the intricacies of photosynthetic light management, photoprotection mechanisms, and the fine balance within photosynthesis. In Chapter 3, our investigation into the photoprotection mechanisms in *C. crispus* revealed the fascinating synergistic interaction at play. We observed that the photonic structure functions as an attenuator, particularly during the gametophyte stage, influencing the collection and distribution

of photon energy. This influence favors the pathway through the phycobilisomes, regulated by an intensity-dependent mechanism. This insight enhances our understanding of the photosynthetic light harvesting mechanism in *C. crispus*, shedding light on the nuanced interplay of light management and photoprotection in marine algae. In Chapter 4, we delved into the fascinating world of spectral properties and their impact on light management in corals. Specifically, we explored the interplay between CFP and GFP emissions and their interaction with chlorophyll absorption. The spectral characteristics of these fluorophores, along with their role in avoiding chlorophyll absorption, alter the light properties reaching the symbionts. Furthermore, the scattering effect plays a pivotal role in regulating the number of photons penetrating the tissue layers. The combined influence of energy transfer and scattering mechanisms was observed in Favia Green, exemplifying their role in controlling the energy reaching the zooxanthellae. Chapter 5 marked a significant advancement in our research, where we introduced a fluorescence lifetime snapshot technique for the measurement and analysis of

Non-Photochemical Quenching. The fine-tuning of parameters, such as laser spot diameter, number of replicates, and actinide light intensity, optimized our experimental system. This allowed us to effectively assess NPQ values in both wild-type and mutant *Arabidopsis thaliana* strains. We further extended our methodology to examine the fluorescence lifetime of *Chlamydomonas reinhardtii* during its dynamic motion. This pioneering step opens new avenues for implementing fluorescence lifetime snapshot measurements in photosynthetic organisms with motile characteristics. In conclusion, our research not only enhances our understanding of photoprotection and light management but also contributes to the broader field of photosynthesis and its intricate regulatory mechanisms. These findings have the potential to influence future research in photosynthetic organisms, offering new perspectives on energy transfer, scattering effects, and dynamic photoprotection mechanisms.

## A COMPREHENSIVE APPROACH TO DEVELOPMENT, CHARACTERISATION, AND IN-VIVO APPLICATION OF THE TIME DOMAIN NEAR INFRARED SPECTROSCOPY TECHNIQUE

Lorenzo Frabasile – Supervisor: Davide Contini

Time Domain Near Infrared Spectroscopy (TD-NIRS) has emerged as a powerful technique in biomedical research, providing valuable insights into the optical properties of tissues. The aim of my thesis work was to comprehensively explore different aspects and applications of the TD-NIRS technique. Considering the current status of TD-NIRS devices, I will discuss the device I worked on, which is identified by its compactness. In fact, TD-NIRS devices face challenges related to portability, fragility and high costs. The efforts have been directed towards overcoming these constraints, resulting in the development of the NIRSBBox system. By addressing these limitations, the NIRSBBox system enables *in-vivo* oximetry measurements on freely moving subjects. The system exhibits compact dimensions, a feature achieved through the customized design and production of various components, based on two compact pulsed diode lasers and homemade electronic circuits, custom cage attenuators, a silicon photomultipliers module and a time-correlated single photon counting system based on a time to digital converter. Over the device structure, I focused on probes designed for

*in-vivo* measurements, starting with the conventional probe used in hairless tissues, such as the forehead and muscle. It then progresses to the V-probe, distinguished by the presence of two teeth in proximity to the launch and detection points designed for veterinary application. This design enhances robustness, allowing penetration through the rigid hair of the animal, and includes a handle for ease of use by veterinary operators. Lastly, the P-probe is designed for generic application on hairy tissues for short-term measurements. We characterized both the instruments employed: the NIRSBBox and the Pionirs device, a commercial device analogous to the NIRSBBox. Applying the Medphot protocol, a comprehensive investigation was conducted to scrutinize the systems' performance. The primary focus encompassed the establishment of linearity, precision, accuracy, and reproducibility across a phantom matrix with varying absorption and scattering parameters. It was observed that the system can be considered linear up to phantoms with  $\mu'_s$  equal to  $15 \text{ cm}^{-1}$ . However, when examining individual wavelengths, the 830 nm laser

exhibited a higher linearity trend than the 670 nm laser. Nevertheless, it became evident that for the highest nominal scattering and absorption values, the error bars became non-negligible, compromising the linearity evaluation. One contributing factor to this degradation is related to the decrease in signal-to-noise-ratio. Regarding the reproducibility of solid identical phantoms, examinations were performed on phantoms obtained from both the same or different preparation batches, referred as intra-batch and inter-batch, respectively. The findings not only reaffirmed the reliability of the NIRSBBox system but also brought to the forefront the critical role played by a specific parameter, the time shift (t-shift) rescaling, between the Instrument Response Function (IRF) and the distribution time of flight (DTOF) during the fitting procedure. The t-shift, denoting the extra photon time of flight added during the acquisition of the IRF that depends on the probe type, experimental condition etc; It emerged as a pivotal factor requiring careful consideration. The analysis underscored the significant influence of this parameter in the intricate process of DTOF fitting, thereby directly impacting the accuracy

and precision of the optical parameters assessments. The thesis explores the practical applications of TD spectroscopy *in-vivo*, particularly focusing on animal applications, including highly perfused muscles in horses and oxygen saturation in dogs. The TD-NIRS technique offers potential for evaluating animal health using non-invasive technologies, enabling easier assessment of different circumstances and therapy effects. A cross-sectional feasibility study across dog and horse species examined the impact of fur on optical parameter evaluation, demonstrating reliable results with necessary precautions. Clinical applications extended to dogs undergoing hyperbaric chamber treatment, revealing breed-dependent variations in oxygen concentration in peripheral tissues before and after treatment. The study highlights an increase in oxygenated haemoglobin in peripheral muscles post-treatment, contrasting with effects observed in the head region, where I noticed an opposite behaviour. Moreover, this study could be useful to analyse the dynamic nature of tissue responses and the benefits conferred by the hyperbaric

chamber treatment. In the end I discussed about the research conducted during my internship at the Biomedical Optical Research Lab (BORL) in Zurich, with a primary focus on overcoming a fundamental limitation associated with TD-NIRS related to the complexity of the detection and acquisition parts that limits the efficiency in the photons detection. The developmental process starts with the laser with a low repetition frequency and high power pick as a foundational component, and subsequently, the entire optical and detection system underwent expansion. Key aspects addressed include the launch and collection optical system, the selection of detectors (with a fast APD for one pulse measurement), signal reading procedures, and the control of trigger signals. The culmination of these meticulous efforts yielded a prototype that demonstrated promising results in the development of the TD-NIRS technique applied on human tissue. The prototype underwent comprehensive characterization measurements on phantoms with varying scattering and absorption properties, revealing the system potentiality in the NIRS field. Notably, the achievable SNR with a reasonable measurement

time demonstrate the possibility to perform measurements, reaching 15.4 cm in transmittance geometry with a low absorption coefficient of  $0.04 \text{ cm}^{-1}$ . Conversely, in scenarios with a higher absorption coefficient ( $0.13 \text{ cm}^{-1}$ ), the penetration was reduced to 6 cm. However, the collection system still has a lot of space for improvement (increase of the detector collection area, optimization of the injected laser power, etc). Despite this, the groundwork laid by these results holds promise for future advancements in the field. To conclude, during my Ph.D. years I provide a comprehensive exploration of TD-NIRS, spanning characterization, *in-vivo* applications, and the development of a novel TD-NIRS devices. The characterization chapter establish the reliability of the NIRSBBox system, with a deep focus on parameters influencing accuracy and precision. *In-vivo* applications demonstrate the system's adaptability to different veterinary research paradigms. The development of a new TD-NIRS system presents promising results, heralding a new era in non-invasive tissue assessment.



# TAILORED NANOSCALE SPIN TEXTURES FOR SPINTRONICS AND THREE-DIMENSIONAL MAGNONICS

**Davide Girardi** – Supervisor: Edoardo Albisetti

Magnetic materials, such as ferromagnets or antiferromagnets, have significant fundamental and technological importance in the field of spintronics, which aims to use the spin of electrons for information encoding and processing. In this context, spin textures such as magnetic domains, domain walls and skyrmions have been extensively studied in the last decade due to their stability, nanoscale size and reconfigurability. In addition, spin waves, which are propagating perturbations in the orientation of the magnetization in magnetically ordered materials, have also been thoroughly investigated due to their peculiar properties such as nanometric wavelength and absence of Joule losses. Controlling the static and dynamic magnetic properties of materials at the nanoscale is then crucial for manipulating the configuration of magnetic moments for both conventional and unconventional computing and signal processing applications. This PhD activity has been developed in the framework of the European Union's Horizon 2020 research and innovation program for the B3YOND project, which aims to use the innovative phase-nanoengineering methodology to fine-tune the physical properties of materials at the nanoscale.

Specifically, the goal of this PhD research was to exploit the direct, tuneable control of the magnetic properties of thin films using highly localized heating via thermal scanning probe lithography (t-SPL) and direct laser writing (DLW). This allows the controlled stabilization of 2D domains of arbitrary shape and spin configuration, 1D domain walls, and 0D magnetic solitons, as well as the point-by-point spatial fine-tuning of the energetic landscape to control local hysteresis loops and stabilize multiple magnetic states at remanence. In terms of applications, the engineering of the magnetic properties of thin films can be used for the design of skyrmion-based spintronic devices for memory applications and for the manipulation of two- and three-dimensional spin-wave emitters in the field of

magnonics. The first part of this research activity was devoted to the magnetic nanopatterning by DLW of two sets of exchange-biased magnetic multilayers with out-of-plane magnetization. For both sets of samples, a ferromagnetic layer (CoFeB and NiFe/Co, respectively) is in contact with an antiferromagnetic IrMn layer, which allows to establish the exchange bias interaction. In addition, the multilayers were designed to exhibit strong perpendicular magnetic anisotropy and Dzyaloshinskii-Moriya interaction, both of which are fundamental for the stabilization of skyrmions. The main challenge of this step was to identify the best laser power intensities and laser pulse durations needed to finely manipulate the direction and intensity of the exchange bias. The corresponding parameters

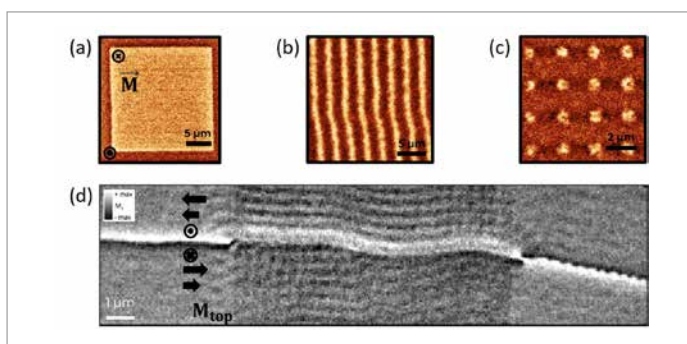


**Fig.1** -MFM characterization of magnetically nanopatterned 2D (a), 1D (b) and 0D (c) spin textures; d, STXM imaging of emission and propagation of spin waves in SAF

were also identified for the t-SPL technique. This optimized process was applied to the stabilization of 2D reconfigurable magnetic domains, 1D domain walls, and 0D skyrmion lattices. Such spin textures, which were characterized by magnetic force microscopy (Fig. 1a,b,c). These results demonstrate that the phase nanoengineering method is an important tool for controlling the magnetic properties of thin films and that can be used for the future development of skyrmion-based memory devices. After the optimization of the magnetic nanopatterning procedure, the research activity focused on the application of such methodology for the manipulation of spin-waves emission and propagation and their imaging in two- and three-dimensions, respectively. For the first set of experiments,

synthetic antiferromagnetic (SAF) multilayers consisting of CoFeB/Ru/CoFeB/IrMn were grown on top of SiN membranes via magnetron sputtering with different thicknesses for the ferromagnetic layer, ranging from 45 to 100 nm for each layer. Each sample was then magnetically characterized and nanopatterned, to stabilize the domain walls used for the spin wave emission. Spin-wave imaging was performed on these samples using 2D-STXM (Scanning Transmission X-Ray Microscopy) at the Swiss Light Source synchrotron facility at the Paul Scherrer Institute (PSI), and the results are shown in Figure 1d. The last part of this research activity focused on the demonstration of 3D imaging of spin waves. Indeed, in the field of magnonics, the exploitation of the third dimension has become one of the

most desired capabilities for the introduction of new functionalities. However, experimental visualization of propagating spin waves in 3D has been elusive due to the challenging requirement of combining nanoscale spatial resolution in 3D and time resolution in the GHz frequency range. NiFe 40 nm/Ru 0.9 nm/CoFeB 50 nm SAF microstructures were grown by magnetron sputtering on SiN membranes and studied using the newly developed synchrotron technique Time-Resolved Soft X-Ray Laminography at PSI. This allowed to reconstruct the full 3D precession of the magnetization associated with spin-wave propagation and to map the distribution of spin-wave modes throughout the volume of the structure. We observe complex depth-dependent spin-wave profiles resulting in 3D interference patterns that can be controlled by the composition and structure of the magnetic system. An example of the 3D reconstruction of the spin-wave dynamics is shown in Fig. 2. These results open up unprecedented possibilities for the study of complex spin-wave modes and for the design of novel functions in 3D magnonic devices.

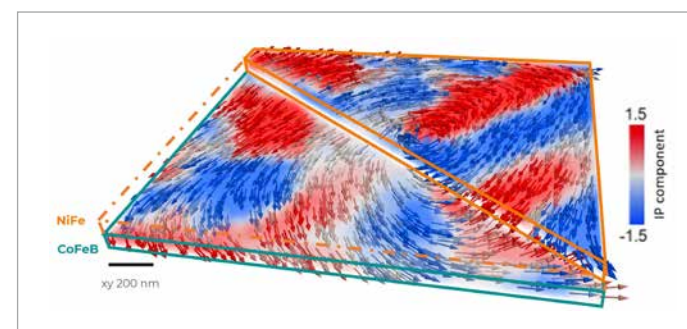


**Fig.2** - three-dimensional reconstruction of propagating spin waves in NiFe 40 nm/Ru 0.9 nm/CoFeB 50 nm SAF microstructure

# BISMUTH THIN FILMS ON VICINAL GE(111) SUBSTRATES: A SPIN-RESOLVED PHOTOEMISSION STUDY

**Francesco Goto** – Supervisor: Gianlorenzo Bussetti

Bismuth represents a well known case-of-study in the field of spintronics for its notable electronic properties such as significant spin-orbit coupling and low carrier density. Bismuth (Bi) crystals and thin films were widely investigated for their peculiar electronic properties attributed to non-trivial topological phases. In this study ultra-thin Bi films are deposited on vicinal germanium (Ge) substrates with the aim to provide a vicinal bismuth film, at the date missing, in the attempt to unveil the controversial Bismuth topology. The thesis has two main objectives: to provide a vicinal Bi sample for investigating Bi's topological properties, and to investigate for the first time the electronic structure above the Fermi level on Bi films. Challenges in surface preparation and the impact of substrate properties on film growth are addressed, with a focus on achieving highly oriented Bi(111) surfaces. Bi films, deposited in vacuum, are characterized by Low Energy Electron Diffraction (LEED) and Spin Polarized Angle Resolved PhotoEmission and Inverse PhotoEmission spectroscopy (SP-UPS, SP-IPES). In figure 1(a-c) the crystallographic structure of the vicinal Ge substrates, used as template for the deposition of Bi thin films, is shown. The atomically flat

Ge(111) surface has the hexagonal symmetry typical of the (111) plane. The Ge(223) substrate, with a miscut angle of  $11.4^\circ$  towards the [001] direction, exhibits a stepped surface expected to have a terrace width of  $\approx 1.6$  nm (5 atoms). The Ge(443) substrate, with a miscut angle of  $\approx 7.3^\circ$  towards the [110] direction, has a terrace width of  $\approx 2.5$  nm (7 atoms). The vicinal Ge substrates have opposite miscut angle with respect to the [111] direction, possibly affecting the growth and the electronic structure of the deposited Bi film. The results obtained by LEED exoeriments, at a beam energy of 70 eV, are presented in Figure 1(d-f).

The LEED analysis of a 10 nm

thick Bi film on Ge(111) reveals hexagonal symmetry, indicative of high-quality Bi(111) bilayers, and on Ge(223) shows a diffraction pattern with a hexagonal lattice showing single and double diffraction spots along [10], indicative of stepped Bi(111) films. The inclination angle of the (111) terraces on Ge(223) matches the substrate's inclination, with terrace width, estimated by LEED, of approximately 5 Bi atoms. On Ge(223), the Bi(111) film forms periodic, directional terraces similar to bulk-truncated Bi(9 9 11) crystals, with the substrate's inclination guiding the film's terrace formation. The LEED pattern for Bi on Ge(443) showcases hexagonal spots with

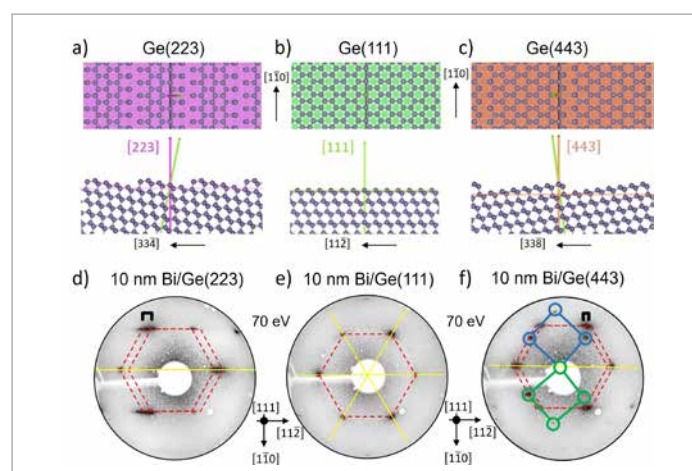


Fig.1 - a-c) schematics of Ge(223), Ge(111) and Ge(443) substrates. d-f) LEED results obtained on 10 nm Bi samples, beam energy 70 eV.

spot splitting due to stepped surfaces and a pseudo-square lattice indicating two domains separated by a mirror axis, suggesting a complex terrace structure influenced by the different Bi crystallographic phases. SP-UPS experiments have been performed at  $\pm 2^\circ$  emission angles, with respect to the [111] direction, to probe opposite momenta at the (111) surface and to confirm the quality of Bi films on Ge(111), aligning with previous findings on Bi(111). The spectra are characterized by sharp photoemission peaks close to the Fermi level and broader signals at higher energy. A reversal of the spin polarization for the spectra at opposite momentum is observed, despite stronger asymmetries already reported

in the literature. For Bi films on Ge(223), the SP-UPS results align with those on flat Bi(111) films, with a small shifts in energy of the electronic states possibly due to terrace size effects on the electronic structure. Bi films on Ge(443) show a similar SP-UPS spectra despite the presence of pseudo-cubic domains at the surface. However the SP-UPS data strongly suggest that the Bi(111) layer is rotated by  $180^\circ$  with respect to the Bi film on the Ge(111) and on the Ge(223) substrates. Electronic states are investigated also, for the first time, by spin and angle resolved Inverse photoemission spectroscopy, the results (not shown) obtained on the flat Bi(111) and vicinal Bi(9 9 11) films, above the Fermi level, are schematized in figure 3.

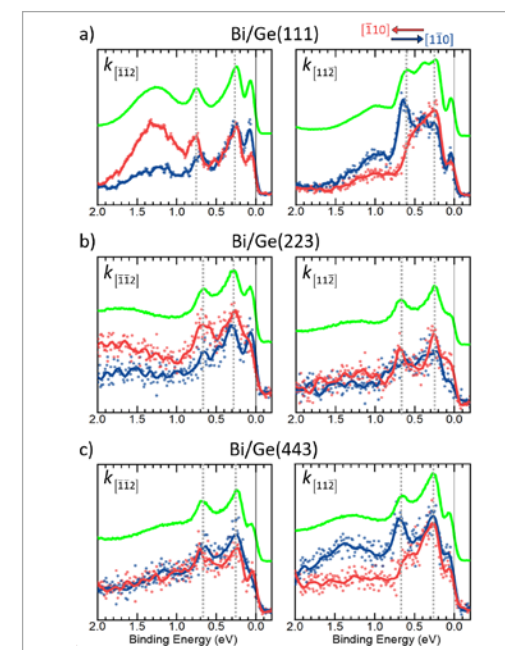


Fig.2 - SP-ARUPS results obtained for 10 nm Bi films deposited on Ge(223), Ge(111) and Ge(443), (a-c).

This research highlights the impact of the substrate's miscut angle on the film's properties and reports the first realization of a vicinal Bi(111) film is obtained, overcoming limitations encountered with Si substrates. Differences in Bi films growth on Ge(223) and Ge(443) are revealed, showing the influence of miscut orientation on atomic structure and spin properties. For the first time the spin-polarized electronic states have been investigated also above the Fermi level, possibly contributing to the problem of Bismuth topology and its potential in spintronics.

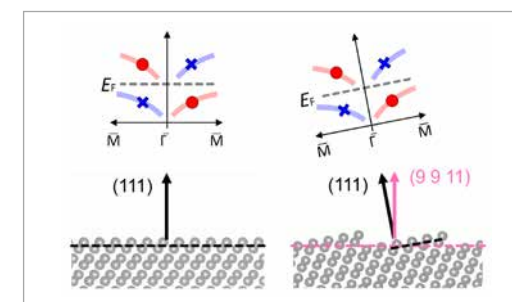


Fig.3 - Summary of the electronic states, close to the Fermi energy, for flat and vicinal Bi films.

# ULTRAFAST HOLOGRAPHIC WIDEFIELD MICROSCOPY

**Martin Hörmann** – Supervisor: Franco V. A. Camargo

Recent developments in the fields of ultrafast spectroscopy and optical microscopy extends the research possibilities in both areas and paves the way for a variety of new applications. Particularly, combining these two well-developed fields gives rise to the technique of transient absorption microscopy (TAM), enabling the spatio-temporal investigation of excited state dynamics in heterogeneous and complex analytes at femtosecond timescales with diffraction-limited spatial resolution. Until recently, confocal microscopy was the preferred choice in TAM due to its excellent signal-to-noise ratios, and hence ability to detect small signals. However, thanks to current developments in fast-acquisition cameras, widefield configurations can also be applied in TAM microscopes. Widefield configurations are attractive due to the experimental simplicity and their potential faster acquisition compared to confocal point scanning. Moreover, the combination of femtosecond pulses with techniques from widefield imaging holds promise to revolutionise prior TAM techniques. This thesis addresses key problems from the transition of confocal to widefield TAM and presents new techniques thereof

by integrating the phase-sensitive technique of off-axis holography. One part of the PhD consisted in using off-axis holography for an all-optical demodulation scheme for widefield TAM microscopes. As a result, shot-to-shot detection of the pump-induced signals is achieved, independent of the camera frame rate. This enables to acquire TA data with strongly reduced noise. We used this technique to study ultrafast transport phenomena of charge carriers in the perovskite MAPbBr<sub>3</sub>. For this purpose, we further implemented a scheme to perform 81 diffusion measurements simultaneously, by distributing diffraction-limited excitation spots over the

entire FOV. This reduces the data acquisition times proportionally to the number of excitation spots. We resolved a fast diffusion of hot-carriers in the first picosecond with a diffusion coefficient larger than 300 cm<sup>2</sup>/s, followed by slower diffusion of cold carriers with a diffusion coefficient of 0.20 cm<sup>2</sup>/s, which matches with previously reported values. Since resolving diffusion and transport phenomena of, e.g. charge carriers, excitons or heat, is one of the main applications of TAM, we believe that the approach developed during the PhD is a better statistical and quantitative method, thanks to its simultaneous evaluation of several spots across a

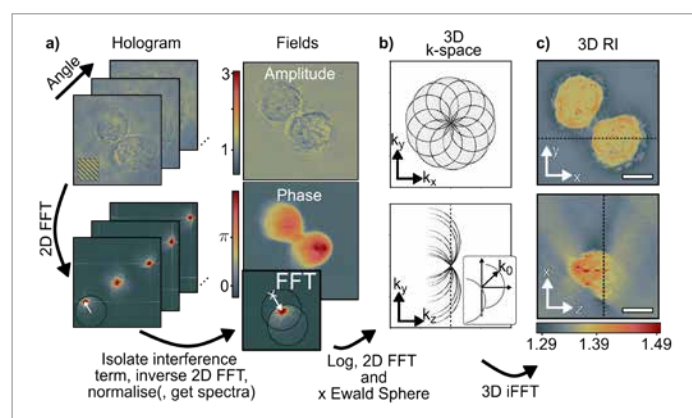


**Fig.1 - Sketch of the reconstruction of two HeLa cells. a) From the hologram the amplitude and phase information is retrieved. b) Around sixty images are placed into different positions in a three-dimensional box (Fourier space). c) An inverse Fourier transform retrieves a three-dimensional refractive index distribution.**

large sample area. Also, the holographic implementation measures the real and imaginary part of the refractive index/third order polarisation, which may be exploited in future applications. Further, during the PhD, a universal method to perform balanced detection in widefield TAM was developed. To this end, the idea of self-referencing was applied. Laser noise contaminating the TA signal was removed by making sure that parts of the field of view are from TA signal. A detailed experimental and theoretical description and validation of this approach was elaborated, and it was tested on various samples and configurations. The implementation is simple and applicable to almost any TA microscope working in a widefield configuration. Further, it can be extended to interferometric methods, e.g. the method was also used by us to remove noise in the transient phase of holographic measurements. To summarise, this technique brings the measurement performance close to the shot-noise limit while being independent of the camera frame rate. In other words, it removes the need to perform measurements at high demodulation frequencies to avoid excess laser noise (1/f noise) contaminating the signals. Due to its relative simplicity, we believe that this technique will boost widefield configurations in TAM, SRS and photothermal imaging in the future. We also established a microscope which measures the transient ultrafast polarisation changes.

It uses an existing off-axis holographic scheme to perform polarisation-resolved imaging with two cross-polarised reference waves and extends it to ultrafast imaging. The measurement of both polarisation components is performed with the same pulse, thereby canceling excess laser noise and enabling shot noise limited detection. In this way, small changes of the probe polarisation are measured. We used the microscope to perform ultrafast Faraday rotation microscopy in the mixed halide perovskite. We also showed methods to tailor the pump excitation to small excitation spots in order to observe spin diffusion phenomena. Furthermore, we established a model to represent the main features of the experiments. As a result, we could observe carrier density dependent diffusion phenomena within the first two picoseconds in this specific specimen. We believe that this technique will establish as a powerful tool to observe spin resolved (transport) processes on ultrafast time scales. It is worth noticing that thanks to the holographic scheme, it is intrinsically capable to simultaneously resolve circular dichroism and birefringence, which will be explored in more detail in the future. In addition, we worked on a possible method to perform three-dimensional imaging with ultrashort femtosecond pulses. To achieve this, we established a setup, consisting of an imaging system with pulse shaping, to perform the three-dimensional

imaging technique of optical diffraction tomography with pulses having bandwidths of more than one hundred nanometres in a way that would be compatible with compressed few-cycle pulses. Figure 1 shows the flow from the acquisition of holograms to the three-dimensional data. We compared the ground-truth spectra with the holographic retrieved fields and proofed the homogeneous interference of the entire spectrum from ca. 510 to 640 nm, which corresponds to a Fourier transform limited pulse duration shorter than five femtoseconds. As a further validation we acquired spectrally resolved three-dimensional images of HeLa cells. The work bridges the gap between the three-dimensional imaging with optical diffraction tomography and integration of ultrashort and ultrabroadband pulses. If implemented with ultrashort pulses, the presented technique could be useful to quantify and localise species inside biologic environments using transient signals a means of contrast, for instance



# ULTRAFAST OPTICAL SPECTROSCOPY OF INORGANIC SEMICONDUCTORS

Hemen Hosseini – Supervisor: Giulio Cerullo

## Abstract:

Throughout my Ph.D. research, I explored various aspects of ultrafast optical spectroscopy in the domain of inorganic semiconductors, with a primary focus on a significant project. The investigation into white light emission perovskites, specifically  $\text{Cs}_2(\text{Ag}_{0.6}\text{Na}_{0.4})\text{InCl}_6$  doped with bismuth, unveiled a high quantum yield and broad visible emission arising from self-trapped excitons. Utilizing ultrafast transient absorption techniques, I revealed an ultrafast thermalization process occurring within 50 fs, followed by the formation of self-trapped excitons in 250 fs. Additionally, I successfully extracted impulsively excited phonon modes.

## Time-domain observation of ultrafast self-trapped exciton formation in lead-free double halide perovskites

Metal halide perovskites, central to solution-processed optoelectronics research, exhibit remarkable properties such as high charge carrier mobilities, extended diffusion lengths, and defect tolerance. This positions perovskite optoelectronic devices as competitive alternatives to silicon-based counterparts, showing significant potential across various

market applications. Notably, three-dimensional lead halide perovskites in this category offer a narrower emission spectrum, enabling a more extensive color gamut compared to traditional III-V group LEDs.

Advancements in perovskite materials, encompassing low-dimensional perovskites, double perovskites, and perovskite-derived materials, unveil efficient broadband luminescence. This phenomenon results from strong electron-phonon coupling, triggering ultrafast lattice distortions in response to photo-generated electrons and holes. These distortions lead to the formation of self-trapped excitons (STEs) characterized by broad bandwidth, microsecond photoluminescence lifetime, large Stokes shift, and high exciton binding energies surpassing 1 eV. The remarkable high quenching temperature for STEs enables perovskite materials to maintain luminescence efficiency at room temperature, rendering STE emitters well-suited for white-light illumination applications. In the specific case of the double perovskite  $\text{Cs}_2\text{AgInCl}_6$  and its doped counterpart, theoretical calculations propose that exciton self-trapping is linked to Jahn-Teller distortions of the  $[\text{AgCl}_6]$

octahedra upon photoexcitation. This distortion operates on a timescale of a couple of hundred femtoseconds, necessitating ultra-short pump and probe laser pulses for precise investigation. The employment of ultrafast transient absorption (TA) spectroscopy with sub-20-fs time resolution in the UV range reveals the STE formation process in  $\text{Cs}_2\text{AgInCl}_6$  and the Na-alloyed version  $\text{Cs}_2\text{Ag}_{0.6}\text{Na}_{0.4}\text{InCl}_6$ . The observed carrier cooling process with a time constant of 53 fs is followed by the STE formation process with a time constant of 252 fs, aligning well with theoretical predictions. Fourier transforming the TA signal identifies the  $140\text{ cm}^{-1}$  phonon

mode as the Jahn-Teller mode, consistent with theoretical expectations. Figure 1 presents femtosecond transient absorption (TA) measurements for  $\text{Cs}_2\text{AgInCl}_6$ . Panel (a) displays the TA map, while panels (b) and (c) showcase the dynamics at specific probe energies and spectra cuts at various time delays, respectively. The observations reveal the development of a broad photo-induced absorption (PA) band across the visible region. Notably, at the band's center (around 2.3 eV), a dip in the signal is identified, attributed to the simultaneous emergence of the stimulated emission (SE) signal superimposed with the PA.

We detected a modulation in the transient absorption (TA) map, attributed to vibrational coherence impulsively induced by the 20 fs pump pulse. To isolate the oscillatory behavior, we subtracted the fitted exponential decays, obtained from Global Analyses after chirp correction, from the TA map. Subsequently, Fourier Transform (FT) analysis, performed without filters to preserve accuracy, identified four frequency modes:  $127\text{ cm}^{-1}$ ,  $152\text{ cm}^{-1}$ ,  $240\text{ cm}^{-1}$ , and  $307\text{ cm}^{-1}$ . In parallel Raman measurements, three frequency

modes were identified:  $140\text{ cm}^{-1}$ ,  $165\text{ cm}^{-1}$ , and  $297\text{ cm}^{-1}$ . Comparing the FT results with Raman measurements revealed red shifts in the frequencies of  $127\text{ cm}^{-1}$  and  $152\text{ cm}^{-1}$ , and a blue shift in the  $307\text{ cm}^{-1}$  mode. Notably, the Raman spectrum did not exhibit the  $240\text{ cm}^{-1}$  mode..

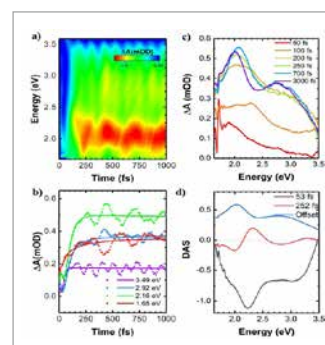


**Fig.1 - (a) Transient absorption map of  $\text{Cs}_2\text{AgInCl}_6$  following broadband excitation around 284nm. (b) Representative kinetics at selected probe photon energies. (c) Sequence of transient spectra for different pump-probe delay times. (d) Decay associated spectra obtained from the data global analysis.**



# HIGH-BRILLIANCE ATTOSECOND SOURCE FOR X-RAY SPECTROSCOPY

**Bogdan-Constantin Ispas** – Supervisor: Caterina Vozzi

Femtosecond ( $10^{-15}$  s) laser pulses have been used in recent years for research, as well as industrial and medical/biological applications, exploiting their unprecedented temporal resolution and high peak intensity. However, technology is continuously evolving, and femtosecond resolution no longer suffices. Electronics are getting smaller and faster, breaching the barrier between the classical and quantum realms. Biology and chemistry have also reached a saturation in the knowledge on this timescale. Many fields are now in need of tools to unlock the study of even faster dynamics. Whilst femtosecond pulses can be generated by simply putting the right gain medium between two mirrors (albeit not very powerful), going faster is going to require clever manipulation of these pulses to drive the generation of Extreme Ultraviolet (XUV) laser pulses to reach timescales three orders of magnitude shorter: attoseconds ( $10^{-18}$  s). Thanks to the high intensity of focused femtosecond infrared (IR) pulses, the High-order Harmonics Generation (HHG) process can be triggered in gases to give rise to XUV attosecond pulses. But because, unlike other common nonlinear optical effects that depend on the intensity profile of the electric field, HHG depends

on the driving electric field itself, so to ensure the reproducibility of attosecond pulses, the carrier-envelope phase (CEP) of the IR pulses must be stable. The goal of this thesis is to realise a table-top source of high-brilliance isolated XUV attosecond pulses through a series of innovative techniques: 1. Generation of passively-stable CEP mid-IR ultrashort pulses; 2. Efficient generation of intense trains of XUV attosecond pulses in microfluidic devices, driven by the previously mentioned source; 3. Isolation of a single XUV attosecond pulse for time-resolved spectroscopy of matter. As illustrated in Figure 1, an initially 25-fs laser pulse, centred around 800 nm (red line), is

split in three branches: the first replica is further compressed to ~5 fs (yellow line) by exploiting the self-phase modulation (SPM) nonlinear effect induced by propagation inside a gas-filled hollow-core fibre (HCF), followed by a complementary pair of chirped mirrors (CM). This ultra-broadband light pulse drives an intrapulse difference-frequency generation (DFG) process inside a nonlinear crystal, generating a seed pulse, centred around  $1.5 \mu\text{m}$  (dark red line) with a stable CEP thanks to the peculiar properties of the DFG effect. This signal is then amplified up to hundreds of microjoules in a cascade of two optical parametric amplifiers (OPA), pumped by the other two

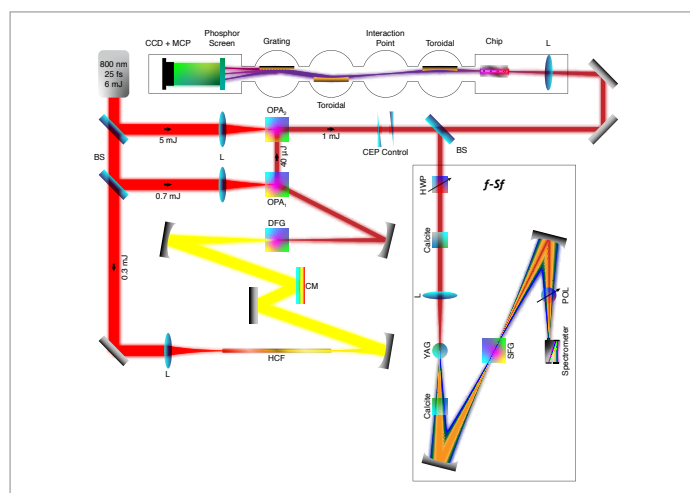


Fig.1 - Setup layout.

replicas of the pulse that was split at the beginning. The concept of CEP refers to the relative position between the peak of the electric field oscillation and the peak of its envelope. As stated above, the generation mechanism of high-order harmonics is sensitive to the electric field so the CEP will play a crucial role in guaranteeing that the attosecond pulse trains are reproducible. Unfortunately, because of this field-dependence, XUV pulses will be generated every half-cycle of the impinging mid-IR optical field, resulting in a fringed spectrum due to the interference, however the work presented in this thesis aims to isolate one of these highly-energetic attosecond pulses. The price to pay for such a source is indeed the increased sensitivity to disturbances and fluctuations in the driving laser source. As mentioned before, DFG takes care of stabilising the CEP, fixing the position of the carrier under the envelope, however air fluctuations, temperature fluctuations, laser beam drifts, they will all slowly shift the phase during operation. Thankfully, the long-term stability can also be dealt with by feeding, in real-time, this drift to a feedback loop,

comprised of a pair of wedges and a white-light interferometer that keeps track of the changes in the phase. Typically, this interferometry method is based on two major nonlinear optical effects: 1. Whitelight generation (a broadening of the spectrum of the driving field through SPM); 2. Second- Harmonic Generation (SHG) of the fundamental pulse. The requirement is that the induced SPM spectrum has to cover at least one octave so that the white-light tail with frequency  $f$  overlaps with the second harmonic with twice the frequency. This is called the  $f$ -to- $2f$  interferometer, and, sadly, its design flaw is that it tracks not only the CEP variations, but also the fluctuations due to the white-light generation (WLG) process. One way around it is to, instead, split the pulse in two polarisation states and taking the sum-frequency between the fundamental and some colour of the broadened spectrum. This way, the  $f$ -to- $Sf$  shows only the fluctuations of the CEP. In the figure above, a preliminary measurement taken with the  $f$ -to- $2f$  interferometer and without the active feedback loop is presented to showcase the

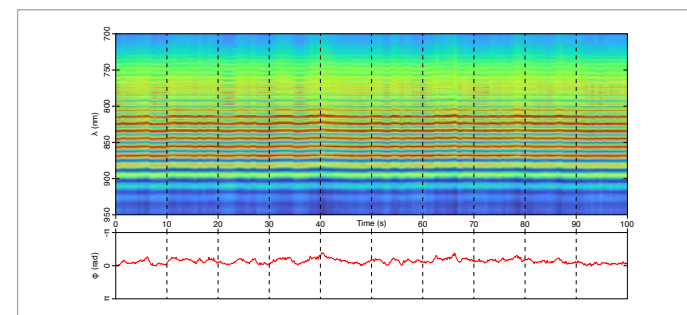


Fig.2 - Interferogram

performance of the source. The standard deviation extracted from the movement of the fringes is ~200 mrad, a good starting value which will be further improved upon after setting up the feedback loop and switching to the  $f$ -to- $Sf$  interferometer. Moving on, this CEP-stable 1.5-micron pulse is focused inside a microfluidic chip, another novelty of the experiment. The chip is produced in-house, as a collaborative work with the National Research Council. As opposed to HHG in gas jets, this microfluidic device has a waveguide with four gas-delivery nozzles, increasing the generation length and the number of jets. What's interesting is that the increase in gas jets provides the capability to deliver the gas as pressure gradient, ensuring that the phase-matching conditions are fulfilled throughout the entire propagation length, yielding a much better conversion efficiency. Up to here, a reproducible attosecond pulse train is achieved. The isolation involves some more optical elements in the path of the  $1.5 \mu\text{m}$  pulse, but that is not a big deal, since this wavelength choice is nothing but opportunistic – it lies in the 'zero-dispersion' region of most transparent media, leaving the pulse duration virtually unaffected. A quarter-wave plate will shape the optical field in such a way that the tails will become circularly polarised, while the peak remains linear, which is going to be the only part of the field capable of driving the HHG process.

# PRINTED ORGANIC MICRO-THERMOELECTRIC GENERATORS

**Nathan James Pataki** – Supervisor: Mario Cairon

Organic thermoelectric generators (TEGs) are a prospective class of versatile energy-harvesters that can enable the capture of low-grade heat and provide power to the growing number of microelectronic devices and sensors in the Internet of Things (IoT). The abundance, low-toxicity and tunability of organic conducting materials along with the scalability of the fabrication techniques, promise to culminate in a safe, low-cost and adaptable device template for a wide range of applications. Despite recent breakthroughs, it is generally recognized that significant advances in organic thermoelectric materials must be made before organic TEGs can make a real impact. In addition to the need for higher-performing organic thermoelectric materials, progress in the field of organic thermoelectric towards devices that could make a substantial impact in the energy landscape will require increased focus on practical application-focused design of organic TEGs, which are scarcely addressed in the field today. The goal of this thesis was to substantially increase the power density of scalable, solution-processed organic TEGs beyond  $1 \mu\text{W cm}^{-2}$ , thus representing meaningful

progress towards supplying renewable energy to future IoT applications. The work was carried out under the framework of the European Commission-funded Marie Skłodowska-Curie Innovative Training Network (ITN), HORATES. All members of the HORATES project focused on different aspects of advancing organic thermoelectrics research, therefore this thesis is a result of collaboration among many different universities, research institutes and companies within the project. The large majority of this work focused on the design and fabrication of efficient and practical organic TEGs within Dr. Mario Caironi's Printed and Molecular Electronics group at Istituto Italiano di Tecnologia's

Center for Nano Science and Technology. In current organic thermoelectrics research the challenges of designing and fabricating organic TEGs suitable for real scenarios are scarcely addressed. Small sensors and wearables, two of the high-value applications proposed for organic TEGs, demand micro-thermoelectric generators ( $\mu\text{TEGs}$ ) with high power density architectures and small form factors, while typical demonstrations of organic TEGs are characterized by  $< 10$  thermocouples (TCs) per  $\text{cm}^2$ . This thesis presents a versatile  $\mu\text{TEG}$  architecture that exploits in-plane, large-area solution-based fabrication techniques on micron-thin substrates and a rolling process to produce a

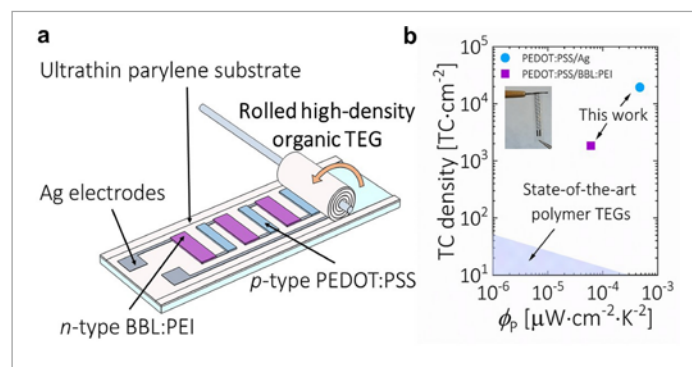


**Fig.1 - (a)** Depiction of the high-density  $\mu\text{TEG}$  architecture after planar fabrication in which the alternating p-type (blue) legs, n-type (purple) legs, and metallic connections/electrodes (grey) are shown. **(b)** TEG power factor,  $\phi_P$ , and thermocouple density of the  $\mu\text{TEGs}$  presented in this work compared to the state-of-the-art organic polymer-based TEGs.

device with a high-density of thermocouples. The proposed architecture was validated using PEDOT:PSS (p-type) and BBL:PEI (n-type) as the active thermoelectric materials, exploiting complementary deposition techniques, inkjet printing, and spray-coating. The PEDOT:PSS/BBL:PEI  $\mu\text{TEG}$  represents the largest thermocouple density for any fully-organic TEG previously reported in literature, at 1842 TCs- $\text{cm}^{-2}$ , while exhibiting a  $P_{\text{density}} = 0.15 \mu\text{W cm}^{-2}$  at  $\Delta T = 50 \text{ K}$ . In addition, this thesis presents an architecture that enables the use of high-performing aligned polymer films. Studies have consistently reported that macromolecular engineering and secondary crystallization control of polymer thin films can induce high degrees of anisotropy in the morphology of polymer films which can then be exploited to improve the thermoelectric performance of such materials by orders of magnitude. That being said, there currently exist no

instances of polymer-based TEGs specifically designed to utilize the superior performance benefits of highly aligned polymeric films. This section of the thesis capitalizes on the exceptional performance of aligned thin films documented in previous studies, incorporating them into a fully operational TEG for the first time. Thin films of regioregular poly(3-hexylthiophene) (P3HT) and poly(2,5-bis(3-alkylthiophen-2-yl)thieno[3,2-b]thiophene) (PBTtT) were aligned via the well-studied high-temperature rubbing technique to induce high-degrees of anisotropy in the charge transport properties of the films. An optimized multi-stage fabrication technique was developed to integrate monolithic aligned films into a TEG architecture (Figure 2a), which was finalized through the application of local inkjet doping. The P3HT and PBTtT aligned TEGs exhibited exceptional power densities of  $0.8 \mu\text{W cm}^{-2}$  and  $2.7 \mu\text{W cm}^{-2}$  (Figure 2b), respectively. Although not the primary focus of this thesis, work on the

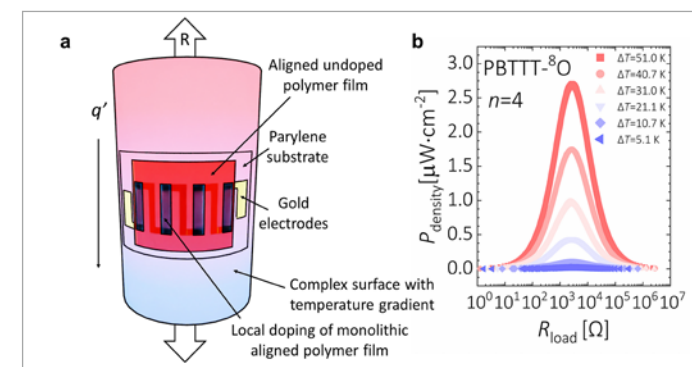


**Fig.2 - (a)** Depiction of the conformable aligned TEG on a hypothetical surface with an existing temperature gradient. The white arrow shows the rubbing direction during the alignment process, such that it is parallel to the direction of the heat flux. **(b)**  $P_{\text{density}}$  with respect to  $R_{\text{load}}$  for the aligned PBTtT-O ( $n=4$ ) TEG.

development of high-performing organic thermoelectric materials through doping and processing studies was conducted and is presented here. Doping studies were conducted on novel n-type polymers consisting of BDF (benzodifuranone), isatin, and thiophene-based units, with single-oxygen-containing branched side chains designed to solubilize the polymer. The solubility, optoelectronic and thermoelectric properties of the BDF-thiophene copolymers were characterized, finding that the electrical conductivity of chemically doped polymers is found to scale with molar mass, reaching  $\sim 1 \text{ S cm}^{-1}$ , a respectable value for n-type organic thermoelectrics.

In conclusion, this thesis presents work on the design and fabrication of organic TEGs with a specific focus on practical design, scalable fabrication, and efficient active materials. In the context of the goals outlined at the beginning of the project, this work represents a significant step forward in the design and performance optimization of application-focused organic  $\mu\text{TEGs}$ .

*This project has received funding from the European Union's Horizon 2020 research and innovation program under the Marie Skłodowska-Curie grant agreement No 955837 – HORATES.*

# HYBRID LINEAR/NONLINEAR INTEGRATED QUANTUM PHOTONIC DEVICES

Hugo Jorge da Nóbrega Abreu Ferreira – Supervisor: Roberto Osellame

## 1. Demonstration of an integrate 3-photon Greenberger-Horne-Zeillinger state factory

After the recent first demonstration of quantum advantage, there has been an increasing need for a scalable paradigm and platform for quantum computation. While optical computing (with associated low decoherence and established encoding and manipulation strategies) is a convincing platform, it is notoriously difficult to conciliate with the circuital paradigm, which requires two-photon interactions to form gates. Measurement-based quantum computation offers a solution, by shifting the non-linearity from the gates to the measurement itself. While the teleportation-based version requires stringent phase control, the one-way proposal takes a further step, delegating the entanglement from teleportation-based measurements to the computational substrate, designated the cluster state, which is then subject to simpler one-qubit measurements. There are several proposals to build this state from simpler states, tracing back to the minimum entanglement building block, the 3-partite Greenberger-Horne-Zeillinger states, a coherent superposition of three “1” qubits

with three “0” qubits.

This work demonstrated an integrated photonics approach for the generation of these states. The qubits were encoded on a pair of waveguides, following the dual-rail encoding. The photonic circuit was fabricated by femtosecond laser writing on a borosilicate glass substrate, and consists of 12 waveguides, where half of the outputs implemented the three logical qubits, and the other half represent heralding channels. The circuit will be fed with six single photons from a quantum dot source which are subject to linear optics components to probabilistically generate the desired states. The existence of three ancillary photons circumvents the necessity of actually measuring the the generated state to validate its entanglement, which results in its destruction. The low footprint device layout (15x33 mm<sup>2</sup>)

demonstrates the scalability of the state factory, while the active components (thermo-optical phase shifters) enable fast actuation to generate a specific Greenberger-Horne-Zeillinger state, based on the information contained in the ancillae detection pattern.

## 2. Demonstration of an high heralded photon purity photon source

Single photon play a crucial role in quantum information, and are nowadays primarily generated through either quantum dots or spontaneous parametric down conversion. Quantum dots offer unparalleled brightness but suffer from lower purity and photon-pair source efficiency. On the other hand, spontaneous parametric down conversion (on which this work was based), while providing high purity states, is probabilistic, so that one has to rely on one

photon of the generated photon pair to herald for the presence of the other.

For applications in quantum processors, it is crucial that the detection of heralds does not project the heralded photons onto distinguishable states. This condition is satisfied when dealing with completely uncorrelated signal and idler pairs, resulting in a separable Joint Spectral Amplitude (a sort of probability density function in the spectral domain). In cases where this perfect correlation does not exist, a Schmidt-mode decomposition (analog to an eigenvalue decomposition) can still be performed, and the level of correlation between the pair of photons assessed by calculating the heralded photon state’s purity (varies between 0 and 1), which should be as close to one as possible.

A simulation software was developed to systematically approach for global purity maximization under specified process constraints such as material properties, pump characteristics, and generation wavelength. The software was optimized in terms of discretization and numerical

algorithms to ensure the affordability of numerous successive queries for purity calculations. Different materials and wavelengths of generation were simulated, resulting in the identification of an experimental configuration producing highly pure and non-degenerate bi-photon states.

The configuration was experimentally tested using an ion exchange waveguide in periodically poled potassium titanyl phosphate, pumped by femtosecond pulses in the visible range. Crystal temperature and pump wavelength tunability provides a margin of tolerance against waveguide fabrication deviations, and the non-degenerate spontaneous parametric down conversion facilitated spatial separation of generated photons for routing to heralding or quantum processor channels. Purity values higher than 0.92 were obtained. Verification of similar central signal and idler wavelengths across various waveguides was achieved through stimulated emission tomography and spontaneous parametric down conversion spectra measurements. To

precisely quantify this wavelength similarity, additional Hong-Ou-Mandel experiments involving signals (or idlers) sourced from different origins must be carried out in the future. Assuming these signals are indistinguishable, the experiment’s visibility should provide insights into the purity of the single-photon states. Additionally, the presence of single photons was confirmed by measuring the second order correlation function, achieving generation at 40.7 MHz/mW of coupled pump power. Considering the low reproducibility of ion exchange waveguides, a potential hindrance to scalability, we pursued also waveguide inscribing in potassium titanyl phosphate with the technique of femtosecond laser writing. This technique, known for its reliability in inscribing photonic circuits on transparent media, aims to overcome integration limitations of spontaneous parametric down conversion for future applications. In perspective, it is intended to achieve multiple waveguides generating identical photons.

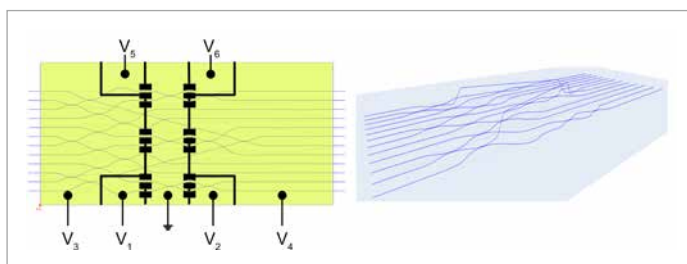


Fig.1 - On the left, two dimensional top view of the fabricated circuit, with the waveguides in blue, the isolation trenches in black and the resistances surrounded by the common ground and the several voltage inputs. On the right, three dimensional view of the same circuit.

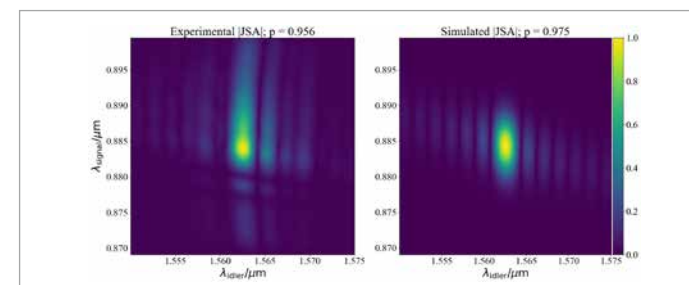


Fig.2 - Plots of the absolute value of the joint spectral amplitude reconstructed from the stimulated emission tomography measurement, and simulated, for one waveguide.

# ULTRAFAST TRION FORMATION DYNAMICS IN ELECTRICALLY TUNABLE MONOLAYER WS2 AND WSe2 BASED TRANSISTORS

**Irantzu Landa García** – Supervisor: Christoph Gadermaier

Atomically thin transition metal dichalcogenides (2D-TMDCs) have garnered increasing interest on the last decades due to their remarkable novel properties, which render them promising candidates for optoelectronic and photonic applications. Among others, the strong quantum confinement and reduced dielectric screening coming from their 2d nature lead to significant exciton and trion binding energies, which dominate their optical response. Thus, investigating exciton and trion dynamics post-optical excitation provides insights into fundamental interactions within these materials, crucial for the fundamental understanding, evaluation and improvement of their use in device applications. In particular, trions offer an avenue to explore the charge carrier-excitonic complex interplay, enabling a deeper understanding of many-body physics within the materials.

In this work, we performed pump-probe experiments at low temperatures of 9K on monolayer WS2 and WSe2 based-transistors. Our aim was to investigate the doping-dependent trion formation following optical excitation by tuning the doping level via the electrical gate voltage ( $V_g$ ). Notably, in both

the cases the monolayers were encapsulated with hBN, which significantly improved the quality of the acquired spectra. We observe two different scenarios, as illustrated in two of the pump probe measurements obtained for the WSe2 based transistor shown in Figure 1. At  $V_g = -1V$  (Figure 1a), transient measurements show a photoinduced absorption (PA) of the trion, emerging rapidly within our time resolution of  $\sim 150fs$ . Conversely, at  $V_g = +2V$  (Figure 1b), we detected a photobleaching (PB) signal, which also forms quasi-instantaneously. In the former scenario, in which there is a lack of free charges in the material, the PA signal indicates that trions are formed as a consequence of previous pump excitation, being absent in the material's equilibrium response.

We attribute this to pump-excited excitons dissociating into free charges and subsequently interacting with other excitons to generate trions. In contrast, in the doped case ( $V_g = +2V$ ), given the availability of free electrons, trions are present in the material's equilibrium response, leading to a PB signal. Furthermore, investigating intermediate doping levels (see fig. 2), we observe a gradual transition between the two aforementioned scenarios. Through simulations, we confirm that this effect arises as a result of the simultaneous presence of the PA and the PB signals at these intermediate doping levels. The relative ratios of these different signals vary depending on the specific doping level, contributing to the observed dynamics. The measurements conducted

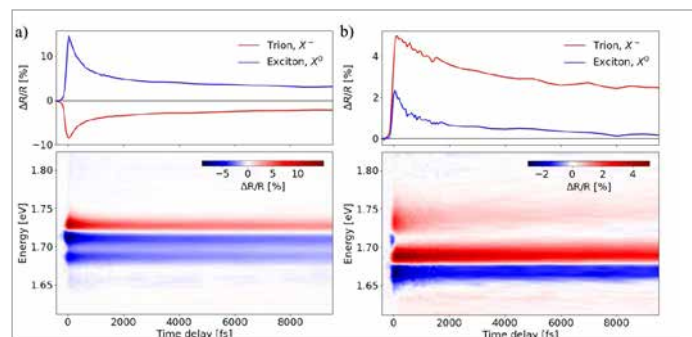


**Fig.1** - Pump-probe maps together with the temporal traces of trion and exciton features, obtained for the WSe<sub>2</sub>-based transistor. Panel a) and b) show the results obtained at  $V_g = -1V$  and  $V_g = +2V$ , respectively.

on the WS2-based transistor (fig. 3) exhibit a similar doping-dependent trion formation trend. In this case, specifically focusing on the doped regime, our observations reveal a clear change in the positive signal of the trion. Characterized by a slow buildup of the order of few picoseconds at lower applied voltages, this signal transforms into an ultrafast buildup of  $<150fs$ . However, as mentioned earlier, this apparent change is the result of the superposition of two distinct signals, a PA signal arising from pump-induced trions, and a PB signal of trions formed upon the free charges available within the material. This phenomenon has been previously interpreted as a pure PB signal indicative of slow trion formation, but here we show that both PA and PB processes, signature of the true nature of the trion formation, occur on an ultrafast timescale.

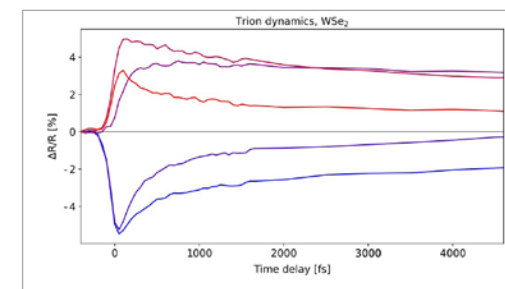


**Fig.2** - Trion dynamics on the WSe<sub>2</sub>-based transistor under various applied gate voltages.

In summary, we unveil, for the first time, the pure trion formation dynamics of WS2 and WSe2, occurring on an ultrafast timescale of  $<150fs$ . Our findings shed light on the inconsistency observed in previously reported trion formation times, which ranged from slow timescales of few ps to fast timescales of hundreds of fs in different cases. This finding may significantly impact our understanding of trion formation in 2D-TMDCs and pave the way for the development of more efficient optoelectronic and photonic devices.

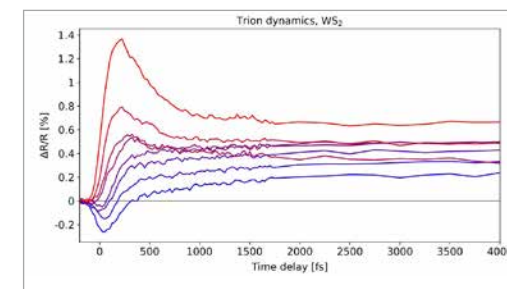


**Fig.3** - Trion dynamics on the WS<sub>2</sub>-based transistor, obtained for different applied gate voltages.



# DEVELOPMENT AND TEST OF TIME-RESOLVED REFLECTANCE SPECTROSCOPY TECHNOLOGY FOR NON-DESTRUCTIVE OPTICAL CHARACTERIZATION OF FRUITS AND VEGETABLES

Pietro Levoni – Supervisors: Lorenzo Spinelli

## 1 Introduction

The near infrared spectroscopy (NIRS) technique provides non-destructive optical characterization of highly scattering media. NIRS measures absorption ( $\mu_a$ ) and reduced scattering ( $\mu_s'$ ) coefficients of the sample within the 600–1000 nm range. When probing fruits and vegetables,  $\mu_a$  evaluates the concentration of the main constituents (e.g., chlorophyll, water, carotenoids), while  $\mu_s'$  assesses the equivalent size and density of the scatterers: depending on the specific sample, both parameters can be linked to various features (e.g., maturity degree, firmness). Continuous-wave NIRS systems are commercialized worldwide, but they present some drawbacks, which are overcome by time-resolved reflectance spectroscopy (TRS, also named time-domain NIRS) devices: such instruments can disentangle  $\mu_a$  and  $\mu_s'$  by a single measurement, and they are little affected by the peel of fruits and vegetables. The application of TRS technology at industry level (e.g., implementation in selection lines) is prevented by the slowness of the measurements, since the optical probe must be kept in contact with the sample. Therefore, in the horticultural sector the most common internal quality control techniques are destructive and sampling. Thus,

the production chain suffers from waste issues, and the evaluation of the quality of the marketed products is undermined. To improve the applicability to the industry of TRS devices, i.e. to improve the sustainability of the production chain, a crucial step would be represented by the development of technology based on a non-contact approach. During my doctoral program, I developed and tested two TRS systems: a state-of-the-art device and a non-contact laboratory prototype.

## 2 Contact time-resolved reflectance spectroscopy system

The contact TRS system is based on a supercontinuum fiber laser providing picosecond pulses. Wavelength selection is provided by 14 band-pass interference filters in the range 540–1064 nm. Light is delivered to the sample via a

62.5  $\mu\text{m}$ -core graded-index optical fiber, and the pulse reemitted by the sample is collected via a 1mm-core graded-index fiber. The fluorescence signal originated from the sample is quenched by a set of interference filters identical to the one in the injection module. The pulse is detected by a Silicon PhotoMultiplier module and the photon distribution of time-of-flight (DTOF) is measured by a time-correlated single-photon counting (TCSPC) board. The instrument response function (IRF) has a full width at half maximum (FWHM) of about 100 ps. The data analysis is based on a semi-infinite model for photon diffusion in turbid media. The contact system was tested within several measurements campaigns on fruits (e.g., pears, melons), especially within the ESPERA Project, assessing the sustainability of the production chain of Mantuan PGI pears. We

performed measurements on large sets of pears. The main point was measuring the optical properties of the pears at harvest, to sort the fruits into maturity classes. Then, the pears were stored in refrigeration cells. After storage, we measured the fruits once again, both by our TRS device and by some state-of-the-art devices. The results for 'Abate Fetel' pears show that  $\mu_a$  at 671 nm, assessing the chlorophyll content of the pears, i.e. related to their maturity degree, retrieved at harvest is correlated with some features of the fruits retrieved after storage. Pears classified more mature at harvest resulted less green and more sweet than less mature pears. Moreover, more mature pears were perceived as firmer, less juicy, and more astringent than less mature pears.

## 3 Non-contact time-resolved reflectance spectroscopy system

Figure 1a shows a scheme of the non-contact TRS prototype. The system shares the injection module with the contact device. The injection optical fiber enters a measurement box (Figure 1b) minimizing ambient light. The pulse is directed towards the sample via a collimator mounted on the tip of the fiber, 10 cm apart from the sample itself. Next to the collimator, a linear polarizer filters the collimated pulse before it impinges on the sample.

The collimator and the polarizer are mounted on a rotating breadboard, enabling various measurement configurations (e.g., reflectance, transreflectance, transmittance). The sample holder is placed at the center of the rotating breadboard, where a portion of the breadboard itself is removed, so that the sample does not move when the breadboard rotates. Next to the breadboard, the detection module is placed, consisting in a hybrid photomultiplier detector. To quench light reflected or backscattered after travelling through superficial layers of the sample, the detection module and the sample are separated by a bulkhead, with an 8mm-diameter hole through which light reemitted by the sample can pass. Beyond the bulkhead, a set of lenses collects light and focuses it onto the detector. In between the collection optics, light is filtered by two linear polarizers crossed with respect to the one in front of the collimator, to quench direct reflections, and by a bandpass interference filter centered at 671 nm, assessing the chlorophyll content of fruits and vegetables. The photon DTOF is measured by a TCSPC board. The IRF has a FWHM of about 180 ps. The data analysis is based on Monte Carlo models for photon diffusion in turbid media, whose geometry is tailored to the shape of the sample (e.g., spherical,

cylindrical). The non-contact prototype was tested within a shelf-life experiment on 'Abate Fetel' Mantuan PGI pears. The fruits were sorted into maturity classes by the contact TRS system and stored in shelf-life conditions, then we performed measurements by both TRS devices on day 1, 2, 3, 4, and 7. The results show that the non-contact system can recognize the relative differences in  $\mu_a$  at 671 nm between more and less mature pears, i.e. it is suitable for applications like sorting into maturity classes. Therefore, our prototype represents a step towards application at industry level of TRS technology. The next step consists in implementing the system in selection lines.

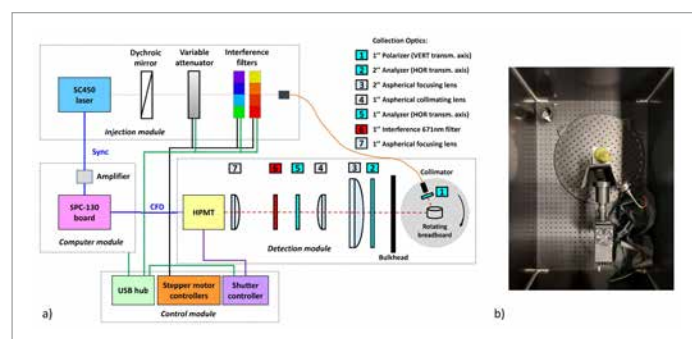


Fig.1 -a) Scheme of the non-contact TRS system. b) Measurement box housing the detection module.

# ORGANIC POLYMERS FOR GENELESS, OPTICALLY-DRIVEN MODULATION OF INTRACELLULAR REDOX BALANCE IN CARDIOVASCULAR CELLS

Camilla Marzuoli – Supervisor: Maria Rosa Antognazza

In cell physiology, redox homeostasis refers to the balance between oxidizing and reducing agents and is recognized as a core concept governing the entire cell cycle, from differentiation and proliferation, up to specific functions and apoptosis. Recent advances in understanding the role of redox reactions in maintaining cellular health have revealed that several pathological conditions are characterized by altered redox states. Over the last few decades, a better understanding of redox-mediated processes has gradually led to the emergence of the concept of “redox medicine”, whose principles are laying the foundation for novel therapeutic strategies addressing a broad spectrum of health issues. From a biochemical point of view, the maintenance of redox homeostasis in cells is strictly correlated to the intracellular presence of Reactive Oxygen Species (ROS), derivatives of molecular oxygen which play the role of secondary messengers. The term ROS includes both free radical and non-radical oxygen intermediates, such as singlet oxygen, the highly reactive hydroxyl radical and superoxide anion and the less reactive but more abundant hydrogen peroxide. The role of ROS in pathophysiology

appears to be a highly pleiotropic phenomenon, strictly dependent on their intracellular concentration. Modulation of ROS levels can have a dual impact on intracellular signalling: balancing ROS towards a positive, oxidative eustress can induce responses that trigger physiological processes, whereas shifting the balance towards oxidative distress levels may have detrimental effects, leading to apoptosis. The possibility to gain control on ROS intracellular concentration could potentially enable control over diverse biomolecular pathways, such as calcium dynamics, and ultimately affect the regulation of specific functions. Employing physical stimuli for precise manipulation of intracellular signaling pathways, including ROS-related ones, offers important advantages compared to traditional pharmacological methods, as well as chemogenetic, magnetic and electrical approaches. In particular, the possibility to stimulate cells by light provides high spatial and temporal resolution, simultaneously minimizing invasiveness. As living cells do not naturally respond to visible light, optogenetics has become the most widely known method

of conferring light sensitivity. Since this technique involves the genetic modification of cells to express light-sensitive proteins, it carries some of the potential risks associated with genetic modification. For this reason, although it is widely used as a research tool, its transition to clinical application is still at an early stage. As an alternative strategy to confer light sensitivity to cells, our research group has recently suggested the use of photosensitive materials that can act as phototransducers. These phototransducers offer a minimally invasive, gene-less approach that potentially has fewer drawbacks when applied *in vivo*. The ideal material should satisfy criteria such as high phototransduction efficiency, stability in an aqueous environment, and long-term biocompatibility. Organic-based compounds, in particular polythiophene-based semiconductors, have recently emerged as promising candidates due to their distinctive optoelectronic properties. In our research group, poly(3-hexylthiophene) (P3HT) has been successfully employed as photoactive layer for both *in vitro* and *in vivo*

applications. There are different phototransduction mechanisms at play at the interface between the synthetic material and the living cell membrane, which can efficiently trigger cell response activation, including photo-thermal, photo-capacitive and photo-electrochemical (PEC) transduction.

In this PhD thesis we target the possibility to optically modulate the intracellular ROS balance, focusing specifically on the study of PEC reactions. Under illumination, P3HT acts as photocathode: its energetic levels are well aligned with the reduction potential of oxygen towards superoxide radical anion, which further evolves in ROS. These exogenously generated ROS have been shown to play a key role in the effective modulation of cell activity. For this purpose, we have developed two approaches, based on the use of polymer thin films, acting as cell culturing substrates, and polymer nanoparticles (NPs), which internalize within the cell cytosol. This allows us to achieve extracellular or intracellular ROS production, respectively. The use of polymer thin films enables the possibility to ad hoc engineer the device architecture, and to parallelize *in vitro* experiments, thus offering new simple tools for redox biologists. Conversely, the use of NPs is more attractive for *in vivo* applications, as they can be injected and delivered to the site of interest, without the need for surgical implantation, and they also offer the possibility of fine-tuning the efficiency of ROS production by playing with their concentration.

In addition to material form and concentration, we also considered other parameters, that may play a key role in ROS production and biological modulation, namely: material morphology, surface chemistry, charge recombination and charge transfer efficiency, optical band gap. This way, we have extended the toolkit of materials available as phototransducers. More specifically, control of material morphology was achieved by increasing the surface area available for PEC processes, i.e., by introducing porosity. The addition of electrochemically active functional groups, such as a TEMPO unit, served as a useful approach to chemically enhance the photocathodic behaviour of P3HT and the optical triggering of oxygen reduction. Composite structures, including electron- and hole-conductive layers, as well as surfactants and aptamers, conferred additional efficiency and cell selectivity to the bare photoactive material. As an alternative to P3HT, we have also employed other low bandgap conjugated polymers to achieve deeper penetration into the tissue. Examples of such polymers include PBDB-T, PTB7, and PCPDTBT. A comprehensive microscopic and opto-electrochemical characterization was carried out to evaluate materials performance and stability in an aqueous environment. Among other potential applications where ROS balance play a key role in cell homeostasis maintenance, we focused here on cardiovascular cell models.

No toxicity signs were evidenced, thus confirming that the proposed strategy works in a eustress condition. Most interestingly, we have successfully demonstrated the possibility of fine-tuning the intracellular ROS production in a spatially and temporally precise manner. Among others, two valuable examples of promising therapeutic applications are extensively discussed in the thesis: (i) modulation of electrical activity and calcium dynamics at the polymer thin film/cardiomyocyte interface through PEC reactions, leading to a significant impact on beating frequency; (ii) bimodal modulation of the angiogenesis process in endothelial cells using ad hoc engineered NPs, achieved through optically activated ROS production. Summing up, results obtained in this PhD work represent an important step forward in the development of new tools for precise, non-invasive, geneless and wireless modulation of intracellular ROS. Broadening the toolkit of materials available as phototransducers allowed to obtain higher photoelectrochemical efficiencies with respect to P3HT, taken as a benchmark material, while reducing the power density required for photostimulation. Aiming at redox medicine applications for therapeutic purposes, we demonstrated the possibility to modulate cardiovascular cell functions *in vitro*, paving the way for *in vivo* exploration of innovative redox-based interventions in the cardiovascular field.

## BLENDED AND HYBRID TEACHING/LEARNING: EXPERIENCES AND DATA ANALYSIS

**Roberto Luca Mazzola** – Supervisor: Maurizio Zani

With over two decades of experience as a high school Physics teacher, I have devoted considerable time to reflecting on and evaluating my pedagogical approaches and techniques. My philosophy has always been to strike a balance between various strategies and methodologies, especially in the context of STEM (Science, Technology, Engineering, and Mathematics) education, as recommended by scholarly literature and researchers. The trend of globalization has shown that countries focusing on developing their human capital, particularly in STEM fields, can achieve significant growth and influence. Numerous studies have pointed out the strong link between a robust STEM education system and a nation's competitiveness on a global scale. The job market has seen an increasing need for STEM-trained professionals, a trend attributed to the rapid technological evolution and the demand for innovation in diverse sectors.

In the realm of education, there's an ongoing concern to enhance student outcomes and reduce dropout rates, which might call for a revision of traditional teaching methods. New Information and Communication Technologies (ICTs) provide promising prospects for enriching higher education

by offering alternative methods of creating, distributing, and accessing educational content. The concept of "Teaching-learning innovation" has become a central theme in the strategies of universities globally, including those in Europe. This challenge is often linked to the adoption of strategies that transform traditional teaching methods, moving from didactic lectures and summative assessments to more student-centric approaches. These methods are designed to promote active learning in supportive environments that utilize digital tools, encouraging students to solve real-life problems and apply various assessment strategies. Some approaches also aim to unleash students' creative potential.

Teaching-learning innovation is a dynamic and evolving process within the educational environment, not just reliant on specific methods or approaches. It focuses on enhancing the overall learning experience. The current phase of heightened focus on teaching-learning innovation is about identifying the most effective didactic practices. For institutions that have traditionally relied on frontal teaching and summative assessment, initiating a change process to develop programs that encourage learning

innovation is crucial.

A key consideration is how educators engage with learning design. In many schools and universities, there is a prevalent model of the teacher as a lecturer, delivering content in a one-way manner without much evaluation of its effectiveness. In contrast, students are often passive recipients of this information. Transitioning from a content-centric to a learner-centric approach, and the change in the teacher's role that accompanies it, is neither straightforward nor simple. It represents a significant aspect of change management in education and requires dedicated focus.

The future of education is complex and challenging: it's about ensuring that the teaching-learning experience not only imparts essential knowledge and skills but does so through an active, creative learning process that develops crucial competencies for an uncertain and rapidly evolving future.

The key question is whether online components can effectively replace certain aspects of classroom instruction while maintaining educational quality and performance. The COVID-19 pandemic brought unprecedented disruptions to various sectors, including education. With the

abrupt closure of educational institutions globally, educators faced the challenge of ensuring uninterrupted learning. In this context, blended learning, which combines face-to-face instruction with online learning's flexibility and accessibility, emerged as a practical solution. Also known as hybrid learning, this method integrates digital technologies with traditional classroom techniques to create a cohesive and engaging educational experience. The pandemic's demand for social distancing and remote learning necessitated a swift shift to online platforms. However, a fully online approach introduced challenges like limited student-teacher interaction and unequal access to resources. Blended learning was a strategic response, combining online and offline components to offer a comprehensive learning experience.

Blended learning uniquely balances the benefits of in-person instruction with digital tools' flexibility. By integrating virtual platforms like video conferencing and learning management systems with traditional classroom settings, educators could create a dynamic and adaptable learning environment. This approach enabled students to engage in collaborative activities, participate in discussions, and receive immediate feedback, fostering an interactive and immersive learning experience.

Moreover, blended learning allowed educators to tailor their teaching strategies to meet diverse student needs. By using digital resources, teachers could personalize learning, provide additional

support, and offer differentiated instruction to suit individual learning styles and paces. This adaptability was invaluable during the pandemic, as students encountered varying levels of technological access and different home learning environments. The success of blended learning during the pandemic has highlighted its potential as a transformative educational approach for the future. This paper aims to examine the impact of blended teaching and learning during the pandemic, exploring its advantages, challenges, and possible long-term effects on education. Specifically, in the first part of this work, Chapter 2 delves into remote teaching perceptions, analyzing data collected from over 3500 engineering students. We have scrutinized data from an extensive questionnaire focusing on different aspects of the learning process, including the organization of emergency remote teaching, subjective well-being, metacognition, self-efficacy, identity, and socio-demographic factors.

Several intriguing insights have emerged from the analysis of these data, two of which are particularly highlighted in this study. Firstly, the challenges perceived by students in relation to remote learning appear to be gender-neutral, affecting both male and female students alike. However, these challenges seem to be correlated with the academic year of study. Secondly, this research delves into one of the analyzed factors, namely metacognition. It appears that remote teaching has facilitated the employment of

cognitive strategies and cognitive tools by students to navigate the complexities of online instruction. In Chapter 3, we investigate the results and methods used in a Physics vocational training project for high school students conducted at an Italian school, named PCTO. This project encompassed webinars, self-organized laboratory group experiences, and peer evaluation. Our team meticulously planned the project from both logistical and educational standpoints and conducted a detailed analysis of the data gathered, focusing on satisfaction and peer evaluation. The students demonstrated a favorable reception towards the blended learning approach implemented in the project. Additionally, the study yielded insights regarding formative peer assessment as juxtaposed with the evaluations conducted by faculty members.

In Chapter 4, two distinct educational paths designed by the ST2 group are outlined, targeting prospective students and new entrants at Politecnico di Milano. The first path involves preparing and delivering refresher courses in Physics for incoming engineering students, scheduled one week before the start of academic courses. The second focuses on preparatory courses for the Politecnico di Milano entrance examination, aimed at students in the fourth and fifth grades of high school. This final chapter describes the organization of these two paths from an educational design perspective, offering descriptive results on the degree of satisfaction achieved.

## TIME-DOMAIN DIFFUSE OPTICAL MONITORING AND PREDICTION OF NEOADJUVANT CHEMOTHERAPY RESPONSE FOR PERSONALIZED BREAST CANCER MANAGEMENT

**Nikhitha Mule** – Supervisor: Paola Taroni

NeoAdjuvant Chemotherapy (NAC) is a type of therapy administered in order to downsize the tumor before it can be surgically removed. It is widely being accepted these days to treat patients with locally advanced breast cancer as it could allow for breast conserving surgery. The early assessment and prediction of the cancer response to this therapy is essential as it could allow healthcare providers to evaluate tumor response, monitor side effects, and make informed decisions regarding further treatment strategies. However, currently there are minimal to no clinically accepted biomarkers that can provide insights into the likelihood of a patient responding to the NAC treatment. Hence, there is a need to explore and identify objective biomarkers that can help associate with therapy response. Several routine imaging modalities such as x-ray mammography, ultrasound, magnetic resonance imaging (MRI) and positron-emission tomography (PET) are being tested for their capabilities to predict the therapeutic efficacy. While X-ray mammography and ultrasound may be utilized, they do not readily provide metabolic and physiological information, which could be the

key parameter that reflects initial changes rapidly. MRI and PET have the potential to provide such metabolic information. Nevertheless, factors such as longer examination times, cost, and the use of radioactive contrast agents render them unsuitable for frequent monitoring. Given that metabolic changes in cancer due to therapy can precede morphological changes, there is a potential to track for any such supplementary information. Here comes the possibility of new imaging modalities, like diffuse optical spectroscopy (DOS), that could be examined for this type of application. Diffuse Optics studies the propagation of light in highly scattering media, like the breast tissue, which helps to investigate it down to a depth of few centimeters using near-infrared light (650–1000 nm). It provides information on tissue composition, that includes blood, lipid, water, and collagen concentrations, through its absorption properties, as well as tissue microstructure through the scattering properties. In the context of breast cancer, this information can be utilized for various purposes, including risk assessment, identifying lesion nature, monitoring therapy progress, and predicting

treatment outcomes. The advantages of using non-ionizing radiation, non-invasiveness, relative cost-effectiveness compared to other imaging modalities, ability for frequent monitoring, and more importantly provision of quantitative physiological information, render it suitable for exploring its potential in this particular application of therapy monitoring. With this aim, an optical mammograph that uses DOS technique in time domain was developed at Politecnico di Milano. It is a seven-wavelength (635–1060 nm) optical mammograph that is designed to collect projection images of the compressed breast, i.e., in the same geometry as used for conventional x-ray mammography, but with soft compression of the breast. The seven wavelengths were chosen based on the main breast chromophore spectra: water, lipids, collagen, oxy and deoxy-hemoglobin. The breast is raster-scanned by the light transmitted through an injection fibre, which is axially aligned with a detection probe composed of silicon photomultipliers. The output signals are then amplified and directed to the Time-To-Digital Converter, that reconstructs the time-dependent distribution

of the re-emitted photons, i.e. the transmittance curves, from where the optical properties of the tissues are then derived using a model based on diffusion approximation of the radiative transport theory. The instrument is now at San Raffaele Hospital, Milan, for a clinical study on breast cancer patients. The purpose of this study is to monitor NAC effects through time-domain diffuse optical spectroscopy, correlate the optical results with conventional imaging techniques and patient's pathologic outcome, and eventually predict the efficacy of NAC in breast cancer patients to discriminate responders from non-responders. So far, 10 patients have completed their participation in this study. Before the start of the measurement, a signed informed consent was obtained from each patient. Each subject undergoes six optical sessions with the optical mammograph: a baseline before starting NAC, 2–5 days after starting NAC, 6–8 days later, 2 weeks later, at mid-treatment and one at the end of the treatment. In each session, 4 scans are acquired, to probe the combinations of both breasts (right – R – and left – L) and views (Cranio-Caudal – CC – and Oblique – OB). Each patient received multicycle and multi-regime NAC treatment. Considering the mean of 10 patients and averaging on both CC and OB views to have an approximate overview of the present results, the optical data analysis shows that there is significant reduction in

the concentrations of total hemoglobin (–41%), water (–17%) and collagen (–54%) and increase in lipids (+20%) by the end of therapy in the tumor bearing breast, indicating a response to the therapy. These trends correlate with standard imaging modalities and histopathological reports, that have indicated that all 10 patients indeed responded to the therapy (either partially or completely). The literature also supports these expectations, indicating that blood, water, and collagen concentrations are typically higher in malignant tumors compared to healthy tissue, likely due to factors such as angiogenesis, hypermetabolism, and intravascular pressure within the tumor, while the lipid content in tumors tends to be lower than in normal tissues, often as a result of the replacement of breast adipose tissue by tumor cells. Therefore, positive response to the NAC therapy is anticipated to result in decreased blood, collagen, and water concentrations, alongside an increase in lipid content compared to baseline levels. Besides, we hypothesize that collagen could be a possible biomarker relating to the NAC efficacy, as it shows a maximum reduction in its concentration with therapy, and it is known to be involved in breast cancer development and progression. Comparing the baseline and end therapy measures, compositional changes occurring during the course of NAC were observed even on the contralateral healthy breast. A reduction

in the concentrations of total hemoglobin that includes oxy and de-oxy hemoglobin (–35%), water (–5%), collagen (–11%) and increase in lipids (+16%) was noticed. This could be due to the systemic nature of NAC, and it is worth noting that these variations are smaller compared to the variations in the tumor bearing breast. In conclusion, it is observed that DOS is sensitive to the changes occurring in the breast tissue due to the therapy. Data from more patients is necessary to strengthen our hypotheses. We also aim to see any regimen-dependent changes related to response in breast tumors throughout NAC. Future work includes identifying reliable parameters that can help us predict the tumor response for the evaluation of neoadjuvant therapy's effectiveness as early as possible. This work is being carried out as part of the PHAST project that has received funding from the European Union's Horizon 2020 research and innovation programme under grant agreement No. 860185.



# LAYERED 2D MATERIAL HETEROSTRUCTURES FOR APPLICATIONS IN PHOTO AND INTEGRATED ELECTRONICS

**Nikil Paithankar** – Supervisor: Roman Sordan

Two-dimensional (2D) van der Waals heterostructures provide a platform for theoretical investigations in physics and realization of the next generation of highly integrated nanoelectronic devices. The combinations of 2D materials are virtually limitless in heterostructures, given the myriad of discovered 2D materials of different electronic properties. Moreover, 2D semiconductor materials could be encapsulated in insulating and screening 2D materials, greatly enhancing their electronic properties. Heterostructures could, therefore, preserve the intrinsic properties of single-layered 2D semiconductor materials, making it advantageous to encapsulate the 2D semiconductor layers of interest in other 2D materials free of dangling bonds. This work explores how the 2D heterostructures can be utilized both for fundamental investigations in optoelectronics and realization of digital complementary inverters. Fundamental investigations in optics involving 2D materials often require specific structures exhibiting near-ideal conditions, as such materials are very sensitive to the surrounding environment. Passive circuit elements in the device could

also affect the outcome of the measurements. Therefore, a proper isolation of 2D materials is fundamental. An hBN/graphene/hBN van der Waals heterostructure was used for the realization of graphene photoelectronic Corbino field-effect transistors (FETs), shown in Figure 1a. The encapsulation of graphene in hBN was performed to preserve its high carrier mobility and provide a platform to investigate the exchange of orbital angular momentum (OAM) from a vortex light beam to electrons in quantum Hall states of graphene. The electrical characterization of the locally gated Corbino ring GFETs revealed almost

no hysteresis in the measured I-V curves, as shown in Figure 1c. The hBN flakes, used as insulating layers in the gate stack, provided sufficiently large gate capacitance, allowing to efficiently modulate the drain current. The photocurrent (PC) measurements, performed at the Joint Quantum Institute (shown in Figure 1e), provided an experimental proof of the expected exchange of OAM from a vortex light beam to electrons in quantum Hall states of graphene. The hBN/graphene/hBN heterostructure were found to be an optimal platform for the investigation of such phenomena. 2D materials offer a solution to overcome the problems

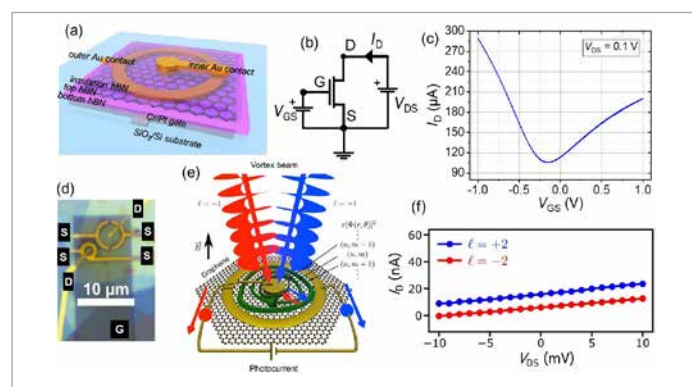


**Fig.1 - Graphene photoelectronic Corbino devices based on van der Waals heterostructures. (a)** 3D view of the Corbino ring, where the different contacts and layers are labelled. **(b)** Circuit schematics of the Corbino ring GFET. **(c)** Transfer curve of one of the biased Corbino ring GFETs. **(d)** Optical image of the Corbino rings. **(e)** Schematic of the experimental setup. **(f)** The measured  $I_D$  as a function of the applied  $V_{DS}$  at a magnetic field  $B = 9$  T. The photocurrent is observed as non-zero  $I_D$  at  $V_{DS} = 0$  V.

related to the downscaling of FETs in semiconductor technology. Leveraging the low dimensionality of 2D FETs allows for the suppression of short channel effects and higher scale integration. The latter can be achieved by stacking the 2D devices in the third dimension. All-2D material complementary inverters were fabricated and electrically characterized. A manual transfer of the 2D material flakes by hot pick-up technique was used to fabricate the devices in this work. The hot pick-up technique is an effective method for research purposes, as it provides a fast assembly of the heterostructures and a great freedom of choice of the used 2D materials. The technique is capable of transferring a great variety of 2D materials. The all-2D material complementary inverter is based on a fully stacked heterostructure comprising the p-type (WSe<sub>2</sub>) and n-type (MoS<sub>2</sub>) FETs in a gate-all-around (GAA) configuration, as

shown in Figure 2a. The hysteresis is almost completely suppressed thanks to the full encapsulation of the 2D material channels in hBN. The static voltage transfer characteristics (VTC), shown in Figure 2d, exhibits rail-to-rail operation and correct logic level inversion. To reach a higher integration density, all-2D material complementary vertical inverters were fabricated. Their structure is shown in Figure 3a. To improve the matching of the threshold voltages of the FETs, an  $\alpha$ -ruthenium(III)chloride ( $\alpha$ -RuCl<sub>3</sub>) bottom gate was used to p-dope WSe<sub>2</sub>. The static VTC, shown in Figure 3d, exhibits again rail-to-rail operation and correct logic level inversion. An increased drain current was observed, suggesting higher gains and bandwidth of the inverter. This results demonstrate the potential use of 2D materials to obtain higher integration density in future large scale production integrated circuits. CVD-grown 2D

materials are the most promising candidates to fabricate the all-2D complementary vertical inverters in a large scale. This work focused on the demonstration of two applications of a large variety of possible applications of 2D material heterostructures. Their promising electronic properties and low dimensionality provide a foundation for theoretical investigations in physics, and position them as the key building blocks in the development of highly integrated nanoelectronic devices.

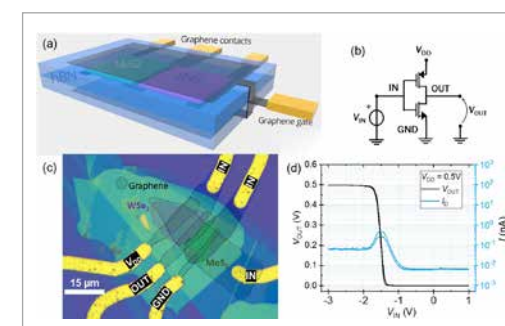


**Fig.2 - All-2D-material complementary inverter. (a)** 3D view of the inverter. **(b)** Circuit schematics of the inverter. **(c)** Optical image of the all-2D complementary inverter. The shaded areas delimited by the dashed lines highlight the different encapsulated flakes: the WSe<sub>2</sub> flake (purple), MoS<sub>2</sub> flake (green) and FLG flakes used for the gate and source-drain contacts (dark contrast). **(d)** Static VTC of the all-2D complementary inverter (black). The drain current  $I_D$  (blue) is also shown.

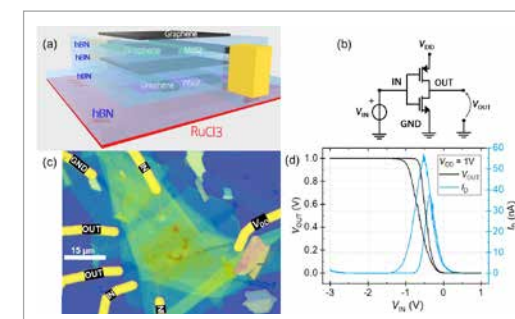


**Fig.3 - All-2D-material complementary vertical inverter. (a)** 3D view of the inverter. **(b)** Circuit schematics of the inverter. **(c)** Optical image of the all-2D complementary vertical inverter (black). The drain current  $I_D$  (blue) is also shown.

# FEMTOSECOND LASER WRITTEN UNIVERSAL PHOTONIC PROCESSORS

**Ciro Pentangelo – Supervisor: Roberto Osellame**

Photonic integrated circuits (PICs) have emerged as a promising tool for use in quantum information processing and quantum communication, providing a scalable and stable platform that surpasses traditional bulk optical systems in terms of stability and scalability. Among the multitude of integrated photonic platforms, Femtosecond laser writing (FLW) stands out for its ability to fabricate 3D photonic circuits swiftly and cost-effectively. In recent years there has been growing interest in the development of universal photonic processors (UPPs), which are programmable PICs that can implement any unitary transformation, allowing for multiple transformations to be implemented on the same circuit. A UPP consists of a mesh of programmable Mach-Zehnder interferometers (MZIs). This programmability is primarily achieved through thermo-optic phase shifters (TOPSs), favored for their simplicity in fabrication and minimal impact on optical performance, as well as their high stability and reliability. Moreover, TOPSs can be fabricated simply by depositing a single metal film (such as gold) and then patterning it by ablation using FLW. This simplifies the fabrication at the cost of a large surface area

being occupied by contact pads, which have to be large enough to minimize the parasitic series resistance. Recent advancements have significantly reduced optical losses and expanded the modal capacity of UPPs across various photonic platforms, culminating in the creation of large-scale UPPs, particularly in the silicon nitride platform where a 12-mode UPP was demonstrated at the start of this PhD work, followed by a 20-mode UPP less than two years later. However, until the onset of this research, the FLW platform had only seen modest achievements, with the largest UPP being a 4-mode circuit lacking comprehensive universal control. This doctoral thesis marks a significant leap in FLW UPPs,

beginning with the introduction of 6-mode processors that incorporate thermal isolation trenches. These trenches, fabricated by FLW, enable efficient phase shifting with markedly reduced power consumption (tens of mW instead of hundreds for a  $2\pi$  phase shift), a crucial step forward in the development of energy-efficient photonic circuits. A novel and fully automated calibration protocol has been devised and optimized for these processors, relying solely on optical power measurements. This method, applicable to FLW UPPs of any scale featuring a rectangular MZI mesh, has been validated through the calibration of two 6-mode FLW UPPs operating at wavelengths of 785 and 1550 nm. The calibration process

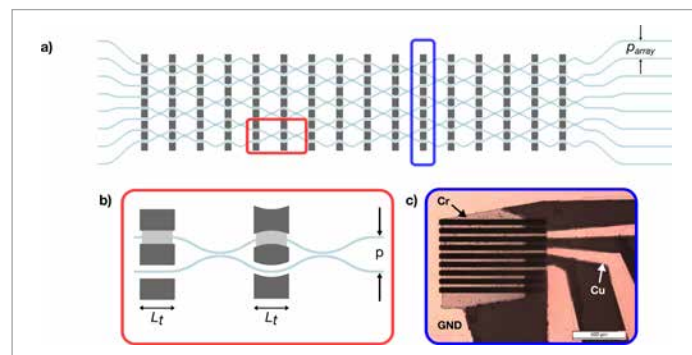


**Fig.1 - (a) Circuit scheme of the 8-mode FLW UPP. (b) MZI cell scheme featuring both rectangular and curved trench structures. (c) Microscope image of a single column of TOPSs. Arrows indicate chromium (Cr) and copper (Cu) features, while GND indicates the ground plane.**

exhibited exceptional fidelity in executing numerous Haar random transformations (above 99.7%). Furthermore, ultra-high fidelity (above 99.95%) was demonstrated with single unitary optimization, showing how some of the potential performance of these processors remains untapped and hinting at future improvements in the calibration protocol. Polarization insensitivity, one of the key advantages of FLW PICs, has been verified using these processors, an attribute that significantly enhances the utility of FLW in quantum information processing by allowing for the encoding of quantum information in the polarization state of light. A modular Quantum-to-Quantum Bernoulli factory was experimentally implemented with high fidelity using these UPPs, exemplifying the practical applications of FLW UPPs in quantum information processing tasks. The high fidelity achieved in this quantum experiments acts as another verification of the high quality of the calibration protocol, and the modularity of the Bernoulli factory showcases the main advantage of using such a universally programmable

processor.

The limits of the single gold film TOPS technology were reached with the 6-mode UPP fabrication, prompting the development of a new dual-film design. A novel photolithographic fabrication process, utilizing chromium and copper for resistive microheaters respectively, has been developed from the ground up in this work. Its development required the introduction of dry film photoresist along with wet etching of metal films, to maintain compatibility with thermal isolation trench structures. The significant improvements brought on by this new TOPS technology, particularly in terms of integration density but also including higher thermal stability and lower parasitic series resistance, has allowed for the demonstration of an 8-mode FLW UPP featuring double the amount of TOPSs as the 6-mode UPP. This processor, which integrates compact MZI cells with curved trenches, represents the pinnacle of FLW UPP development, featuring universal programmability within the constraints of current fabrication technologies.

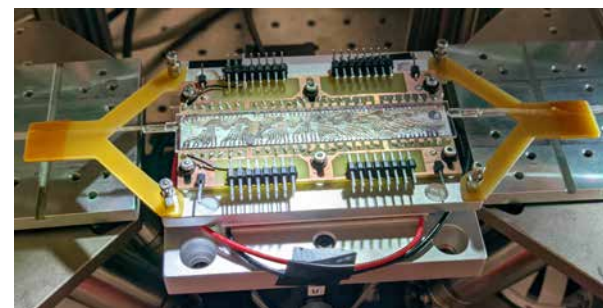


**Fig.2 - Photograph of the fully packaged 8-mode FLW UPP.**

In conclusion, the research conducted in this thesis has significantly improved the state of the art for FLW UPPs, demonstrating high-fidelity control over 6- and 8-mode processors. The introduction of a novel calibration procedure, along with advancements in TOPS fabrication technology, has not only improved the performance and scalability of FLW UPPs but also opened the door to future developments that could see FLW UPPs reaching up to 20 optical modes: a level of complexity that was difficult to envision in FLW PICs before this PhD work. These breakthroughs address and overcome multiple previous limitations of the FLW platform, placing it in a much better position with regards to the state of the art for integrated UPPs.

# ULTRAFAST OPTICAL PHENOMENA IN ADVANCED NANOSTRUCTURED MATERIALS FOR LIGHT HARVESTING AND ALL-OPTICAL MODULATION

**Silvia Rotta Loria** – Supervisor: Margherita Zavelani-Rossi

The advancement of ultrafast optical techniques has marked a significant milestone in exploring the properties of matter as well as in investigating its interaction with light. Indeed, ultrafast lasers can reach high intensities so as to trigger nonlinear processes and they can be used to resolve the materials response on the femtosecond temporal scale. Ultrafast pump-probe spectroscopy is a widely exploited experimental technique, through which we can monitor the response of a sample perturbed by a fs-laser pulse, in the first instants of its excited state dynamics, with high temporal resolution, down to a few fs. At the same time, the evolution of fabrication techniques has enabled the manufacturing of materials with lower and lower dimensions, shrinking the photonic structures down to the nanoscale. This has brought to remarkable changes in the field of optics and electronics, leading to the birth of nanophotonics, which focuses on light-matter interaction at the nanoscale, with the aim of controlling such phenomena to develop new technologies and devices. Both high temporal resolution spectroscopy techniques and the development of nanophotonics are crucial in order to address,

among the others, two important challenges of today's society. Nowadays, the search for energy sources alternative to fossil fuels is mandatory. In this regard, the study of light-harvesting devices has played a pivotal role in the last decades. Semiconductor nanocrystals such as silicon (Si) and titanium dioxide ( $\text{TiO}_2$ ) have been broadly employed for this purpose due to their abundance, good electron transport and low cost. However, the efficiency of these materials alone is often limited, for example due to a rather low absorption coefficient (Si) or because of the high energy of its bandgap ( $\text{TiO}_2$ ), which limits the amount of absorbed solar light. On the other hand, contemporary society demands for faster and faster information processing and transport capabilities. If silicon transistors can be downsized to nanometer dimensions, electronics is inevitably affected by signal delay and thermal issues due to the massive on chip interconnections. Conversely, optics interconnects would possess much higher speed, which would totally innovate data processing (for example in next generation chips, made of a large number of electronic computing cores connected with ultra-rapid links). The novel

field of ultrafast nanophotonics pushes the frontiers even further, by realizing the modulation of light signals through a control light beam, potentially leading to an all-optical manipulation of information. However, optics is intrinsically limited by diffraction. In this context, plasmonics plays an important role, bridging the gap between these two worlds, with the ability of squeezing light into nm-sizes and controlling its interaction with matter so as to have unprecedented optical effects. For both goals, the search of novel materials is central to overcome the main limitations of present technologies. In the case of solar cells made with wide-gap semiconductors, for example, one way is to sensitize the material using particular molecules called dyes, which broaden the absorption spectrum of the cell. The search on dyes has turned more and more towards organic molecules, due to their non-toxicity, easiness of extraction and low cost. Other than dyes, also quantum dots (QDs) have been used as sensitizers in quantum dots sensitized solar cells (QDSSCs), solar concentrators and multi-junction solar cells. In order to improve the performance, doping is exploited to obtain an elevated Stoke shift, but also to increase the electron

transport and luminescent lifetime.

For what concerns materials for plasmonics, noble metals (and in particular gold) have been the primary choice. However, they suffer from high interband losses in the visible, non tailorable dielectric permittivity, low melting point and incompatibility with the silicon industry. In order to overcome these issues, in the last decade a lot of attention has risen towards transition metal nitrides. Among the others, titanium nitride (TiN) was brought into the spotlight as a refractory metal, with good chemical stability, tailorable permittivity and lower interband losses than gold at optical frequencies.

The study of the ultrafast optical relaxation mechanisms of the carriers photogenerated in these materials is essential both to understand their properties at a fundamental level and to exploit them in devices with enhanced opto-electronic functionalities. Ultrafast pump-probe spectroscopy together with other experimental techniques (photoluminescence, photocurrent measurements...) provide data that ought to be paired with theoretical and numerical models to achieve a complete picture of the photophysical processes. This is important in view of providing useful tools to design new devices. In the case of TiN, the material presents the huge optical nonlinearity of a metal, but also an extremely strong carrier-phonon interaction, which gives relaxation times for the hot-electrons below 100 fs, more than one order of

magnitude faster than for noble metals; these characteristics make it the perfect candidate for all-optical modulation. Because the efficient realization of photon interaction relies on the optical media nonlinearity, the study of TiN nonlinear optical response, that is presented in this work, is pivotal. This step is not straightforward, involving multiple numerical models stemming from thermodynamics, thermoelasticity and nonlinear optics, with the calculations being performed on a broad spectral range. Accurate simulations are needed in order to mimic all the light-matter interaction mechanisms at the nanoscale. Quantitative predictions of the ultrafast optical response of TiN structures will enable the design and engineering of these samples for practical applications. This thesis is organized as follows:

First, we describe time-resolved pump-probe spectroscopy, in terms of the main concepts and of the experimental setups exploited in this work. Furthermore, we show the information we retrieved on the photophysics of two interesting systems for light harvesting: 3-hydroxyflavone (3HF) on  $\text{TiO}_2$  and cadmium selenide sulfur ( $\text{CdSeS}$ ) nanocrystals engineered with sulfur vacancies. Then, we introduce TiN interesting features and stationary optical properties, and we detail a novel numerical model for TiN optical nonlinearity. The latter is structured into three sections: the two-temperature model (2TM), the thermoelastic model and the disentanglement

of the material permittivity modulation.

After that, we present the model validation, by comparing our numerical data with experimental data obtained through pump-probe experiments. We analyze two different cases. The first one is a TiN film measured with our aforementioned pump-probe setup. The second consists of TiN nanoparticles whose measurement results are reported in literature. As a last set of results, we present further outcomes on the study of TiN ultrafast optical properties, both on the modelling side and on the experimental one. Further calculations involve a comparison of the Fermi smearing effect in TiN and gold thin films and the refinement of the numerical model presented in Chapter 3 (through the addition of a further interband transition). More experiments show the tuning of the ultrafast optical response of TiN films through stoichiometry control and a preliminary study on coherent phonons in TiN films.

# SIMULATIONS FOR POSITRONIUM INTERFEROMETRY AND GRAVITATION

**Michele Sacerdoti** – Supervisor: Rafael Ferragut

The Phd thesis mainly describes the simulations that I have done to confirm the feasibility of the QUPLAS experiment to measure the gravitational acceleration of positronium.

After a chapter about the theoretical foundations of the experiment and the description of ongoing experiments with antihydrogen the thesis analyses the various parts of the experiment with positronium (Ps) to be able to define the formulae that should be used in the simulation.

The Ps negative ion (Ps<sup>-</sup>), bound state of two electrons and one positron, is generated at the surface of a positron/Ps<sup>-</sup> converter (alkali metal coated tungsten) and then focused using a very compact system to form and guide a Ps<sup>-</sup> beam before it decays (see figure “Schematic representation of the optics”). A laser removes the extra electron by photo-detachment to create a Ps beam which enters a Mach-Zehnder interferometer specifically designed to measure gravitational acceleration. This measure requires a large amount of Ps atoms parallel to the axis of the interferometer.

The velocity distribution of Ps<sup>-</sup> produced by the converter, the trajectory of Ps<sup>-</sup> in the electric field and the photo-detachment

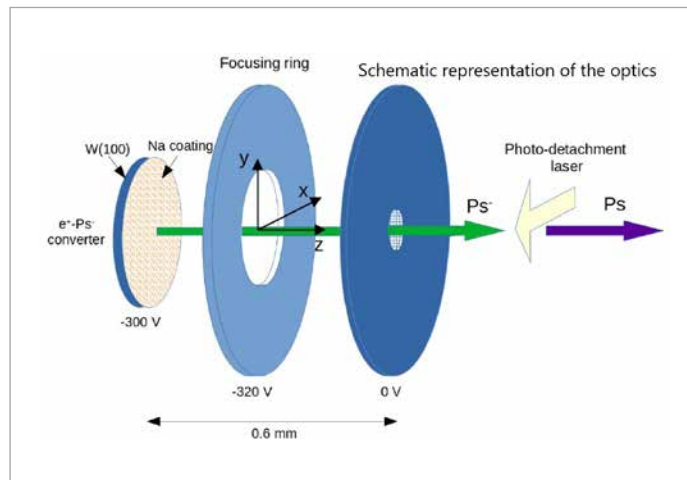


Fig.1

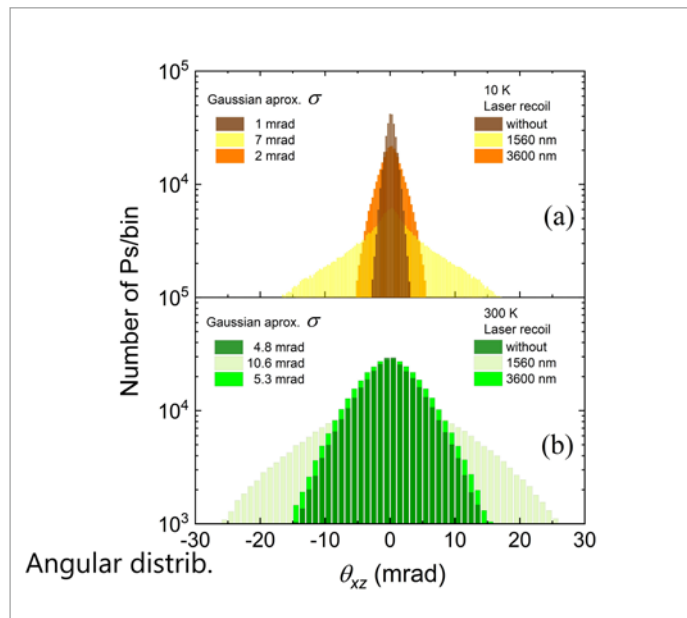


Fig.2

with the recoil of Ps have been modelled.

I have obtained the angular distributions of Ps at the entrance of the interferometer with a laser with 1560 nm and 3600 nm and a converter temperature of 10K and 300K (see figure “Angular distrib.”).

The Monte Carlo results presented in the table last row illustrate the number of Ps entering the interferometer with the required angles of 170 μrad and 125 μrad with the X and Y axis.

The results of the simulation with these cases show that the experiment is feasible with a precision of 10% after a year of measurements.

Laser wavelength	1560 nm	1560 nm	3600 nm	3600 nm
Temperature	10 K	300 K	10 K	300 K
Ps <sup>-</sup> decayed before the laser	327.184 (354)	326.962 (355)	327.184 (354)	326.962 (355)
Ps <sup>-</sup> decayed in the laser	331.710 (641)	324.309 (564)	301.658 (462)	288.459 (544)
Ps <sup>-</sup> arrived at the laser	341.106 (464)	348.730 (410)	371.158 (305)	384.580 (349)
Ps <sup>-</sup> detached by the laser	325.145 (434)	337.506 (445)	362.546 (273)	382.214 (361)
Ps decayed in the laser	241 (13)	249 (9)	273 (14)	289 (12)
Laser photo-detach. efficiency	95% (1)	97% (1)	98% (1)	99% (1)
Ps entering the Mach-Zehnder interferometer	324.904 (436)	337.256 (447)	362.273 (278)	381.955 (354)
Ps with θ <sub>xz</sub> lower than 170 μrad	6.878 (87)	4.461 (30)	24.216 (157)	9.628 (137)
Ps with θ <sub>yz</sub> lower than 125 μrad	5.157 (107)	3.318 (44)	18.248 (153)	7.291 (94)
Ps inside θ <sub>xz</sub> and θ <sub>yz</sub> (125 μrad x 170 μrad)	278 (20)	51 (7)	1.546 (53)	223 (8)

Montecarlo results

Fig.3



# DEEP ENSEMBLE LEARNING AND TRANSFER LEARNING METHODS FOR CLASSIFICATION OF SENESCENT CELLS FROM NONLINEAR OPTICAL MICROSCOPY IMAGES

Salvatore Sorrentino – Supervisor: Dario Polli

Successful chemotherapy and radiotherapy anti-cancer treatments may result in either tumour suppression or senescence induction. Until recently, experts agreed on the fact that senescence was a condition of durable growth arrest, promoting it as a favourable therapeutic outcome. However, recent advancements in oncology research evidence senescence as one of the culprits of cancer relapse. Senescence is a complex phenotype, and while newly developed markers provide promising results, no marker is completely specific for senescence, requiring multiple consecutive assays. A possible solution for fast, non-invasive and label-free detection of therapy-induced senescent cells comes from nonlinear optical (NLO) microscopy. We recently studied cultured human hepatic cancer cells, in which senescence was induced either via a chemotherapeutic drug or by radiotherapy treatment. Compared to proliferating ones, senescent cells show disaggregation of mitochondria, aggregation of lipids and increase of cell area. These hallmarks were quantified using a combination of two-photon-excited fluorescence (TPEF), stimulated Raman scattering (SRS) and linear optical

transmission microscopy. Here, I present the development of a deep learning approach to perform binary classification between senescent and proliferating human cancer cells, based on the three imaging channels acquired using the multimodal NLO microscope. A major challenge to overcome was the very limited number of labelled data, amounting to 224 images acquired from different biological samples, distributed in 99 images of proliferating (control) cancer cells and 125 coming from senescent cells. The images in the dataset were then split in a training set of 127 images (for the learning process) and a validation set of 43 images (to prevent the training from overfitting). The performances were validated on a test set of

further 54 images, never seen by the network. To overcome the limitation given by the small dataset for the training of a neural network, I relied on the so-called Transfer Learning technique, an approach in which a pretrained neural network on a larger dataset is used as the first part of a more complex network for a given classification task, which leverages on the knowledge of the pretrained network. On top of this pretrained network, a smaller neural network is then built to accomplish the senescence classification. The input channels I used for the network are the SRS, TPEF and Optical Transmission signals. Apart from the use of Transfer Learning, I used other two approaches to reduce the problem of lack of data to train a

network. These two approaches are the Data Augmentation technique and the Ensemble Learning technique. Data Augmentation consists in applying some transformations (like rotations, translations and flipping) to the images in the dataset which do not modify the information present in the images themselves, to increase the number of data available for the training. Ensemble learning is an approach which relies on the use of multiple learning algorithms to obtain better predictive performances compared to the single constituent learning algorithms. In this work, I used seven neural networks as constituents of the ensemble, where the difference among these seven networks is given by the pretrained network used as first part of the entire architecture. Specifically, I used the following open source pretrained networks: Inception V3, EfficientNet B4, ResNet 50, DenseNet 121, MobileNet, Inception ResNet V2, Xception. All the seven networks were trained on randomly different train and validation sets (Fully trained EL network). After the training, the final predictions on the test set are given by the average of the seven predictions of the seven networks. The performance of the network is evaluated on the test set using the common metrics for classifiers, namely accuracy, F1 scores, precision, and recall, together with the standard deviation calculated on the different training and validation splits. I achieved a classification

accuracy of over 90%. Moreover, I compared these results with different approaches which all underperformed, on the same test set, the ensemble learning network built on the seven pretrained networks. Namely, I trained: a convolutional neural network from scratch, an SVM classifier on top of the features extracted from the pretrained networks (Hybrid TL/ML approach), and the seven networks cited before individually. All these comparisons were performed to prove both the transferable capability of ImageNet features in Transfer Learning and the stability and increase in performance of Ensemble Learning, also on non-RGB images. In Figure 1 A) are reported the total performances in terms of accuracy, precision, recall and F1-score of the Fully trained network and the comparative networks cited before. Furthermore, I inspected which features in the input images are the most significant in distinguishing between images of senescent cells and proliferating ones. To extract these features, I used the Grad-CAM approach, building the so-called heatmaps, which highlight the most important pixels in the input channels that activated the neural network to separate between the two classes of cells. Figure 1 B) and C) show that, when the predicted class is 'Senescence', the activated pixels (bottom panel) correspond to the pixel locations of mitochondria and lipid droplets (C, upper panel), whereas there is no activation of

pixels when the predicted class is 'Control' (B). In conclusion, the obtained results prove the possibility of building an automatic, unbiased senescence-cell image classifier starting from multimodal NLO microscopy measurements. It provides excellent performances in terms of classification accuracy. Moreover, I proved the possibility of applying transfer-learning and ensemble-learning approaches to overcome the limitation given by the scarce availability of labelled data also on non-standard images, namely non RGB images. These promising results open the way to a deeper study of senescence classification via deep learning techniques which could lead to new insights in the knowledge of senescence as a cause of cancer relapse.

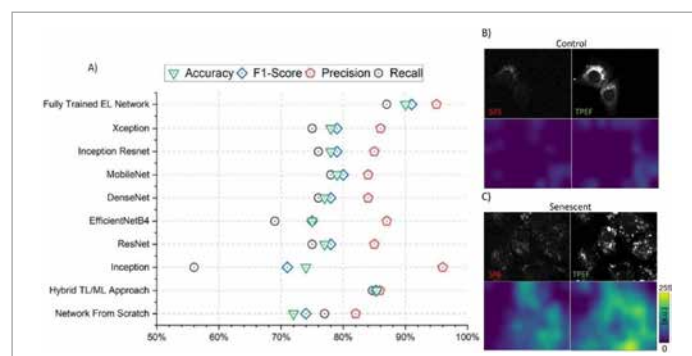


Fig.1 - A) Performance of the different approaches for the classification of senescent cells; B)-C) Heatmap and corresponding optical signal for a control cell (B) and a senescent cell (C)

# NANOSCALE MODULATION AND IMAGING OF OPTICAL, ELECTRICAL AND MECHANICAL PROPERTIES OF 2D MATERIALS

**Giacomo Venturi** – Supervisor: Antonio Ambrosio

The emergence of two-dimensional (2D) materials dates back to 20 years ago, when in 2004 a group of researchers at the University of Manchester reported the first image of a single layer of carbon atoms – graphene – that was produced from a piece of bulk graphite through mechanical exfoliation. This finding triggered the development of a completely new research field, whose main actors are van der Waals crystals, which nowadays is embracing several disciplines from solid-state and condensed matter physics to optics and photonics, as well as materials science.

In the past decade, several tens of monolayer materials have been exfoliated (and synthesized) that span a range of different chemistries and crystal structures, such as hexagonal boron nitride (hBN), transition metal dichalcogenides, Xenes, MXenes, and many more. In their 3D bulk form, these materials share a common crystal structure made of a vertical stack of atomically-thin (i.e., 2D) layers, where covalent bonds provide in-plane stability and weaker vdW forces keep the stack together. It is the very nature of vdW forces that defines this class of materials, enabling a layer-by-layer exfoliation of the bulk

crystals down to a single layer. The fact that the same weak vdW forces are shared by 2D materials makes also possible to combine them in stacks in a Lego-style, without any lattice matching constraint (as it happens for bulk 3D heterostructure), as sketched in Figure 1a. In this case, we speak of vdW heterostructures, which significantly change or enrich the features of the resulting material. This flexibility, and the ability to reach the ultra-flat limit with unique electronic and optical properties, allow 2D materials to offer significant advantages for a wide range of applications. The most renowned example concerns graphene, whose most attractive aspect lies in its linear electronic band structure compared to bulk 3D crystals. This has opened avenues for exploring relativistic physics within a solid-state framework.

Additionally, graphene's exceptionally high carrier mobility (several times greater than that of copper) attracted a high interest in developing new types of transistors.

On top of this, the recent discovery that two vertically stacked graphene layers with a specific relative twist angle behave as a superconductor at room temperature widened the range of potential applications of 2D materials and paved the way for the rise of twistronics: the field that studies how the relative angle between the layers of a vdW heterostructure affects its properties. In this context, the registry of the layers and the associated change in their functional properties are spatially modulated by the emergence of a larger periodicity (compared to their individual lattice constants), called moiré superlattice (see

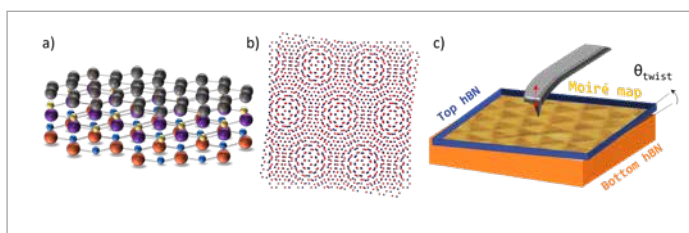


**Fig.1 - Two-dimensional van der Waals materials. a)** Sketch of vdW heterostructure made of different 2D materials. **b)** Representation of vertical stacking of two hexagonal lattices (in this case: hBN) giving rise to a long-range moiré superlattice. **c)** Illustration of moiré pattern imaging with atomic force microscopy.

Figure 1b), determined by the twist angle. This induces the formation of a composite structure with a unique band structure and new properties that differ from those of the individual crystals.

In this thesis, we delve deeper into this phenomenon, showing how the electrical (and mechanical) properties of twisted hBN can be modified by layer twisting, and how this nanoscale modulation can be imaged with scanning probe techniques (Figure 1c). Specifically, we provide an innovative approach, based on atomic force microscopy modes, for visualizing the effects of the moiré structural modulation. These results also evidence how moiré superlattices can be used to generate tunable electrostatic patterns for 2D materials functionalization. Transitioning from the mechanical and electrical to the optical domain, we delve into the

study of light-matter interaction in 2D materials. Specifically, we pose our attention to the ability of confining light to sub-diffractive volumes and enhance light-matter interaction using hybrid excitations called polaritons, which can be imaged by scanning-probe optical microscopy (Figure 2a). Just as the inter-layer coupling and induced band structure modifications enable advancements in computing, energy storage, or surface functionalization, the manipulation of polaritonic states opens new avenues for the development of sub-wavelength photonic devices, including waveguides, modulators, and sensors, as well as for efficient light-emitting devices and lasers or boosting nonlinearities at the nanoscale for high-frequency generation.

Finally, another field that could benefit from 2D materials concerns the realm of quantum

technologies. Here, a pivotal role is played by hBN, which has a large bandgap (nearly 6 eV) able to accommodate crystal defects with energy levels acting as artificial isolated atoms at room temperature. This turns hBN into a suitable host for single photon emitters, with potential applications in quantum information technologies and quantum sensing. In this scenario, the introduction of crystal imperfections in hBN represents another way of engineering its properties, allowing for a non-trivial optical response in spectral ranges where the unmodified crystal is inert. In the present dissertation, we will discuss a practical avenue to selectively control the defects' emission spectral range and their spatial distribution at the same time (Figure 2b).

In the end, the final goal of this work is to introduce new techniques for imaging and controlling 2D materials properties at the nanoscale, highlighting the potential for technological advancements offered by atomically thin materials.

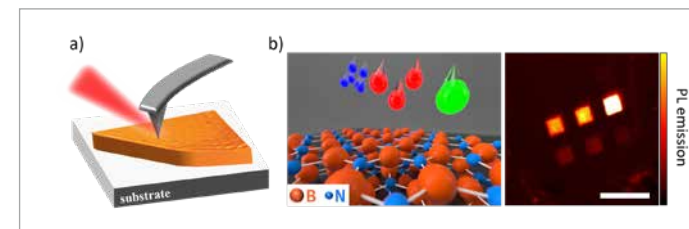


**Fig.2 - Visualization and manipulation of 2D materials optical properties. a)** Optical nanoimaging of polaritons with scanning probe microscopy. **b)** Defects generation in hBN with ion beams for optical emission structuring.

## LIGHT DRIVEN BIO-HYBRID ACTUATORS

**Ilaria Venturino** – Supervisor: Guglielmo Lanzani

Bio-hybrid actuators are soft robotic devices that combine a soft polymeric scaffold with an active biological component. The deformation of the substrates by the biological element regulates the movement of the device. Researchers have explored diverse biological elements for these actuators, including bacteria, fungi, algae, and muscle cells. These devices are trying to mimic the biological world in terms of performance and movements. Muscle cells stand out due to their intrinsic properties: high power/weight ratio, high energy storage capability, high motion control and precision, low environmental impact, and safe interaction with the human world. In addition to their applications in robotics, muscle cells are promising in medical applications. They can serve as platforms to study disease, carriers for drug delivery, and fluid transport devices. From a futuristic perspective, it may one day become possible to fabricate functional organs, such as the heart, or bioengineered prostheses, all originating from cellular materials. The contraction of the muscle tissue conventionally involves the placement of electrodes for the biological element, a well-developed technique in both

robotics and medicine. However, it presents some drawbacks, such as the low spatial and physical constraints given by the electrodes and the possible generation of an inflammatory response or reactive oxygen species that may damage the biological tissue. For this reason, other triggering mechanisms are being studied. Light presents itself as an alternative approach due to its high spatial and temporal resolution, wireless controllability, and non-harmful nature for the cells. Nevertheless, eukaryotic cells are not light-sensitive. Several strategies may be adopted to induce light sensitivity, such as optogenetics, photoactive materials, and photochromic molecules. Photochromic molecules are interesting since they may be delivered directly to the cells without the necessity of introducing scaffolds or a particular substrate. During my PhD, I focused on the use of a photochromic molecule called Ziapin2 to induce muscle cell contraction. The phototransducer is an amphiphilic molecule that dwells spontaneously inside the plasma membrane, inducing light sensitivity. It has an azobenzene core that allows the photoisomerization of the molecule when stimulated with

a wavelength of 470 nm. It has been well characterised and tested on several cell lines, such as neurons, HEK cells, bacteria, and cardiomyocytes. However, its working mechanism has never been tested with skeletal muscle cells. These particular types of cells are suitable for robotics since they do not contract spontaneously and do not require animal sacrifice, eliminating some ethical constraints. Even though skeletal muscle cells are promising, they require several management strategies. Indeed, muscle tissue is composed of several multinucleated cells called myotubes, which derive from the fusion of single cells called myoblasts. This process is natural *in vivo* but requires some technological effort *in vitro*. The myoblasts were seeded on polydimethylsiloxane (PDMS) substrates, which were previously treated with microcontact printing techniques that induce cell alignment. The organisation of the cells improves their maturation and, consequently, myotube formation. Microcontact printing is a well-established method where PDMS stamps, coated with a protein, are imprinted on a substrate to create a precise pattern. The fabrication of the stamps typically involves soft lithography methods;

however, we adopted a mask-less approach to simplifying the fabrication procedure. We exploit a femto-laser ablation technique to directly engrave the surface of the PDMS block, creating the stamps. The approach used is more adaptable than lithography and can also be used to create 3D scaffolds for cell seeding. Once the cells were mature, we were able to treat them with Ziapin2, testing its efficiency to induce muscle contraction. We evaluate the cells performance by exploiting an object tracking algorithm. The visual recognition code is based on a Kanade-Lucas-Tommasi (KLT) algorithm that can evaluate some relevant features inside the first frame of a video and track down their displacement along the whole video. From this detection algorithm, it is possible to reconstruct the contraction profile of the myotubes and evaluate the mean contraction frequency of each analysed cell. By comparing the contraction rhythm of the cells with the stimulation frequency, it is possible to evaluate the effect of the molecule. We trigger the cellular contractions both with optical and electrical stimulation, underscoring the key points of both stimulations. We were able to perfectly trigger the muscle cell contraction when applying a stimulation frequency of 0.5 and 1 Hz in both cases; however, the electrical stimulation seems to be more effective than the optical one when the frequency is increased up to 2 Hz. Even though the electrical stimulation is more effective, it is also quite toxic.

Indeed, after stimulating the cells for 20 minutes continuously, it is noticeable that the voltage applied to the cells should be lower than 3 volts; otherwise, 90% of the cells died. On the other hand, the power density of the light can be increased without affecting the cell's vitality. To enhance the efficacy of our approach, we tried several strategies. First off, we changed the suspension medium of the Ziapin2, switching from water to dimethyl sulfoxide (DMSO), a polar solvent that decreases molecular aggregation, enhancing the number of free molecules that may trigger the cellular contraction. We also changed the type of substrates to PDMS nanostructured once since cellular growth and maturation are strongly influenced by nano or microstructure. The combination of these two upgrades leads to the possibility of improving the control of the cellular contraction up to values comparable with the electrical stimulation and reaching good contraction control up to 4 Hz. We were also able to induce a vibration of the cells, stimulating them at 10 Hz without damaging them. After the very high-frequency stimulation, the cells were still able to contract at a lower frequency. We are currently developing a light protocol to be applied to cells during their growth phase to improve their maturation. The main idea is to train the cells to increase their reactivity and efficiency. Preliminary results suggest that chronic administration of Ziapin2 to the cells during their maturation

process is beneficial, even though the cells are not light-stimulated. This suggests the hypothesis that the molecule affects the membrane of the cells both in dark and light conditions, maybe because it increases the fluidity of the membranes. Lastly, we are currently working on 3D printing techniques to directly print the cells in a three-dimensional device, increasing the possible application and the force generated. Even though we still have to improve the fabrication process of the 3D-biohybrid actuators, we were still able to induce the contraction of some portion of the system upon light stimulus. In conclusion, in my PhD work, I were able to induce muscle cells contraction with light, showing is non-toxic effect on the cells and increasing the contraction frequency up to 4 Hz. I also show the feasibility of treating the cells several times with the photochromic molecules without damaging their viability and functionality. This effect and the preliminary results of the chronic stimulation on the cells open up the possibility of using Ziapin2 as an inducer of cell maturation. Moreover, the possibility of fabricating 3D light-driven biohybrid actuators that are non-genetically modified may open up a new class of actuators.

# HARNESSING ATTOSECOND PULSE GENERATION FOR APPLICATIONS IN SPECTROSCOPY OF OPTOELECTRONICS MOLECULES

**Federico Vismarra** – Supervisor: Rocío Borrego-Varillas

The advent of attosecond science ( $1 \text{ as} = 10^{-18} \text{ s}$ ) marks a revolutionary phase in our understanding of ultrafast phenomena, radically enhancing our ability to observe and comprehend electron dynamics within atoms, molecules, and solids in real time. This transformation is largely attributed to significant advancements in the capability of mastering high-order harmonic generation (HHG), a cornerstone technology for generating attosecond pulses. In my doctoral research, I extensively explored the intricate physics underpinning HHG, the subsequent production of isolated attosecond pulses (IAP) and their use in ultrafast spectroscopy of optoelectronics molecules.

Understanding HHG from a fundamental perspective is a complex task that necessitates a dual approach: a microscopic description focusing on individual atomic responses to an infrared (IR) laser field, and a macroscopic one that considers the collective and coherent behaviour of an ensemble of atoms within the generating medium. From the microscopic viewpoint, the interaction between an intense laser field and an individual atom requires a quantum mechanical description. This involves delineating how a

time-dependent electromagnetic field influences the evolution of the atomic wavefunction. The key to this description lies in the quantum mechanics of light-matter interaction, particularly how an electromagnetic field impacts matter at the quantum level.

Macroscopically, the generation and propagation of electromagnetic fields in an extended medium are governed by collective response of the atoms. In other words, HHG is predominantly influenced by phase matching – the condition in which the generated XUV radiation constructively interferes as it propagates through the gas medium. Achieving optimal phase matching is crucial for maximizing the efficiency of harmonics generation and was a central theme in my research.

Consequently, a significant portion of my work has been dedicated to enhancing the technology for generating attosecond pulses. This involves optimizing the efficiency of HHG sources, refining the spatial properties of HHG to minimize spatial aberrations, and innovating new methods for producing IAP. The research has been conducted between Politecnico di Milano, in the group of Prof. Mauro Nisoli and Lund University, in the group of Prof. Anne L'Huillier. Key achievements include:

- i) The first experimental demonstration of a new theoretical model that provides guidance for optimizing gas-based HHG sources;
- ii) The introduction of a simple model, supported by

experimental investigation, see Fig. 1, to predict and minimize the transfer of astigmatism from the driving field to the generated harmonics. This is crucial for applications requiring either high-intensity XUV fields (e.g. ultrafast physics) or high-quality XUV beams (e.g. nanoscale metrology).

- iii) The development of a novel technique for generating IAP using a semi-infinite gas cell combined with an engineered gas profile. In this case, supported by a novel theoretical method, we validated for the first time the possibility of using an extended medium to generate isolated attosecond pulses, exploiting time-gated phase matching and harmonics re-absorption.

This advancement not only marks a leap in the widespread adoption of IAP technology but also offers a new versatile tools for a variety of experimental setups devoted to unravel the ultrafast physics of matter.

Then, my research extended to the development of a XUV-IR attosecond spectroscopy beamline. Using this beamline we investigated the ultrafast photophysics of a prototypical donor- $\pi$ -acceptor molecular systems: nitroanilines. As shown in Fig.2, our joint experimental-theoretical study revealed a rapid electron transfer mechanism, occurring in less than 10 femtoseconds driven by the planarization of the  $\text{NH}_2$  group. This early-stage processes is crucial in influencing the subsequent electron

dynamics and the overall charge transfer within the molecular system. Supported by advanced quantum mechanics simulations, these experimental observations provide new perspectives on the charge transfer mechanisms of donor-acceptor systems, with huge implications in photovoltaics, molecular optoelectronics, and in further understanding the intricate interplay between nuclear and electron dynamics beyond traditional adiabatic approximations.

In summary, my dissertation outlines significant advancements in attosecond chemistry and attosecond technology. These progresses have direct consequence for broad applications from: nano-imaging to ultrafast molecular photovoltaic and beyond, heralding an exciting future for attosecond science. The dissertation not only addresses fundamental questions in ultrafast molecular physics but also sets the stage for future research directions, aiming to further unravel complex ultrafast processes and their applications in various scientific and technological domains.

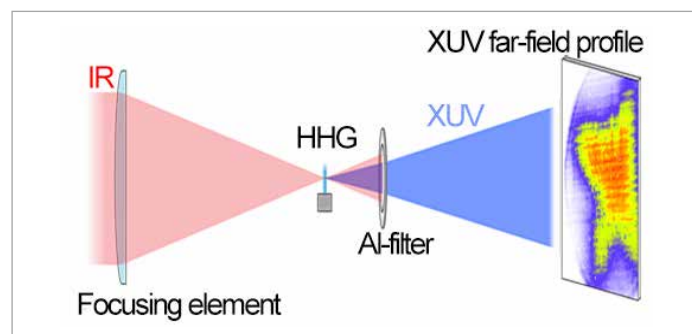


Fig.1 - Experimental evidence of spatial-aberration in HHG (blue area) from an astigmatic IR beam (red area), manifesting as a cross-like pattern in the far-field XUV beam.

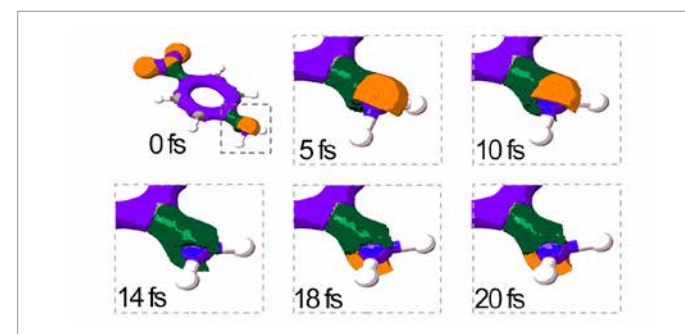


Fig.2 - (a) Sketch of the experimental technique used to initiate and probe a few-fs dynamics in p-nitroaniline. (b) Simulation of the ultrafast charge transfer and hybridization, occurring in 10-femtoseconds.



# ULTRAFAST X-RAY SPECTROSCOPY OF PEROVSKITE SEMICONDUCTORS

**Stavroula Vovla – Supervisor: Eugenio Luigi Cinquanta**

Amidst a semiconductor shortage, the search for alternatives intensifies, with 3D perovskites emerging as promising candidates for light harvesting devices. My research focuses on studying large polaron formation in 3D perovskites using ultrafast x-ray spectroscopy. Large polarons, known to impede carrier recombination and enhance diffusion length in perovskitic semiconductors, form at ultrafast timescales (1) (2). Soft-X transient absorption spectroscopy (XTAS) is pivotal in capturing these events. The experimental setup involves a pump pulse promoting carriers from the valence to the conduction band, with the pulse wavelength determined by the material's band gap. A subsequent probe pulse, delayed with respect to the pump, captures transitions from core orbitals to unoccupied states, revealing absorption edges. For this experiment, I commissioned an experimental line for transient absorption, with IR pulses centered at 800nm and eXtreme UltraViolet (XUV) probe pulses up to 150 eV. The experimental station starts at the exit of the amplified Ti:Sapphire laser system, where a percentage of the beam is used; 35fs pulses of 800μJ energy at 1kHz repetition rate. A 90 – 10

beam splitter is used to divide the radiation in two experimental sub-lines: the 90% is transmitted to the probe line while the 10% is reflected onto the pump line. In XTAS experiments, small signals are expected, making the optimization of the XUV source important. We developed a technology that exploits high harmonics generation in gases in a microfluidic device (3). This source, acts similarly to a hollow waveguide where the impinging IR pulse has multiple instances of interaction with the injected noble gas, which results in higher generation yield and broader energy range compared to most common devices (4)(5). Therefore, the majority of the experimental line is located in a vacuum chamber system, where a pressure gradient is present; from around 10<sup>-4</sup> mbar at the HHG chamber, due to the injected gas

in the microfluidic device, up to 10<sup>-7</sup> mbar at the spectrometer chamber. The generated XUV radiation is directed to the sample holder, where it crosses the IR pump signal non-collinearly. We also developed an Optical Parametric Amplifier (OPA) at 1500 nm to increase the HHG process in Ar (Figure 1). Despite the results obtained with our OPA, further development is needed to increase the photon flux beyond 150 eV. At the Interaction Point, two thin-film samples or a sample and its substrate can be placed and studied in parallel, as well as a BBO crystal. The BBO acts as a cue for the spatial and temporal pump-probe overlap as the nonlinear interaction between the two pulses can be observed visually. After interacting with the sample, the transmitted XUV signal is dispersed by a grazing incidence grating and detected

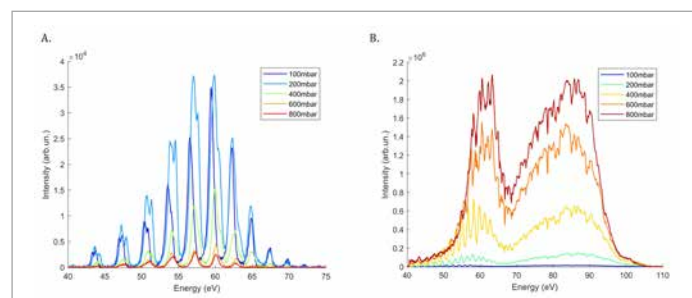


Fig.1 - (A) XUV signal for HHG in Ar with 800nm driving pulses (Ti:Sapphire laser) using the microfluidic device. (B) XUV signal for HHG in Ar with 1500nm driving pulses (OPA) using the microfluidic device.

by a Micro-Channel Plate followed by a phosphor screen. The image displayed on the phosphor screen is acquired by a CCD camera. For benchmarking my beamline, I set up a preliminary XTAS experiment on Silicon, which has already been studied in the literature (6) (7)(8). I targeted the transient evolution of the sharp  $L_{2,3}$  absorption edge at ~99eV. While static measurements yielded satisfactory outcomes (Figure 2), transient measurements revealed certain signal instabilities. Figure 3 shows the measured transient Optical Density (OD) of Si. In this case, OD is defined by the Beer-Lambert Law:

$$OD = -\log_{10} \frac{I_{on}}{I_{off}}$$

The Figure 3 dataset compares signal intensities in the “pump on” and “pump off” states. Eight ten-minute measurements, spanning ~30 ps to 30 ps in 10 ps intervals, were accumulated to avoid laser system instabilities. Signal-to-noise ratio was enhanced by averaging 100 scans for each delay interval. The left panel shows the average OD, and the right panel displays OD after Principal Component Analysis correction (9)(10).

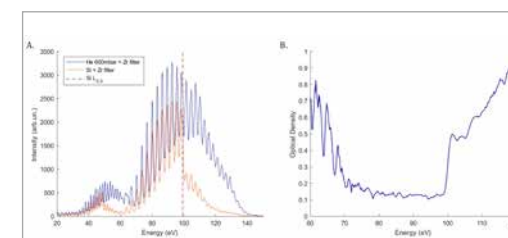


Fig.2 - (A) Comparison of the generated and filtered XUV signal (light blue) and the static absorption of the XUV signal from the L2,3 edge of polycrystalline Si (dark blue). (B) Measured Optical Density

In both instances, a negative signal is evident on the scale of the anticipated signal. This is indicated by the shift from red to blue and back to red along the color scale, around the 99 eV mark, spanning the entire duration of the delay scan. Notably, if this negative signal had originated from the expected carrier dynamics, it would likely have been localized within a narrow delay range, rather than encompassing the entire scan duration. This suggests the involvement of a distinct phenomenon occurring on a slower timescale. Literature suggests a thermal load from pumping pulses (11)(12), prompting two implemented solutions: a rastering system and reducing the laser system's repetition rate with a mechanical chopper. Rastering cycles the sample through different areas for each delay, reducing exposure time. Decreasing the repetition rate extends thermal load diffusion time. While investigating other sources of noise, a problem stemming from the movement of the laser generation device was discovered which was mitigated by a pointing stabilization system with PID

control. Additional investigations revealed a non-reversible six-degree thermal gradient over two hours of irradiation of the microfluidic device during XUV generation. To mitigate these effects, a cooling system is being introduced. Utilizing the Si experiment as a reference, we are conducting similar experiments on perovskitic semiconductors. A preliminary feasibility assessment has indicated that for perovskites with ABX<sub>3</sub> stoichiometry, performing transient absorption measurements on the available edges of the halogen site is appropriate. Additionally, an assessment of material thickness to optimize the signal-to-noise ratio took place. It was determined that two samples, both produced via spincoating, would be most suitable: FAPbBr<sub>3</sub> and FAPbI<sub>3</sub> with Br doping. The perovskite samples required for these studies are supplied by the CNST laboratory at the Istituto Italiano di Tecnologia (IIT).

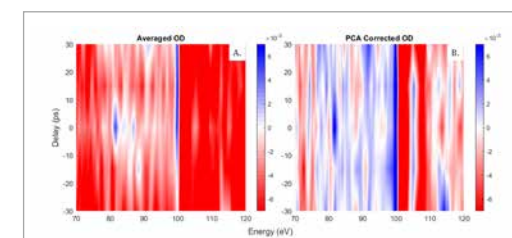


Fig.3 - (A) Calculated average of the Optical Density of a cumulative 80min transient absorption measurement. (B) Corrected Optical Density after Principal Component Analysis.

# TIME-RESOLVED SCANNING ELECTRON MICROSCOPY FOR INVESTIGATION OF MECHANICAL AND CHARGE DYNAMICS

Mohamed Zaghloul – Supervisor: Alberto Tagliaferri

Time-resolved scanning electron microscopy (TR-SEM) is a powerful tool joining nanoscale resolution with time resolution. It allows us to investigate the dynamics down to the ms timescale in real-time mode, and down to the femtosecond timescale in stroboscopic mode. TR-SEM is developing rapidly due to the increasing importance of systems with nanoscale morphologies and photophysics that need novel spectroscopies, imaging strategies, and analytic tools. Examples are micro-electro-mechanical systems (MEMS), including micromirrors and accelerometers, and photonic devices. TR-SEM allows us to visualize their mechanical motion and charge carrier transport at the surface. This thesis work aimed to develop an original *in-operando* setup in a commercial SEM to study the mechanical dynamics of a Tang's comb resonator as a testbed for commercial MEMS devices. The knowledge of their motion is crucial in MEMS design and fabrication. On one hand, We demonstrate the applicability of TR-SEM for capturing stroboscopic motion sequences over the full period of oscillation of the MEMS comb resonator, allowing the *in-operando* characterization of

the in-plane motion on electrically actuated MEMS resonators with few10 nm absolute resolution and 100 ns time resolution. In our setup, a 20 MHz bandwidth beam blanker was used to slice the electron beam in 100 ns pulses. The operation of our setup depends mainly on actuating the device closer to its resonant frequency, 50 kHz. Two acquisition modes were implemented to acquire a wide set of information about the dynamics of the device. First, in the locked phase delay mode, a series of fixed delay images were taken by actuating at a chosen frequency both the device and the electron slicing beam blanker. This mode allows for the visualization of the local motion of the movable part of the device. Fig. 1(a, b) shows the displacement of a tooth of the comb resonator's movable part at delays of  $\pm 1/4$  of the oscillation period, where it reaches the maximum and minimum values of the order of 1  $\mu\text{m}$ . This value is measured with a confidence of a few 10 nm in a single experiment. Fig. 2(a) shows the displacement as a function of time, supporting the reproducibility of automatic motion tracking at arbitrary positions and the lack of strain on the comb's tooth. The Fourier spectrum of the displacement

is shown in Fig. 2(b), where the fundamental component at 50 kHz is accompanied by higher harmonics as large as 3% of the fundamental intensity, gradually decaying with increasing frequency. This testifies the presence of relevant non-linear effects, that were further investigated by a second acquisition mode developed on purpose, the uniformly sweeping phase delay or beating mode. This acquisition mode allows to map in a single image the displacement along a chosen direction over a full period of oscillation, thus making it possible to extract local amplitude versus frequency curves and investigate the non-linear behavior of the device as a function of the position shown Fig. 1(c, d)

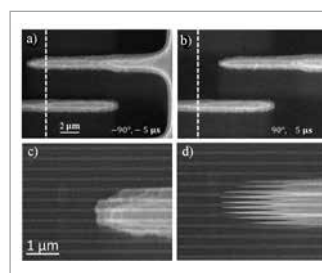


Fig.1 - Stroboscopic TR-SEM delay time series in locked phase delay, dynamics of a tooth of the movable part a) Tooth in the extreme left position. b) Tooth in the extreme right position. (c,d) oscillation mapping acquired at actuation frequencies far and close to the resonance frequency, respectively.

On the other hand, Photoexcited charge carrier dynamics were investigated at the surface of Si(001), by ultrafast TRSEM (USEM) in an ultra-high vacuum environment at 100 ps time resolution. USEM makes use of a photoemitted electron pulse source and of secondary electron (SE) contrast. In this work, we further improved the protocol for contrast pattern analysis to extract the map of induced surface photovoltage (SPV) at the semiconductors' surface. USEM analysis assumes that photoexcited spatial modulations in work function induce SE contrast patterns. Fig. 3 shows the SE contrast intensity at a given position as a function of the delay time between the pump and probe. Si(001) prepared without any surface chemical etching shows negative USEM contrast; the contrast turns positive on the surface prepared by a 40-second HF etching; then

the contrast reverts to negative on the surface treated by a 120-second HF etching. *In-situ* elemental characterization of those surfaces by Auger electron Microspectroscopy (AES) allowed us to correlate the dynamics of SPVs with the sample's surface distribution of contaminants. This evidence demonstrates the extreme surface sensitivity of the technique.

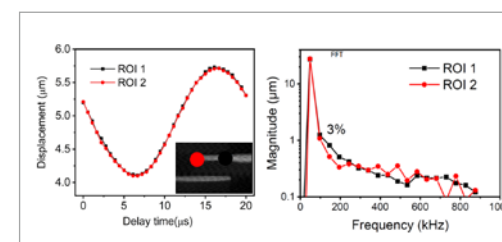


Fig.2 - (a) Tracking recognition of the movable part motion at different delay times and (b) FFT of curve (a)

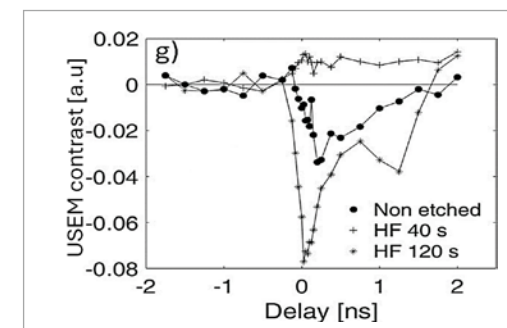


Fig.3 - Dynamics of heavily doped Si at different etching using the ultrafast scanning electron microscope

# LASER WRITTEN VAPOR CELLS DEVICE FABRICATION AND CHARACTERIZATION AS CORE ELEMENT OF MAGNETOMETERS

Andrea Zanoni – Supervisor: Roberto Osellame

In this thesis, a new fabrication technology to create vapor cells of atomic clocks and OPMs (optically pumped magnetometers) is proposed, with a particular focus on this second application. These vapor cells are chambers realized in optically transparent materials (e.g. fused silica, in this work), which contain a vapor of hot alkali atoms, sensitive to magnetic fields variations.

The technology utilized throughout the work to create vapor cells is femtosecond laser writing, followed by chemical etching (FLICE). This fabrication approach unlocks the possibility of creating miniaturized, versatile and easy-to-integrate vapor cells (LWVC) for OPM applications. OPMs are sensors that have existed for at least 40-50 years now, with the first papers about them written by W. Happer in 1972. As such, they are not a new technology in themselves, and this thesis work does not aim to discover any new sensing scheme or improve their sensitivity. This work aims to address some of the unsolved issues in the fabrication of OPMs that have been around for decades, in particular, their limited miniaturization, optical access, and low possibility of integration. The two main fabrication technologies utilized up to

date are glass-blowing and MEMS-related techniques, the limitations above mentioned are generated directly by these fabrication techniques, but with them, it is also possible to reach the highest sensitivities in the field for OPMs.

In this work, the vapor cells fabricated by FLICE (LWVCs) have proven to have, even with increased miniaturization along the sensing channel cross-section, competitive sensitivity (a noise level of  $1 \text{ pT}/\sqrt{\text{Hz}}$  at 10 Hz down to  $40 \text{ fT}/\sqrt{\text{Hz}}$  at 100Hz) with respect to the results available today in literature, and further improvement could be possible finding the correct parameters to operate them in a SERF (spin-exchange relaxation free) regime. This thesis also covers the first steps towards the integration of the LWVCs, where a procedure to create a fiberized system with low losses (roughly 30%) and a more straightforward setup procedure with respect to bulk systems is proposed. Future developments could see the complete integration of the system.

## FABRICATION PROCEDURE:

The fabrication procedure to create LWVCs efficiently and consistently has then been defined. All the LWVCs are composed of at least two main elements: the sensing channel

(mentioned already above), where all the sensing measurements take place in OPM applications, and the activation chamber, or reservoir, where the alkali atoms are inserted.

The procedure consists of several steps, each one of them has been defined and optimized to be highly consistent and repeatable during different fabrications:

• **Laser irradiation.** A pristine piece of fused silica is irradiated with a femtosecond laser following a previously designed geometry. All the critical parameters as laser wavelength, polarization, power of the pulses, repetition rate and writing speed have been defined and optimized.

• **Chemical etching.** An etching process is then carried out on the irradiated samples, by using HF acid. The etching process has been performed at  $35^\circ\text{C}$ , in a solution of HF at a 20% concentration in volume. Optimal acid concentration, temperature, and etching time have been successfully defined in order to obtain repeatable results, given the same irradiation parameters.

• **Polishing.** A polishing recipe has been defined in order to improve the optical quality of the external facets of the sample. For the internal ones (roughness in between e 50 nm and 100 nm RMS), further work is needed

to define and test an optimal annealing procedure, which, up to today, proves to be the only reliable method to reduce the internal roughness (in the literature up to 20 nm RMS).

• **Filling.** The LWVCs need then to be filled with a vapor of alkali atoms (Rb in our case). A preferred filling method has been found, by inserting a solid-state Rb NEG (non-evaporable getter) inside the activation chamber, before the sealing of the LWVC. The Rb NEG can then be thermally activated to release the vapor of Rb in the cell. This procedure is performed under a controlled atmosphere of  $N_2$ , at room temperature and pressure.

• **Sealing and bonding.** In the LWVC, the bottom part of the activation chamber is open, to have a way to insert the Rb NEG. This opening has been closed using a slab of fused silica ( $20 \times 20 \times 1 \text{ mm}$ ); this slab and the cell are bonded together using a UV curing glue. The optimal glue and the procedure to cure it effectively and consistently have been defined. In the future, it could be advantageous to swap to laser bonding techniques, like micro-welding.

• **Laser activation.** The Rb NEG, not only releases vapor state Rb when activated, but also has a gettering effect on all the gases present in the LWVCs, as such, its activation process proves to be critical to realize sensitive OPMs. An optimal procedure to activate the Rb NEG, while maintaining high  $N_2$  pressure inside the cell, has been defined, by using a CW laser with a focal spot on the NEG of  $200 \mu\text{m}$  of diameter, at 5 W, for

20 s.

• **Oven and heaters.** An optimal geometry for the oven heating up the LWVCs (during OPM experiments) has been defined and realized. The oven is heated up by a couple of resistive heaters, working at 40 kHz to average out the magnetic fields created. These heaters have been realized during previous projects.

This procedure has brought to the realization of many different device geometries; this work focuses mainly on two of them.

## LWVCs GEOMETRIES:

The first geometry analysed in detail is the first-ever realized LWVC geometry, which allowed to publish our first proof of principle work, demonstrating that it was possible to use a LWVC as a vapor chamber for OPM or atomic-clock systems.

This LWVC has a 9.5 mm-long sensing channel, with a cross-section of 1 mm, no separation between it and a cylindrical activation chamber (5 mm diameter and 3.5mm height) and a residual  $N_2$  pressure inside the cell of 0.004 amg. This low  $N_2$  is due to a non-perfected (at the time) Rb dispenser activation. This LWVC proved to give high-resolution spectra during SAS (saturated absorption spectroscopy) measurements (linewidth of 70MHz) and, as such, it could be utilized to create atomic clocks; however, it exhibited poor magnetic field sensitivity (in the order of hundreds of  $\text{nT}/\sqrt{\text{Hz}}$ ). The second design presented is the one of the latest LWVC and is the one that is going to be

exploited moving forward.

This LWVC exhibits a 9.5 mm-long sensing channel, with a square cross-section of  $500 \mu\text{m}$  edge, which, up to my knowledge, is the smallest reported in the literature up to today, for a similar system. The sensing channel is separated from a rectangular-base activation chamber ( $9 \times 4 \times 3.5 \text{ mm}$ ) by some micro-channels ( $250 \mu\text{m}$  of section and  $500 \mu\text{m}$  long), which efficiently prevent the Rb NEG activation by-products from getting stuck inside the sensing channel (problem present with the first geometry instead). The NEG inside the cell has been activated by following the activation parameters defined before and, as such, the final pressure of  $N_2$  inside the cell is 0.75 amg. As explained in detail in the thesis, this  $N_2$  pressure did not allow for sensitive AS (absorption spectroscopy) measurements (linewidth of 13.5 GHz), but proved to be adequate to achieve high-sensitivity magnetic field measurements ( $1 \text{ pT}/\sqrt{\text{Hz}}$  at 10 Hz,  $40 \text{ fT}/\sqrt{\text{Hz}}$  at 100Hz). This last design proved to be optimal to realize sensitive OPMs and, as such, it is the design and consequent fabrication procedure, that is going to be used moving forward to push toward better sensitivities. This work paves the way to realize, in future, miniaturized OPMs with a double sensing channel (gradiometer configuration) and the realization of a micro-fluidic, all-in-one, OPM system to sense bacteria or other magnetic-active, small-sized entities.

## FULLY INTEGRATED OPTOFLUIDIC PLATFORMS FOR HIGHLY SENSITIVE, IN-FLOW BIO-SAMPLES DETECTION

Filippo Zorzi – Supervisor: Luigino Criante

Micro Total Analysis System ( $\mu$ -TAS) is a fascinating line of research that is based on the synergy of several fields, from nanotechnology to biotechnology and microfabrication. Its ultimate goal is to condense an entire laboratory within a single chip, incorporating all the components needed to monitor biochemical processes or for specific analytical functions. This microfluidic technology, also known as Lab-on-a-Chip (LoC) consists of complex microsystems that integrate microfluidic networks, to perform different tasks, which in a laboratory are typically performed by different instruments. These tasks can be sample mixing, but also sorting, filtering, and various types of analysis. They are very compact platforms that aim to perform these tasks in an extremely small space (a few  $\text{mm}^2$ ). Thus, they are extremely portable, but also inexpensive (if compared to classical bench-top laboratories instruments) and operate in an automated manner, making them usable even by non-expert users. These factors make them ideal for self-made analysis by the population, as well as for their use in remote and underserved areas. Furthermore, thanks to their robustness, they are proving to be extremely useful

even in contexts with extreme environmental conditions, such as in space or on ocean floors. Over the years, studies conducted on LoC platforms have attracted increasing interest due to their ability to provide increased sensitivity of measurements. Optical detection has proven to be a promising avenue for further developing this technology. Developing a microfluidic device that integrates within it all the components necessary for the analysis of a given sample, including optical elements, would be a great advancement for Lab-on-Chip technology. The potential of such a system is evident. It is extremely compact, minimizing signal losses that occur with optical setups characteristic of larger and more complex instruments. Due to the reduced sample quantity used, it significantly increases the instrument's sensitivity. Furthermore, by integrating optical systems within the chip to enhance signal collection, a level of performance could be achieved that allows detailed analysis of various samples while maintaining high throughput. However, this total integration remains an open challenge for various reasons, from the technical difficulties of implementation to the low

efficiency of some integrated optical elements. Therefore, external instruments are often used, in the case of optical analysis, for example, microscopes and objectives are used for excitation or signal collection, or lasers in the air that must be coupled to the chip, partially negating the positive aspects typical of these devices. Therefore, this doctoral project aimed at developing an optofluidic platform that would integrate a microfluidic network and optical signal-collection systems within it, and enable high-sensitivity, high-throughput measurements of flowing liquid samples. Through the fabrication technique used (Femtosecond Irradiation followed by Chemical Etching), FLICE), it was possible to fabricate an optofluidic flow cytometer with a 3D geometry that contained within it a hydrodynamic focusing stage that allowed the particles of a given sample to be aligned at the center of the outer channel. A detection system was then coupled to this focusing stage, consisting of specially made housings to be able to insert an excitation optical fiber and a signal collection fiber. To increase the signal-to-noise ratio, a spherical micrometric in-plane mirror ( $R=140\text{ }\mu\text{m}$ )

was made, which allowed the signal emitted by the particle to be collected from a greater solid angle than fiber integration alone (in any type of optical analysis – scattering, fluorescence, spectroscopy, etc). Experimentally, it was observed that thanks to the integration of this spherical mirror, the signal-to-noise ratio increased by a factor of 6, allowing us to discriminate signals from different populations of particles and to detect the scattering signal from particles down to  $1.5\text{ }\mu\text{m}$  in diameter, as well as from cells and bacteria. Then a chip was made that in combination with an external optical setup allowed for high-throughput Raman analysis of blood. Blood tests are now mandatory as a preliminary analysis of every patient to determine future treatments. However, with the currently used methods, performing a complete test on a blood sample requires a considerable amount of time (days) from sample preparation to analysis, which risks compromising the effectiveness of the treatment, especially in settings where one is dealing with emergencies. For this reason, it is essential to find a method that can give a complete overview of the blood analyzed in a short time. Raman spectroscopy is an excellent candidate, as it is a label-free method that has high sensitivity, and is capable of detecting several markers related to various diseases. However, due to the weakness of the Raman signal, at present, devices for making Raman measurements

of blood have low throughput, making them unusable in clinical settings. The realized chip can laminate within it the flows from different blood samples (up to four), and thanks to the use of an imaging spectrometer it was possible to acquire the signals from these samples simultaneously, without the use of moving parts within the setup, significantly increasing the throughput of the device. In addition, the setup used brings several advantages over the state of the art, including being able to use an excitation with a wavelength in the visible at a high intensity without running the risk of photodegradation of the cells. Since using a shorter excitation wavelength leads to an increased signal, this factor allows us to make extremely fast measurements, and to maintain a good signal-to-noise ratio while maintaining integration times below one second. The high throughput offered by this device, once combined with machine learning techniques capable of real-time discrimination of different parameters within blood Raman spectra, is extremely promising for its use in clinical trials in hospital settings. Finally, the knowledge gained in the two previous projects was combined to make a chip that would be their natural technological evolution. By modifying the geometry used for the optofluidic flow cytometer made for discrimination of scattering and fluorescence signals of particles in flow, a Lab-on-Chip was made that would allow in-chip Raman spectroscopy

measurements, without the use of external optical elements (microscopes and objectives), but integrating both excitation and signal collection within it. Using a test sample, we again verified the signal enhancement provided by integrating the spherical in-plane mirror, which allowed us to obtain Raman spectra of liquids of interest (e.g., olive oil) while maintaining a good signal-to-noise ratio even with measurement integration times below one second. Furthermore, if we compare the measurement made with this device with the measurement made with bench-top optical instruments, we can say that there is a wide margin for improvement. For example, it is possible to decrease the excitation wavelength and significantly increase the excitation power without incurring into sample photodegradation and modify the spectrometer to get a stronger signal. All these factors lead us to believe that it is possible to make Raman spectroscopy measurements with even shorter integration times (a few tens of milliseconds) while maintaining a good signal-to-noise ratio. It is believed that the devices developed during this thesis can further push optofluidic Lab-on-Chip technology toward new applications in the area of ultra-high sensitivity and high-throughput sensing, all with extremely compact and portable setups, leading to a new era of mass screening and Point-of-Care testing.